DEPARTMENT OF COMMERCE
SINCLAIR WEEKS, Secretary

WEATHER BUREAU
F. W. REICHELDERFER, Chief

MONTHLY WEATHER REVIEW

JAMES E. CASKEY, JR., Editor

Volume 86
Number 5

MAY 1958

Closed July 15, 1958
Issued August 15, 1958

APPLICATION OF RADIATION DATA TO MAXIMUM TEMPERATURE FORECASTING[1]

VANCE A. MYERS

U. S. Weather Bureau, Washington, D. C.

[Manuscript received April 17, 1957; revised November 25, 1957]

ABSTRACT

A method is developed for evaluating the local heating and cooling by radiation and related processes, for predicting the daily maximum temperature at Nashville, Tenn.

1. INTRODUCTION

There is no fact more common in man's life than that each day our environment is warmed by the sun. Yet for the weather forecaster to consider the sunshine in a quantitative way in predicting the daily maximum temperature is far from universal. This paper reports on a method for assessing the net heating by insolation in forecasting the daily maximum temperature at Nashville, Tenn. The method is an expansion of that developed by Neiburger [12] for predicting maximum temperatures at Chicago. Williams [19] recently devised a similar procedure for Las Vegas, Nev., and Phoenix, Ariz. Jefferson [6] has published a note on this type of approach to temperature forecasting in England. Nashville was chosen for the present study because it is both a radiosonde and a pyrheliometric station and because there are neither mountains nor large bodies of water in the immediate environment.

One byproduct of the investigation is the diurnal variation of the clear-weather heat balance. From these data, shown in graphical form for alternate months of the year, the net heating or cooling of the air between any two times of day can be estimated. A second byproduct is the total net daily heating. It was found that insolation absorbed at the ground appreciably exceeds all day and night heat losses under cloudless conditions at Nashville throughout the year, except possibly within a week or two of the winter solstice. This partly accounts for the warming of southward-moving airmasses at the latitude of Nashville.

2. THE LOCAL HEAT BALANCE

The energy-balance equation at the surface of the ground as employed by Neiburger is:

$$H_0 = I_0 - RI_0 - B_0 - S - LE \qquad (1)$$

where H_0 is the heat conducted from the ground to the air, I_0 the solar radiation reaching the ground, R the albedo or reflectivity of the ground surface, B_0 the net long-wave radiation, positive upward, S the heat entering the ground and raising its temperature, L the latent heat of evaporation, and E the amount of water evaporated or transpired. The equation is also valid for the cooling of air at night.

This study seeks to account for the diurnal change in heat content of the layer of air extending upward from the

[1] Paper presented at the 137th National Meeting of the American Meteorological Society, Kansas City, Mo., June 8-10, 1955.

ground a few thousand feet in which the principal daily fluctuation of temperature occurs. In cloudless weather the flux of heat, H_a, into a vertical column of unit cross section through this layer is:

$$H_a=H_0+m(I_a+RI_0)-(B_a-B_0)+A \qquad (2)$$

where m is the fraction of short-wave insolation absorbed by clear air of the column, including water vapor, I_a the insolation at the top of the layer, B_a the net long-wave radiation at the top of the layer, positive upward, and A the advection of heat into the column by horizontal and vertical air movements. The sum of the fluxes on the right in equation (2), excepting A, will be symbolized by H:

$$H_a=H+A \qquad (3)$$

The primary objective of this study was to estimate climatological values of H to enable the forecaster to estimate H_a by inserting his own estimate of A into equation (3), or by neglecting A if it is small.

The absorption of insolation by the air, $m\ (I_a+RI_0)$, is usually the smallest of the energy fluxes in equation (2) and is not as large as probable errors in other fluxes. This term is neglected in the remainder of the present study. With this approximation and combining equations:

$$H=I_0-RI_0-B_a-S-LE \qquad (4)$$

Estimates of the climatological normal values of H in clear weather were obtained by substituting in equation (4) estimates of the five quantities on the right-hand side. This was done on an hourly basis for February, April, June, August, October, and December.

Insolation, I_0.—Essentially cloudless days at Nashville from January 1945 through September 1946 were identified as those on which both 100 percent of possible sunshine from the sunshine recorder ("triple register") and either "zero" or "less than one-tenth" daily mean cloudiness by eye observation, was reported in the Monthly Meteorological Summary [18]. Hourly totals of direct and diffuse solar radiation on those days, as recorded by the Nashville pyrheliometer, were plotted against date, and annual curves of insolation for each hour were drawn to the data. Hourly values of insolation were read from the curves at the 15th day of alternate months and are listed in table 1.

TABLE 1.—*Cloudless-sky hourly insolation on a horizontal surface, Nashville, Tenn. Based on data from January 1945 through September 1946.*

Hour ending local mean solar time	Insolation on the 15th day of the month (langleys/hr)					
	February	April	June	August	October	December
a. m.						
6	0	1	5	2	0	0
7	0	9	20	15	0	0
8	7	30	40	32	10	1
9	21	50	56	49	25	15
10	37	63	70	65	40	29
11	52	74	80	76	54	36
12	58	80	87	81	61	42
p. m.						
1	61	81	86	83	63	43
2	56	76	80	77	57	39
3	41	63	71	66	44	28
4	27	47	57	51	29	15
5	8	30	39	33	11	3
6	1	9	20	15	1	0
7	0	1	5	2	0	0
Total	369	614	716	647	395	251

Albedo, R.—Shaw [15], Fritz [3], and List [11] have tabulated values of the albedo (percentage of sunshine reflected) of various natural surfaces. Some of the values most applicable to the environment of Nashville are those obtained by Kalitin [8] over a field of grass in Poland in spring. His values when the field was dry ranged from 0.18 to 0.23. Neiburger used an albedo of 0.21, the mean of Kalitin's measurements. In the present study an albedo of 0.20 was considered representative for Nashville, that is, 20 percent of each value in table 1 was considered as heat lost to the earth by reflection. Williams used a slightly lower value of 0.17 in consideration of the terrain around his two stations.

Long-Wave Radiation, B_a.—The upward long-wave radiation which dissipates heat from the ground is absorbed by the water vapor of the atmosphere. This energy is reradiated both upward and downward. The net upward radiation through any level may be estimated by use of various radiation charts, if the temperature and water vapor distribution in the atmosphere and temperature of the ground are known. The radiation chart of Elsasser [2] was employed to compute the net upward radiation through the 1.5-km. (mean sea level) surface from selected mean monthly raob soundings at Nashville. In an attempt

TABLE 2.—*Air and ground temperatures (° F.) at Nashville, Tenn. and computed net upward fluxes of long-wave radiation through the 1.5-km. surface during selected months*

Month	Air temperature (observed)				Ground temperature (estimated)	Long-wave flux through 1.5-km. surface (langleys/hr)			
	Departure from normal	Mean for 2115 CST	Mean of daily min. temp.	Mean of daily max. temp.	Mean max. (at solar noon)	2115 CST	Sunrise	1600 CST	Mean local noon (1148 CST)
Feb. 1943	1.6	42	32	54	62	7.5	6.7	8.9	9.6
April 1943	−1.2	56	47	68	89	9.4	8.5	10.4	13.0
June 1945	−1.0	73	65	85	118	9.8	9.0	11.6	14.2
Aug. 1944	0.9	76	69	88	124	9.0	8.4	10.4	13.4
Oct. 1944	−1.3	57	47	72	89	9.4	8.1	10.9	12.5
Dec. 1943	−2.4	38	31	46	61	7.5	6.8	8.2	9.5

to approximate long-term mean conditions, months were selected during which the average surface temperature was close to the long-period normal. The selected months and their temperature departures from normal are shown in table 2. In order to obtain a diurnal curve, the net upward flux through the 1.5-km. surface was computed for the four times a day listed in table 2. The mean monthly temperature soundings for 2115 CST [2] were adjusted to the other three times a day by appropriate small modifications near the ground.

The choice of 1.5 km. as the level at which to compute B_s was made from figure 7. Here mean monthly night temperature soundings at Nash ille and Phoenix are plotted, together with dry adiabats through the mean monthly maximum temperature at the surface. If the latter approximate mean monthly midafternoon soundings, then the intersections of the two curves approximate the height to which heating and cooling are convected daily. The average pressure at the intersections of the six pairs of curves at Nashville is 860 mb., at a height of about 1.5 km. The data for Phoenix were added to figure 7 as a check on whether the Nashville soundings—monthly means including all weather conditions—were nonrepresentative of the desired condition of clear weather. Clear weather predominates a greater percentage of the time at Phoenix than at Nashville. The figure indicates that the two stations are similar to a satisfactory degree, and that therefore the Nashville monthly means are a reasonably good approximation of clear-weather means.

The ground temperature at Nashville for use on the radiation chart had to be estimated from the air temperature. Most of the present study was completed in 1947 before the recent great interest in micrometeorological studies of the surface layer of air and of soil temperatures in the United States. Guidance with respect to the relation of soil temperatures to air temperatures was obtained from two English investigations by Penman [13] and Johnson and Davies [7]. Penman obtained simultaneous continuous traces of soil temperature as close as practicable to the actual ground surface and of air temperature in a standard shelter. He found that during the hours of the day when the ground is cooling the air—from the time of the daily maximum of air temperature to sunrise—the ground temperature was typically only a degree or so (° C.) lower than the air temperature. Air and ground temperatures were assumed to be equal during those cooling hours in the present study and the mean monthly maximum and minimum air temperatures shown in table 2 and the mean "surface" (air) temperature at 2115 CST were substituted for ground temperatures at the appropriate times of day on the Elsasser chart.

During the warming hours of the day, Penman found that the ground is much hotter than the air. The ground temperature rises sharply from sunrise to solar noon when it may attain a value as much as 30° C. above the air temperature, then falls sharply until sunset.

An approximate relation of ground maximum daily temperature to the corresponding air maximum was obtained by plotting mean monthly ground and air maximum temperatures obtained by Johnson and Davies [7] at Salisbury Plain, England, against each other. The air temperature measurement by those investigators was in a standard shelter and the ground temperature 1 cm. below the surface of bare ground. The relationship was used to estimate Nashville mean monthly maximum ground temperature from the air maximum. The ground maximum was considered as occurring at local noon (1148 CST).

The net upward flux of long-wave radiation through the 1.5-km. surface, as computed from the Elsasser radiation chart, is shown in table 2 for the four times a day for the selected months. The intensity of the long-wave flux may be related as a matter of interest to something more personally familiar by comparison with insolation values in table 1. The intensity of this flux is of the same order of magnitude as the intensity of insolation on a horizontal surface about an hour after sunrise or before sunset.

Ground absorption, S.—To obtain estimates of the heat absorbed or released by the ground, profiles of ground temperature from the surface down to a depth of 30 cm. were constructed for every 2 hours throughout the day from Johnson and Davies' [7] tabulations of the mean annual diurnal range at various depths and the mean time of occurrence of the daily maximum at each depth. From these profiles a diurnal curve was constructed of the variation of the mean temperature of the 30-cm. layer, with temperatures expressed in terms of departure from the daily mean. The temperature departures were converted in turn to departures of the heat content of the ground by multiplying by the depth of the layer (30 cm.), and by the density and specific heat of soil. The density of earth was assumed to be 1.5 gm. cm.$^{-3}$, the value for dry packed earth from the Chemical Engineer's Handbook [14], and the specific heat was assumed to be 0.2 cal. deg.$^{-1}$ gm.$^{-1}$ from Brunt [1]. The only significant source of heat to the ground is by transmission through the surface. Therefore the rate of heat absorption by the ground, S, was obtained as the slope of the diurnal curve of heat content of the 30-cm. layer. The diurnal temperature cycle at 30 cm. was small enough to warrant ignoring any heat changes below that level. The foregoing procedure is very similar to that used by Williams for estimating the heat absorbed by the ground in the Phoenix-Las Vegas area.

The mean annual curve of values of S vs. time of day obtained as described above was modified subjectively for each of the 6 months under study in the following way. The curve was reshaped so as to place the maximum upward flux of heat at sunrise in each month instead of at the same hour throughout the year. This was done in such a way that the net area under each diurnal heating curve was zero. Secondly, all fluxes, both upward and down-

[2] Throughout this report, except in the forecast test, raobs at Nashville are considered as at 0915 CST and 2115 CST, the approximate mean time of observation during the years from which data were taken.

ward, were arbitrarily diminished slightly in magnitude for December, in consideration of the small diurnal range of air temperature in that month.

Usually the most important variable controlling the heat absorbed by the ground is the moisture content of the soil. This affects not only the density and specific heat but the conductivity as well. Detailed consideration of soil types is not warranted unless some index of the moistness is also used. Neither moisture content nor soil type was taken into account in the present study. This is not disastrous because the flux of heat into the ground is smaller than the other fluxes in any case.

Evaporation, E.—Hourly values of evaporation from the ground plus transpiration from plants were derived for Nashville by subdividing an estimate of the mean annual total evapotranspiration at Nashville successively into monthly, daily, and hourly amounts.

The mean annual evapotranspiration at Nashville was assumed to be 20 inches. This quantity is intermediate between values of the annual evapotranspiration obtained by different methods. Kittredge [9] and Wilm and Thornthwaite [20] show maps of annual evapotranspiration estimated by subtracting runoff of streams from precipitation. A series of direct measurements of evaporation were made in 1939 by Thornthwaite and Holzman [16] [17] over a field at Arlington, Va., by the turbulent transport method. With interpolation for missing months of February and September, an annual total evapotranspiration of 11.72 inches was obtained for that location. Kittredge's and Thornthwaite's maps show 25 and 28 inches annual evapotranspiration at Arlington, Va., and 31 and 30 inches at Nashville. A value of 20 inches annual evapotranspiration at Nashville is intermediate between the two kinds of measurements.

The Thornthwaite-Holzman Arlington data were used directly by Neiburger. Williams, in view of the climate of his region, ignored evaporation.

The Arlington measurements were considered the best available indication of the annual march of evapotranspiration. Monthly percentages of the annual evapotranspiration during the single year of observations (1939) were smoothed out somewhat for this study. The observed and smoothed percentages are shown in table 3. Some evaporation pan measurements in the southeastern United States showed about the same annual distribution of evaporation. Daily values were obtained by dividing monthly values by 30. The daily energy requirement to produce this evaporation is computed using a value of 590 calories per gram as the latent heat of vaporization.

TABLE 3.—*Monthly and daily evapotranspiration, Nashville, Tenn.*

	Monthly percentage of annual evapotranspiration		Monthly evaporation (inches) [2]	Daily evaporation (inches)	Daily energy requirement (langleys)
	Unsmoothed [1]	Smoothed			
January	3	3	0.6	0.020	30
February	[3] 5	5	1.0	.033	50
March	8	8	1.6	.053	80
April	6	10	2.0	.067	100
May	13	13	2.6	.087	130
June	19	15	3.0	.100	150
July	14	14	2.8	.093	140
August	11	11	2.2	.073	110
September	[3] 8	8	1.6	.053	80
October	5	5	1.0	.033	50
November	3	4	.8	.027	40
December	4	3	.6	.020	30

[1] After Thornthwaite and Holzman [16] [17].
[2] Annual total assumed 20 inches.
[3] Interpolated.

The Arlington data were again used as the standard for the distribution throughout the day of the daily total evapotranspiration with certain necessary substitutions of one month for another. Thornthwaite and Holzman measured the specific humidity and the wind speed at two levels; the evaporation was then computed from the equation,

$$E=0.63\,\frac{k_0^2\,(q_1-q_2)\,(u_2-u_1)}{\left(\ln\frac{z_2}{z_1}\right)^2},$$

where E is the total evaporation in inches over a time interval, k_0 is von Kármán's constant, q_1 and q_2 are the specific humidities at the two levels in grams of moisture per cubic meter of air, u_1 and u_2 are the total wind movement in miles at the lower and upper levels over the time interval, z_2/z_1 is the ratio of the height of the two levels above a reference height h_0. Thornthwaite and Holzman did not publish hourly values of evaporation but rather listed hourly values of specific humidity, temperature, and wind at the different levels, together with monthly means by hours for the months of January and March through August. The percentage of the daily evaporation that occurs in each of the 24 hours of the day was computed by assuming that the evapotranspiration is proportional to the product (q_1-q_2) times (u_2-u_1), the other factors in the equation being constants. The hourly percental distribution of the daily evaporation for January, April, June, and August 1939 obtained in this way (table 4 labeled "1939") were applied to the daily evapotranspiration energy requirements to estimate hourly energy requirements (table 5). The hourly values in tables 4 and 5 do not form a smooth series because values of the wind-speed difference (u_2-u_1) on which they are based were expressed to one significant figure only and did not form a smooth series. Smoothing was introduced when a diurnal curve was plotted.

Another method of estimating hourly distribution of evaporation is based on the assumption that the evaporation is proportional to the difference between the actual vapor pressure and the saturation vapor pressure. The daily distribution of evaporation estimated by this method for Washington in April and June is shown, for comparison, in table 4, under the heading "V. P." The basic data used, hourly temperature and dewpoint normals for Washington, are those published on the back of the Weather Bureau *Daily Weather Map*. It is seen that the vapor pressure method gives a distribution essentially the same as the other method, except in the early night hours when the evaporation has been diminished by a decrease

TABLE 4.—*Hourly percental distribution of daily evaporation, Arlington, Va. 1939 percentages computed from turbulent transport measurements; V. P. (vapor pressure) percentages computed from dewpoints*

Hour ending (EST)	Jan. 1939	April		June		Aug. 1939
		1939	V. P.	1939	V. P.	
a. m.						
1	2.9	2.7	3.0	2.0	2.3	0.5
2	2.6	2.9	2.6	1.9	1.9	0.0
3	2.8	4.2	2.3	1.4	1.9	−0.5
4	0.0	2.6	2.3	1.4	1.5	0.0
5	2.8	1.2	2.1	1.5	1.8	−0.4
6	3.3	2.7	2.0	2.0	1.5	0.0
7	0.0	2.5	2.0	3.2	1.5	0.9
8	2.9	1.4	2.3	4.0	2.2	2.5
9	3.2	1.6	2.6	3.5	2.9	3.8
10	3.2	3.8	3.5	4.8	2.7	5.4
11	3.6	2.0	4.2	5.2	4.9	6.0
12	7.7	6.2	4.7	6.2	5.8	7.8
p. m.						
1	8.0	9.5	5.4	6.7	6.7	7.7
2	4.1	7.7	6.2	8.4	7.2	9.3
3	8.0	6.9	6.6	7.7	7.7	8.4
4	8.2	2.2	7.0	6.8	7.7	11.1
5	8.0	4.1	7.0	6.3	7.7	8.5
6	7.7	4.1	7.0	6.1	6.9	6.7
7	6.1	5.0	6.2	4.7	6.5	5.4
8	3.2	6.7	5.2	4.5	5.2	4.2
9	3.2	4.6	4.8	3.7	4.3	4.7
10	2.9	4.5	4.1	3.6	3.5	2.9
11	2.8	6.5	3.4	2.2	3.5	1.9
12	3.0	4.3	3.1	2.0	2.6	1.4

TABLE 5.—*Hourly evapotranspiration energy requirement, Nashville, Tenn. (unsmoothed estimates)*

Hour ending (local time)	Langleys					
	February [1]	April	June	August	October [2]	December [1]
a. m.						
1	1.4	2.7	3.0	0.6	1.4	0.9
2	1.3	2.9	2.8	0.0	1.5	0.8
3	1.4	4.2	2.1	−0.6	2.1	0.8
4	0.0	2.6	2.1	0.0	1.3	0.0
5	1.4	1.2	2.2	−0.4	0.6	0.8
6	1.6	2.7	3.0	0.0	1.4	1.0
7	0.0	2.5	4.8	1.0	1.2	0.0
8	1.4	1.4	6.0	2.7	0.7	0.9
9	1.6	1.6	6.2	4.2	0.8	1.0
10	1.6	3.8	7.2	5.9	1.9	1.0
11	1.8	2.0	7.8	6.6	1.0	1.1
12	3.8	6.2	9.3	8.6	3.1	2.3
p. m.						
1	4.0	9.5	10.0	8.5	4.8	2.4
2	2.0	7.7	12.6	10.2	3.8	1.2
3	4.0	6.9	11.6	9.2	3.5	2.4
4	4.1	2.2	10.2	12.2	1.1	2.5
5	4.0	4.1	9.4	9.3	2.0	2.4
6	3.8	4.1	9.2	7.4	2.0	2.3
7	3.0	5.0	7.0	5.9	2.5	1.8
8	1.6	6.7	6.8	4.6	3.4	1.0
9	1.6	4.6	5.6	5.2	2.3	1.0
10	1.4	4.5	5.4	3.2	2.2	0.9
11	1.4	6.5	3.3	2.1	3.2	0.8
12	1.5	4.3	3.0	1.5	2.2	0.9

[1] Derived from January hourly distribution (table 4).
[2] Derived from April hourly distribution (table 4).

in the wind velocity while the vapor pressure difference is still relatively high. Thornthwaite and Holzman's evaporation measurement site was on the outskirts of Washington.

Heat Balance Diagram.—Local heat balance diagrams for alternate months from February through December (figs. 1–6) were constructed from the data described above and are a graphical portrayal of equation (4). The various curves on these figures show, for the 15th day of each month, the diurnal progression of insolation I_0 (from table 1), the reflection of a portion of the insolation RI_0 (20 percent), the net outgoing long-wave radiation from the top of the diurnally heated layer B_s (table 2), the heat used in evaporation of water from ground and plant surfaces LE (table 5), the energy used to warm the ground or given up by cooling ground S, and finally, the heat H entering the air and raising its temperature or given up by the air as it cools. The air curve is constructed by adding together algebraically at each hour the ordinates of all the other curves, that is, by performing the operation indicated by equation (4). The air curves depict estimates of climatological values of the heating or cooling of air at Nashville in clear weather. The amount of heat that should be added to the lower end of a raob to predict a later maximum temperature is obtained by integrating the area under the curve between the hours of the raob and the expected maximum temperature. (In this procedure the net area below the zero line is subtracted from the net area above the zero line.) Integrating under the entire air curve gives the net daily clear-weather heating; that is, the excess of a day's sunshine over the energy-dissipating processes for 24 hours.

3. HEATING AND COOLING VALUES FROM RAOBS

Values of clear-weather heating and cooling at Nashville were obtained by comparing successive temperature soundings. In addition to the twice-daily raobs a hypothetical midafternoon sounding was constructed by running a dry adiabat from the maximum temperature for the day up to the intersection with the previously observed temperature curve. The apparent heating or cooling from one temperature sounding to the next was measured on an adiabatic chart and converted to calories in a vertical column of 1 square centimeter cross section. This was done for all instances of cloudless sky during a 21-month period.

Definition of periods of the day.—The 24-hour day was divided into three parts: from the time of morning raob to time of maximum afternoon temperature, approximately 0915 to 1600 CST, called the "day" period; from the time of afternoon maximum temperature to the time of the night raob, approximately 1600 to 2115 CST, called the "evening" period; and from night raob to morning raob, approximately 2115 to 0915 CST, termed the "night" period.

Heating for day period.—The clear-weather days from January 1945 through September 1946 were selected by inspection of 3-hourly surface weather maps, with the following requirement: One-tenth or less of sky covered by cirrus or altocumulus, otherwise no clouds, at 0630, 0930, 1230, and 1530 CST. An original criterion of 100 percent sunshine by triple register measurement was rejected as it was found that thin cloudiness could appreciably reduce the daily insolation even with reported 100 percent sunshine. The morning (0915 CST) raobs together with a dry adiabat through the afternoon maximum temperature were plotted on adiabatic charts for 54 clear days. The maximum temperature was plotted at the surface pressure of the morning raob. The area on the

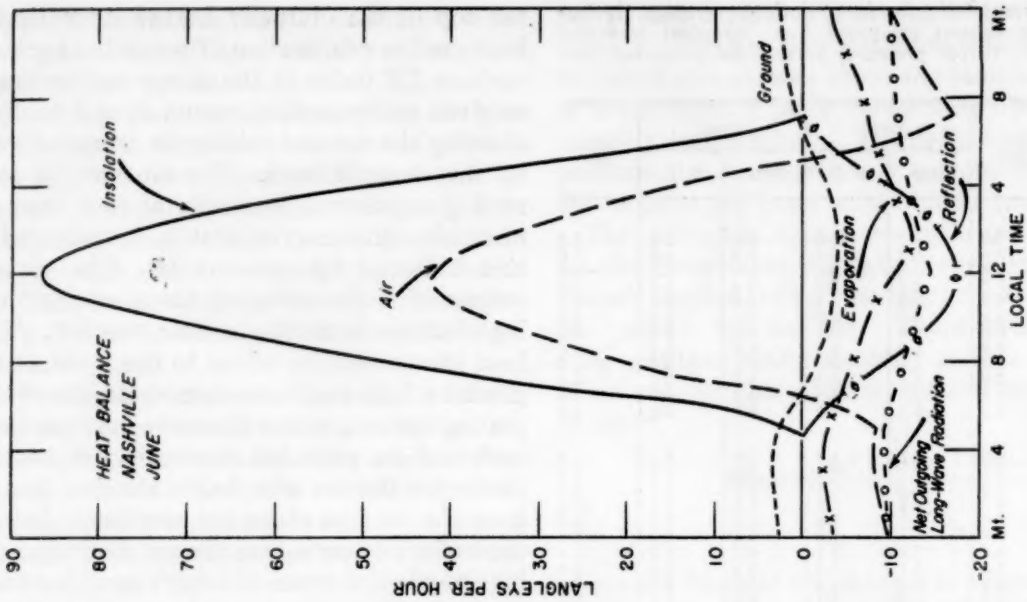

FIGURE 3.—Heat balance diagram for Nashville for June.

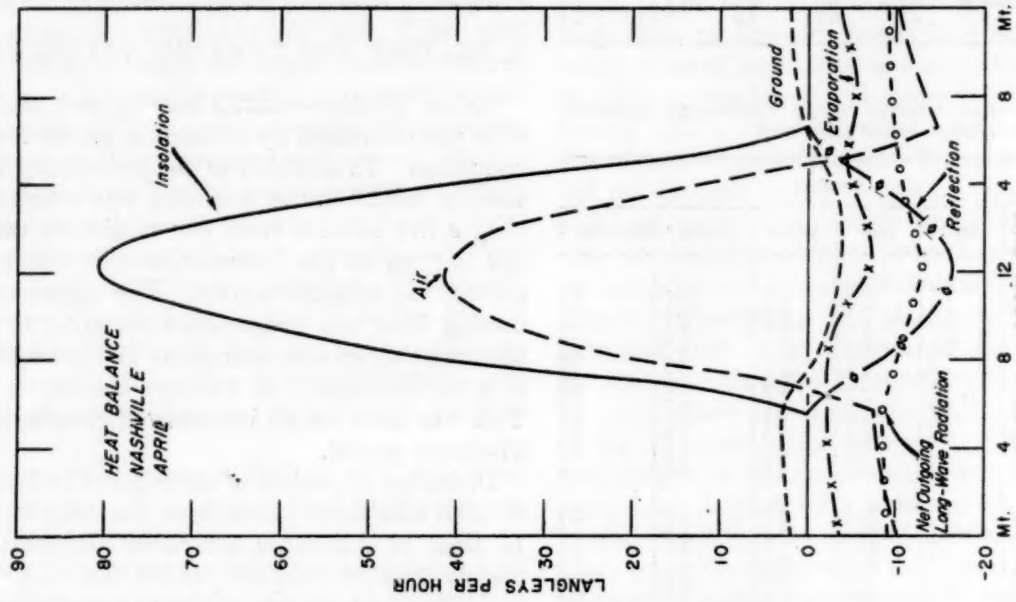

FIGURE 2.—Heat balance diagram for Nashville for April.

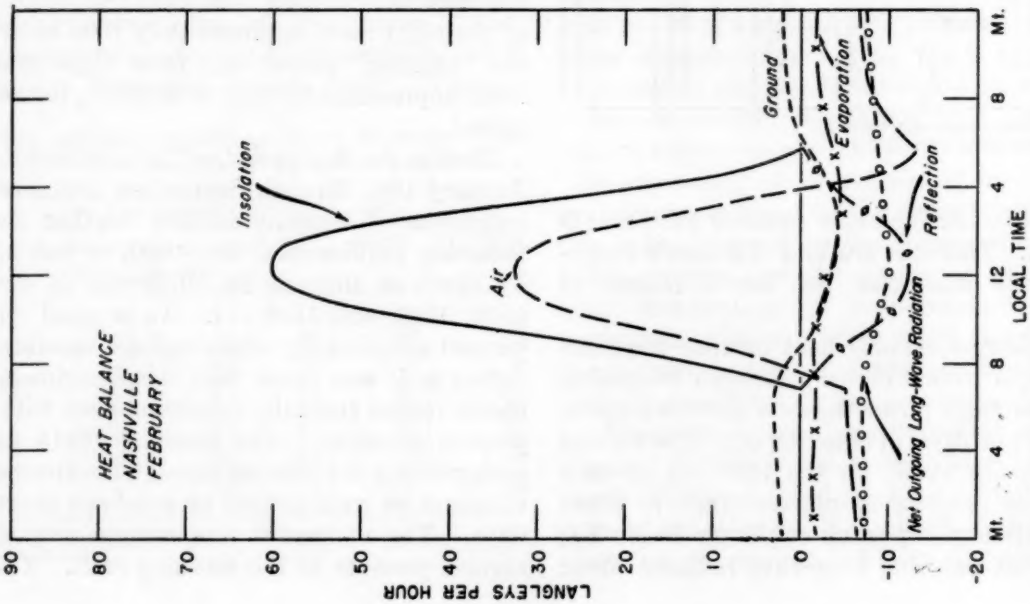

FIGURE 1.—Heat balance diagram for Nashville for February.

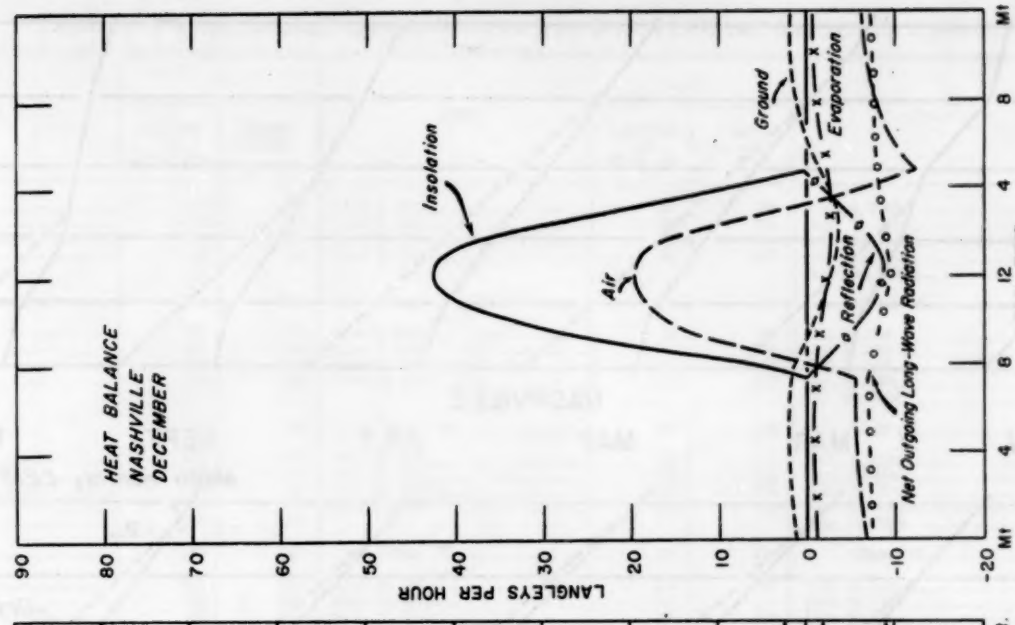

FIGURE 6.—Heat balance diagram for Nashville for December.

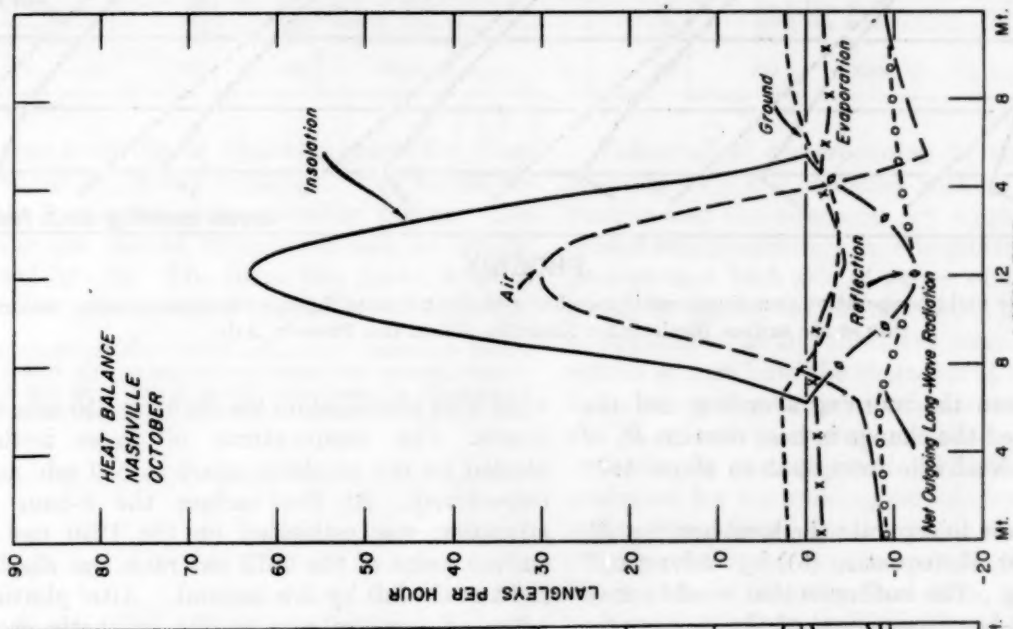

FIGURE 5.—Heat balance diagram for Nashville for October.

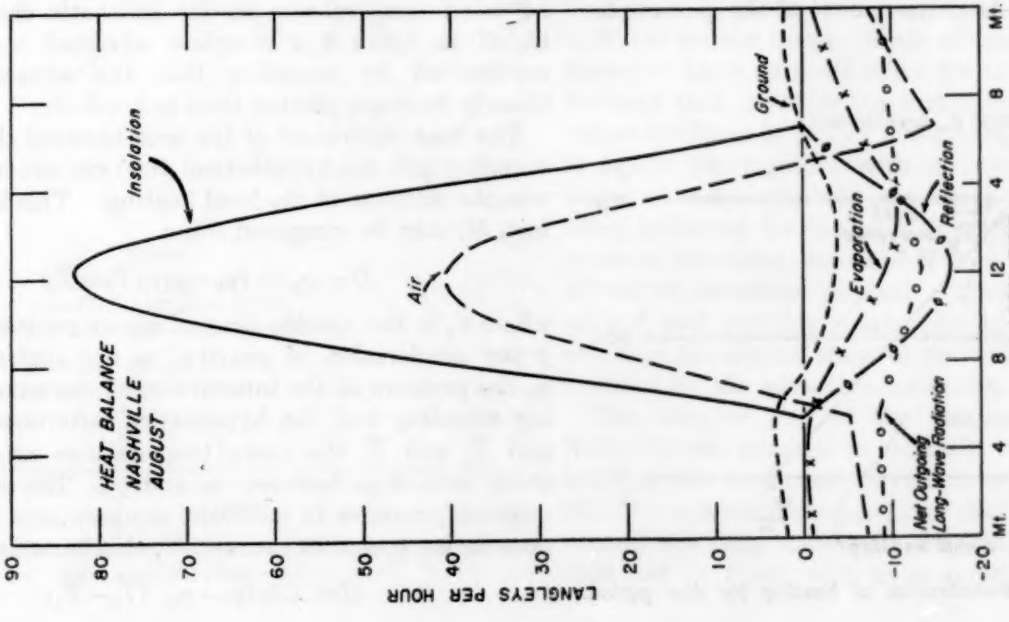

FIGURE 4.—Heat balance diagram for Nashville for August.

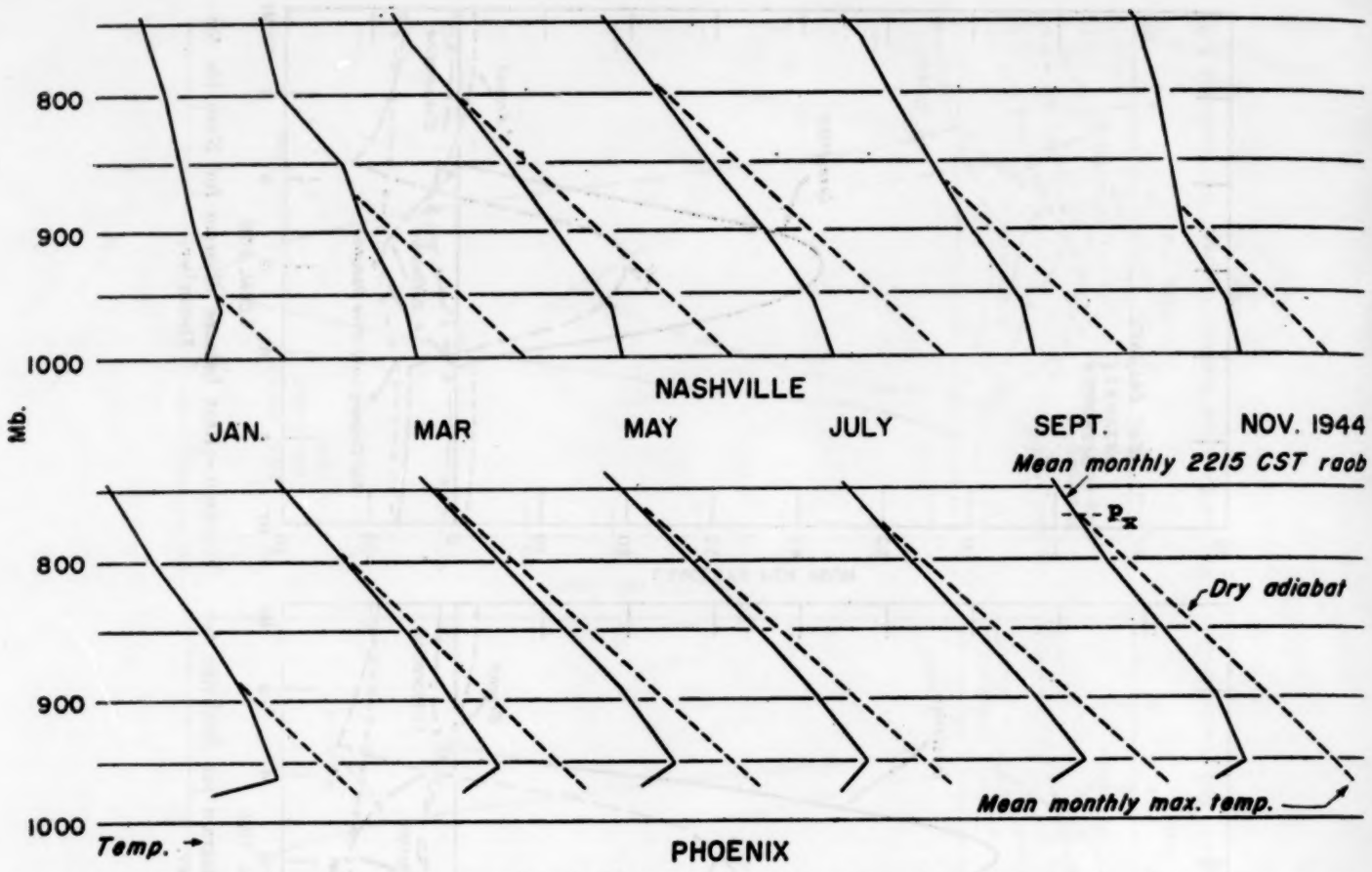

FIGURE 7.—Mean monthly night temperature soundings (solid) together with dry adiabats through the mean monthly maximum temperature at the surface (dashed) for Nashville, Tenn. and Phoenix, Ariz.

adiabatic chart between the morning sounding and the dry adiabat represented the change in heat content H_a of the column of air at Nashville from 0915 to about 1600 CST.

An attempt was made to separate the local heating, H, from the advected heat, A, (equation (3)) by "advecting" the 0915 CST sounding. The isotherms that would arrive over Nashville by a 6-hour movement of the geostrophic wind were identified on the 0915 CST 850-mb. and 700-mb. charts. The temperatures of these isotherms were plotted on the adiabatic chart at 850 mb. and 700 mb., respectively. At the surface the 6-hour geostrophic advection was estimated on the 1230 CST map. The surface point of the 0915 CST raob was displaced to the right or the left by this amount. After plotting the three advected temperatures on the adiabatic chart as illustrated in figure 8 a complete advected sounding was constructed by assuming that the advection varied linearly from one plotted level to another.

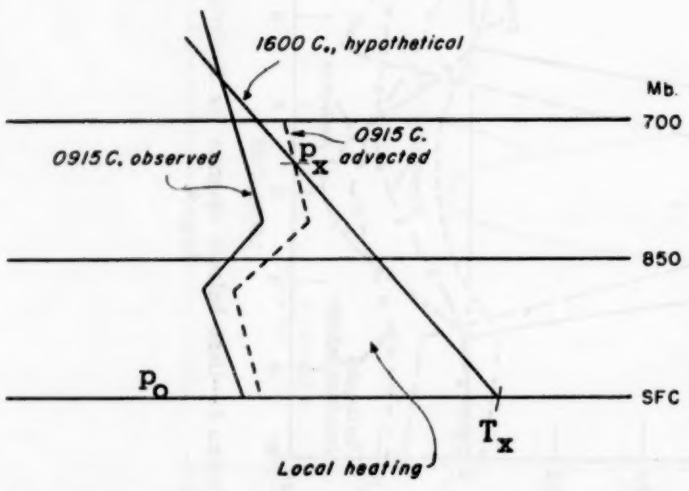

FIGURE 8.—Graphical determination of heating for day period.

The heat equivalent of the area between the advected sounding and the hypothetical 1600 CST sounding (fig. 8) was the estimate of the local heating. This heat equivalent, H, may be computed from:

$$H=(c_p/g)\ (p_0-p_z)\ (\overline{T}_z-\overline{T}_1) \qquad (5)$$

where c_p is the specific heat of air at constant pressure, g the acceleration of gravity, p_0 the surface pressure, p_z the pressure at the intersection of the advected morning sounding and the hypothetical afternoon sounding, and $\overline{T}_z$ and $\overline{T}_1$ the mean temperatures respectively of those soundings between p_0 and p_z. Expressing H in calories, pressures in millibars, temperatures in ° C. and considering g as 1000 cm. sec. $^{-2}$, this becomes:

$$H=.239\ (p_0-p_z)\ (\overline{T}_z-\overline{T}_1) \qquad (6)$$

TABLE 6.—*The heat (langleys) absorbed by the air from 0915 to 1600 CST, (day period), Nashville, Tenn.*

Date	H	
	Adjusted for advection	Unadjusted
Jan. 5, 1945	90	165
Jan. 10, 1945	98	140
Jan. 11, 1945	115	160
Jan. 26, 1945	151	115
Mean: 13	114	148
Jan. 31, 1945	177	115
Feb. 1, 1946	139	235
Feb. 2, 1946	108	175
Feb. 20, 1946	172	140
Mean: 6	150	166
Mar. 3, 1946	171	240
Mar. 22, 1945	176	210
Mar. 27, 1945	92	110
Mar. 31, 1946	254	215
Apr. 5, 1946	219	200
Mean: 24	182	195
Apr. 5, 1945	251	220
Apr. 13, 1946	144	185
Apr. 18, 1946	196	196
Apr. 19, 1945	141	210
Apr. 19, 1946	197	220
Mean: 15	186	206
May 5, 1946	227	227
May 8, 1945	254	160
May 22, 1946	196	196
May 23, 1945	231	160
Mean: 14	228	156
June 4, 1946	194	180
June 5, 1946	237	200
June 6, 1946	107	140
June 23, 1946	305	270
Mean: 10	211	220
July 16, 1945	157	120
July 22, 1944	333	333
July 23, 1946	176	176
July 26, 1946	199	120
Mean: 22	216	157
Aug. 18, 1945	204	195
Aug. 26, 1945	251	195
Aug. 27, 1945	190	200
Aug. 27, 1946	189	200
Aug. 31, 1946	224	250
Mean: 26	212	188
Sept. 3, 1945	226	205
Sept. 11, 1946	149	140
Sept. 25, 1946	155	155
Sept. 26, 1946	168	168
Sept. 30, 1946	172	120
Mean: 19	174	158
Oct. 2, 1946	220	200
Oct. 3, 1946	219	200
Oct. 4, 1946	181	160
Oct. 5, 1946	268	250
Oct. 26, 1945	192	145
Mean: 8	216	191
Nov. 5, 1945	117	170
Nov. 15, 1945	208	208
Nov. 20, 1945	86	105
Nov. 24, 1945	57	130
Nov. 29, 1946	138	125
Mean: 19	121	148
Dec. 12, 1945	179	160
Dec. 16, 1945	145	190
Dec. 20, 1945	48	100
Dec. 21, 1945	80	80
Mean: 17	113	132

H was evaluated from the 54 adiabatic charts for clear-weather days from the above equation. The values are listed in table 6 together with monthly means. The monthly means are plotted in figure 9 and an annual curve was fitted by eye. The curve was drawn so as to be symmetrical about the summer solstice on June 22.[3]

[3] Making the curve symmetrical about June 22 was a practical expedient for fitting a curve to the data. It is by no means certain that it should be symmetrical. Possibly the curve should have been drawn closer to the high point for October. Dryer ground at that season would in part lead to a higher value of H than at the corresponding time in early spring.

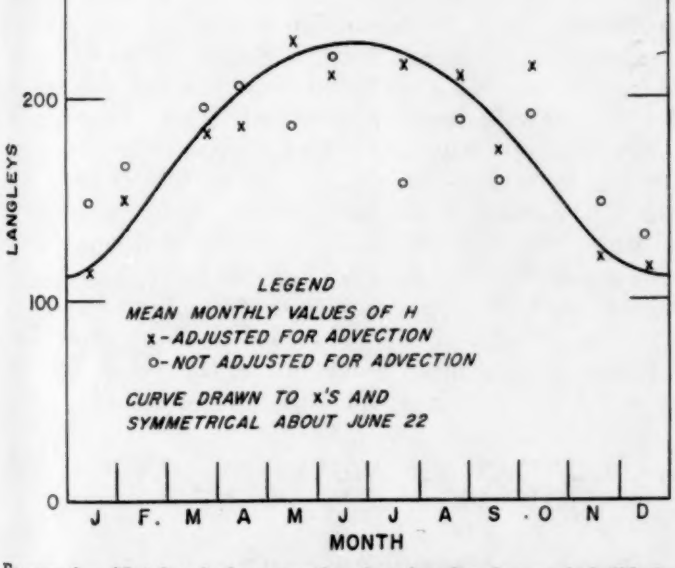

FIGURE 9.—Net local clear weather heating for day period (0915–1600 CST) for Nashville.

Values of H corresponding to the area between the morning 0915 CST sounding without adjustment for advection and the afternoon dry adiabat are also listed in table 6 and the monthly means plotted in figure 9. It can be seen that both sets of values of H fit the same curve except in winter, indicating that in general the net effect of application of the advective correction is small. This results in part from the character of the sample, cloudless days; on many of these Nashville was near the center of a High, where light winds prevailed.

Cooling for evening period.—The heat equivalent H, was evaluated for the evening period, from the time of maximum temperature to the 2115 CST raob, by methods strictly analogous to those used for the day period. There were 57 clear-weather cases, selected on the basis of lack of cloudiness at Nashville on the 1530, 1830, and 2130 CST surface maps. Since advective corrections were shown to have no great effect for the day period, it was assumed that $A=0$ for the first evaluation of H. These values are listed in table 7 and monthly means are plotted in figure 10, together with an eye-fitted curve. The shape of this curve was surprising, the greatest cooling being indicated for the months of longest daylight. To check on the curve, values of H were recomputed with the advective correction applied. These are also listed in table 7 and monthly means plotted in figure 10. It is seen that the original shape of the curve was not materially modified by the advective correction.

The time of day of the maximum temperature at Nashville was checked to ascertain whether any seasonal trend in this time could have affected the curve of figure 10. It was found during one year that the monthly average time of the daily maximum temperature varied between 1545 and 1612 CST, with no systematic seasonal progres-

TABLE 7.—*The heat (langleys) released by the air from 1600 to 2115 CST. (evening period) Nashville, Tenn.*

Date	H	
	Adjusted for advection	Unadjusted
Jan. 1, 1946	64	80
Jan. 4, 1946	90	35
Jan. 17, 1946	75	55
Jan. 27, 1946	34	34
Jan. 31, 1946	65	155
Mean: 16	66	72
Feb. 1, 1946	78	75
Feb. 2, 1946	88	40
Feb. 6, 1946	38	100
Feb. 23, 1945	40	40
Mean: 8	61	64
Mar. 2, 1946	164	40
Mar. 11, 1946	72	35
Mar. 20, 1946	52	50
Mar. 30, 1946	141	100
Apr. 2, 1946	139	155
Mean: 19	114	76
Apr. 4, 1946	30	180
Apr. 12, 1946	37	75
Apr. 17, 1946	78	80
Apr. 18, 1946	96	95
Apr. 19, 1946	106	95
Mean: 14	69	105
May 18, 1946	144	105
May 20, 1945	96	60
May 22, 1945	94	155
May 22, 1946	144	115
May 23, 1945	143	110
Mean: 21	124	109
June 4, 1946	182	220
June 5, 1946	162	170
June 6, 1946	169	55
June 7, 1946	164	105
June 21, 1946	192	155
Mean: 9	174	141
June 23, 1946	293	290
July 6, 1946	111	110
July 16, 1945	138	145
July 22, 1944	229	230
July 26, 1946	172	205
Mean: 13	189	196
Aug. 26, 1946	201	200
Aug. 27, 1945	72	72
Aug. 30, 1946	176	205
Aug. 31, 1945	176	175
Mean: 28	125	163
Sept. 11, 1945	123	160
Sept. 11, 1946	158	175
Sept. 25, 1946	108	140
Sept. 26, 1946	155	155
Sept. 30, 1946	113	130
Mean: 21	131	133
Oct. 2, 1946	214	205
Oct. 3, 1946	152	155
Oct. 4, 1946	171	180
Oct. 5, 1946	184	195
Oct. 16, 1945	61	85
Mean: 8	156	166
Nov. 5, 1945	93	65
Nov. 14, 1945	62	60
Nov. 15, 1945	84	55
Nov. 24, 1945	72	25
Mean: 14	78	61
Dec. 7, 1945	23	35
Dec. 16, 1945	105	95
Dec. 20, 1945	35	30
Dec. 22, 1946	35	25
Dec. 26, 1945	73	85
Mean: 18	54	54

sion. (Days with maximum temperature before 1 p. m. or after sunset were excluded.) The time of maximum temperature on the specific days for which H was evaluated was also examined and no seasonal trend found.

Cooling for night period.—The heat equivalent H, was evaluated for 58 clear-weather periods between the 2115 and 0915 CST raobs. A pressure surface had to be designated as the top of the layer in which H would be computed. This was placed at 850 mb., corresponding to the 1.5-km. level for which B_a was computed.

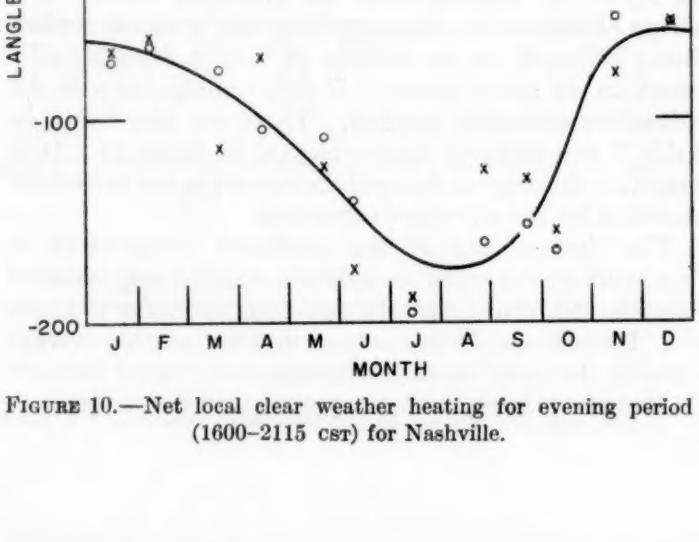

FIGURE 10.—Net local clear weather heating for evening period (1600–2115 CST) for Nashville.

Advective corrections were determined for the night period by assuming that the observed change in temperature at 850 mb. from one raob to the next was all due to advection and that the magnitude of the advection was constant from the ground up to this level. H could then be computed from the following simplification of equation (6):

$$H=(.239)(150)(\overline{T}_1-\overline{T}_2-\Delta T_a) \qquad (7)$$

where $\overline{T}_1$ is the mean temperature between the surface and 850 mb. at 2115 CST, $\overline{T}_2$ the mean temperature at 0915 CST and ΔT_a the change in temperature at 850 mb. over this period (all in ° C.). In equation (6) (p_0-p_x) is set equal to 150 mb., the slight fluctuation of the Nashville surface pressure about 1000 mb. being neglected. The values of H from equation (7) are listed in table 8 and plotted in figure 11, together with an eye-fitted curve.

Several more complex ways of applying the advective corrections were experimented with to find if they improved the scatter of the values of H. None appeared to be superior to the simple method used and some were inferior. These other methods included geostrophic advection of the observed mean surface-to-850-mb. temperature, mean of geostrophic advection on the initial and final 850-mb. charts, mean temperatures advected by the observed 3000-ft. winds, and variations of these.

4. COMPARISON OF VALUES OF HEATING AND COOLING BY THE TWO METHODS

Values of the heating or cooling during the day, evening, and night periods by the heat-balance method were obtained by planimetering the area under the air curve

TABLE 8.—*The heat (langleys) absorbed by the air from 2115 to 0915 CST, (night period) Nashville, Tenn. Advective corrections included in computation of H*

Date	H	Date	H	Date	H
Jan. 5, 1945	4	May 6, 1945	4	Sept. 3, 1945	0
Jan 11, 1945	−132	May 22, 1946	−4	Sept. 4, 1945	0
Jan. 24, 1945	−75	May 23, 1945	−25	Sept. 5, 1946	11
Jan. 31, 1945	−18	May 24, 1945	−14	Sept. 13, 1946	−14
		May 29, 1946	−47	Sept. 27, 1946	64
Mean: 18	−55	Mean: 21	−17	Mean: 10	12
Feb. 2, 1946	−32	June 4, 1946	−72	Oct. 1, 1946	−21
Feb. 15, 1945	−111	June 5, 1946	11	Oct. 2, 1946	−18
Feb. 23, 1945	−25	June 7, 1946	72	Oct 3, 1946	47
Feb. 24, 1945	−36	June 8, 1946	58	Oct. 4, 1946	−4
Mar. 1, 1946	50	June 9, 1946	0	Oct. 13, 1946	−18
Mean: 19	−31	Mean: 7	14	Mean: 5	−3
Mar. 3, 1946	−61	June 23, 1946	14	Nov. 5, 1945	−107
Mar. 9, 1945	18	July 16, 1945	−29	Nov. 15, 1945	−125
Mar. 12, 1946	4	July 16, 1946	−29	Nov. 16, 1945	4
Mar. 27, 1945	−11	July 17, 1945	104	Nov. 24, 1945	−89
Mar. 28, 1945	−21	July 23, 1946	−82	Nov. 26, 1945	−50
Mean: 16	−14	Mean: 13	−4	Mean: 17	−73
Apr. 3, 1946	−50	Aug. 27, 1946	−25	Dec. 8, 1945	−68
Apr. 5, 1946	−72	Aug. 28, 1945	−4	Dec. 21, 1945	−39
Apr. 7, 1945	−25	Aug. 29, 1945	25	Dec. 22, 1946	21
Apr. 18, 1946	18	Aug. 31, 1945	11	Dec. 23, 1946	14
Apr. 19, 1946	−18	Aug. 31, 1946	21		
Mean: 10	−29	Mean: 29	6	Mean: 18	−18

in figures 1 to 6 between the hours of 0915 and 1600 CST, 1600 and 2115 CST, and 2115 and 0915 CST. These are compared with the curves for H from raobs in figure 12. The correspondence between the two curves for the night and the day periods is gratifyingly close; for the evening period the difference is surprisingly great.[4]

Difference in placement of the top of the layer from which the cooling was computed was eliminated as an important cause of the disparity between the two evening period curves. The long-wave radiational loss for the heat-balance diagrams was computed at the 1.5-km. surface. The top of the cooled layer on the adiabatic charts for the evening period, was frequently at a higher elevation than 1.5 km. To determine the order of magnitude of additional upward long-wave radiation from moist layers above 1.5 km., the flux for the mean June 1945 sounding was computed through the 3-km. surface on the Elsasser chart. The comparative data are:

Flux through 1.5-km. surface.. 29 ly/3 hr.
Flux through 3-km. surface.. 35 ly/3 hr.

It is seen that the additional increment of radiational flux between 1.5 and 3 km. over a 6-hour period would rarely exceed about 12 langleys, only a fraction of the discrepancy between the two evening period H curves.

If the lapse rate at the time of maximum temperature were appreciably superadiabatic the effect of assuming an adiabatic lapse rate in this study would be to exaggerate both the cooling during the evening period and the heating during the day period. Improvement of the correspondence of the curves of figure 12b by constructing superadiabatic lapse rates would be at the expense of the good fit of the curves of figure 12a.

[4] It is perhaps worth placing in the record that the H curves from raobs in figures 8, 9, and 11, which are subjectively drawn to scattered data, were constructed *before* the more objective corresponding heat-balance curves, with no prior knowledge of what the shape or level of the heat-balance curves would be.

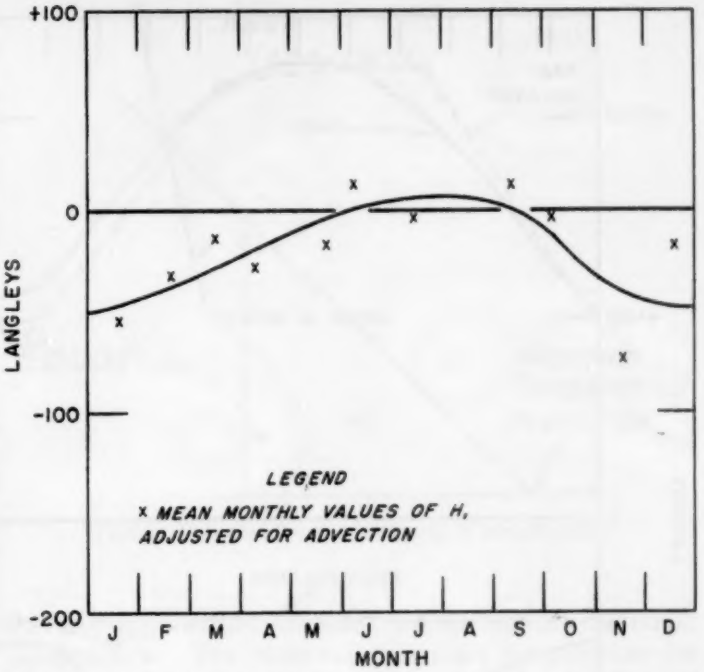

FIGURE 11.—Net local clear weather heating for night period (2115–0915 CST) for Nashville.

Another factor to take into account is that the heat-balance curve of figure 12b is for mean soundings while the raob curve is for selected clear-weather cases. It is reasonable to suppose that the mean moisture content would be lower for the latter than for the overall mean. The net upward long-wave radiation, B_a, could be greater for the drier cases because of less return downward radiation from above the level where B_a was determined.

None of the foregoing seems to be a fully adequate explanation of the discrepancy of figure 12b. Resolving the discrepancy awaits more data of this nature from other investigators.

5. MAXIMUM TEMPERATURE FORECASTS

Values of H for maximum temperature forecast.—The idea with which this investigation started was to develop values of the heating area to add to the night raob for predicting the maximum temperature the next afternoon. This value is the sum of H for the night period and for the day period. Curves of this sum are shown in figure 12. Lacking a reason for choosing one curve over the other, the average of the two curves (dashed on the figure) was selected for forecasting. The heat H (in langleys) read from the curve for a particular date is converted to a triangular area on the adiabatic chart by use of equation (6) converted to the form:

$$H=.239\Delta p(\Delta T/2) \tag{8}$$

Δp and ΔT are the legs of a triangle on the adiabatic chart as shown in figure 13, scaled in millibars and ° C. respectively. Another equation in Δp and ΔT is:

$$\Delta p=K\Delta T \tag{9}$$

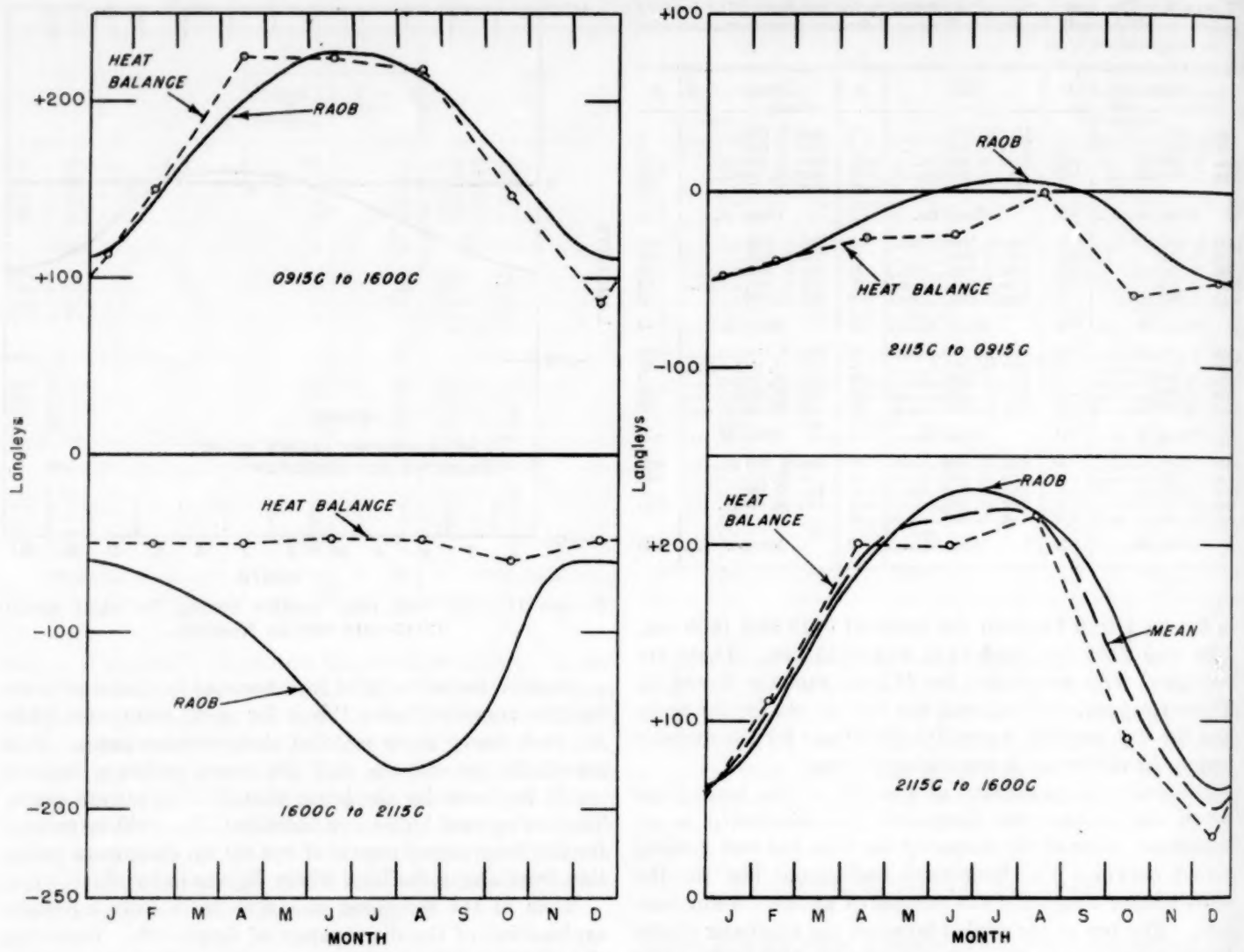

FIGURE 12.—Heating or cooling of air in clear weather, Nashville. Curves marked "heat balance" were obtained by planimetering the area under the air curve in figures 1–6.

K is evaluated by constructing any triangle similar to the one in figure 13 in the region of the adiabatic chart to be used, and depends on the slope of the dry adiabats. Solving the simultaneous equations (8) and (9) yields specific values of Δp and ΔT for laying out the triangle of the desired area corresponding to H. This may be done on a transparent overlay. The H area is then added graphically to the raob temperature curve to obtain the maximum temperature forecast in the familiar manner shown in figure 14. A permanent transparent overlay may be constructed on which various H values are represented by triangles having two sides coincident and the third side as a family of parallel lines labeled with the H values.

Test of forecasting curve.—The mean curve of the lower right panel of figure 12 was applied to forecasting the maximum temperature at Nashville from the raob of the night before for each day from March 1 through November 30, 1954. The winter months were omitted so as not to confound the results with too many days when the radiative balance was relatively unimportant as compared with advection. These were after-the-fact forecasts but were made in a strictly objective manner. Two departures from field forecast conditions were permitted so as not to introduce subjective elements. First, no adjustment was made for advection. Second, observed cloudiness instead of forecast cloudiness was used in making an allowance for reduction of insolation. Completely cloudless days are few in number. The intent in designing this test was not only to obtain an idea of the forecast accuracy for near-cloudless days but also an idea of the amount of cloudiness that could be tolerated in applying this technique. Therefore, a forecast was made for every day during the forecast period. It turned out that on the average the forecast errors for cloudy days were not appreciably larger than for clear days. Therefore all days were included in the final verification statistics.

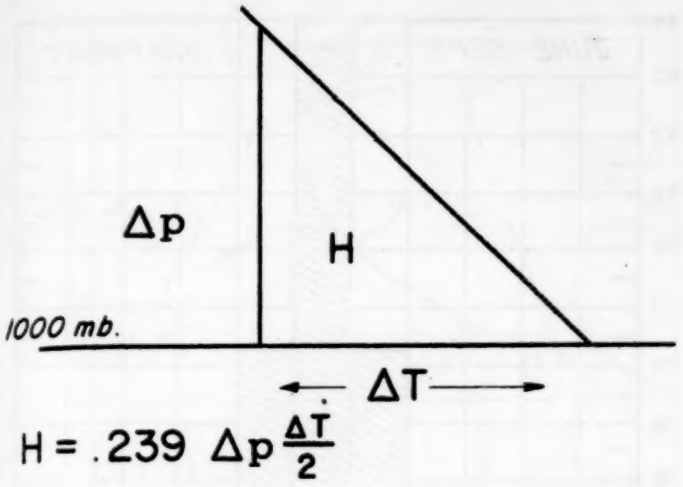

FIGURE 13.—Laying out area corresponding to H on an adiabatic chart.

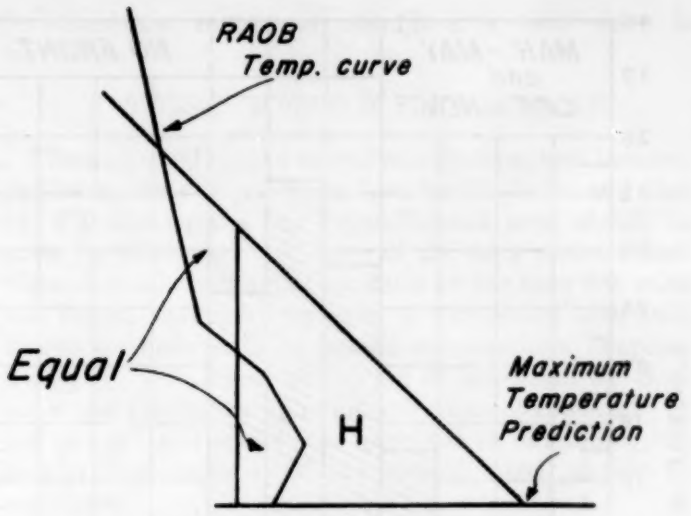

FIGURE 14.—Graphical addition of H area to raob.

Steps in each verification forecast were:

(a) Clear-weather H read off mean curve of figure 12 for particular date.

(b) Kind and amount of cloudiness at Nashville at 1200 CST noted from surface observation form (WBAN 10B). Using the cloudiness from a single observation during the forecast period as representative of the whole period is somewhat comparable in reliability to a cloudiness forecast, when changes during the period would be considered.

(c) Values of H reduced for cloudiness on the following scale:

Overcast	Percent transmission of sunshine
Cirrus	84
Cirrocumulus	78
Altocumulus	50
Altostratus	41
Cumulus	25
Stratocumulus	25

These values are given by Haurwitz [5]. He cautions against application to partial sky covers because of reflection from sides of clouds and other effects. Nonetheless for simplicity proportionate allowances were made for fractional sky covers. For example, one-tenth of altocumulus is considered to reduce H 5 percent. Strict logic would require that the insolation and not H be reduced for cloudiness, and also that the net outgoing long-wave radiation should be diminished. However, the simple correction indicated above was considered adequate for present purposes of approximating field forecast conditions.

(d) Triangle laid out as in figure 13 corresponding in area to the adjusted H.

(e) Area added graphically to the bottom of the 2200 CST raob and the maximum temperature read off. Plots on adiabatic charts prepared daily by the National Weather Analysis Center from teletypewriter data were used for this purpose.

(f) Forecast error determined by subtracting the observed maximum temperature from the forecast maximum temperature. The observed maximum temperature for the day, midnight to midnight, was used regardless of the time of day it occurred.

Monthly mean forecast errors are shown in table 9. These are separated into two classes depending on whether or not a front, either warm or cold, passed Nashville during the forecast period. Frontal passages were identified on 3-hour Analysis Center surface charts. If a front was approaching Nashville on one chart but was frontolized on the next chart, it was not counted as a frontal passage.

The forecast errors were separated into four groups: cold season without frontal passage at Nashville during forecast period (March–May and October–November), warm season without frontal passage (June–September), cold-front passage during forecast period (all months), and warm-front passage (all months). The separate frequency distributions are shown in figure 15. The bars are for class intervals of 3° F. centered on the number indicated. The frequency distributions show an encouraging degree of reliability in the forecasts. Forty-two of 98 warm-season forecasts without frontal passages had an error between −1° F. and +1° F. This frequency distribution is quite symmetrical, indicating lack of bias of the warm-season portion of the H curve toward values

TABLE 9.—*Mean monthly errors in daily maximum temperature forecasts (°F.) Nashville, Tenn. Number of forecasts in parenthesis*

Month (1954)	Days without frontal passages	Days with frontal passages
March	4.6 (24)	11.4 (7)
April	3.3 (21)	6.9 (9)
May	3.0 (23)	4.2 (8)
June	2.4 (26)	7.5 (4)
July	1.6 (25)	4.7 (6)
August	3.0 (23)	7.6 (8)
September	2.6 (25)	7.2 (4)
October	2.8 (26)	8.0 (4)
November	3.7 (22)	3.4 (8)

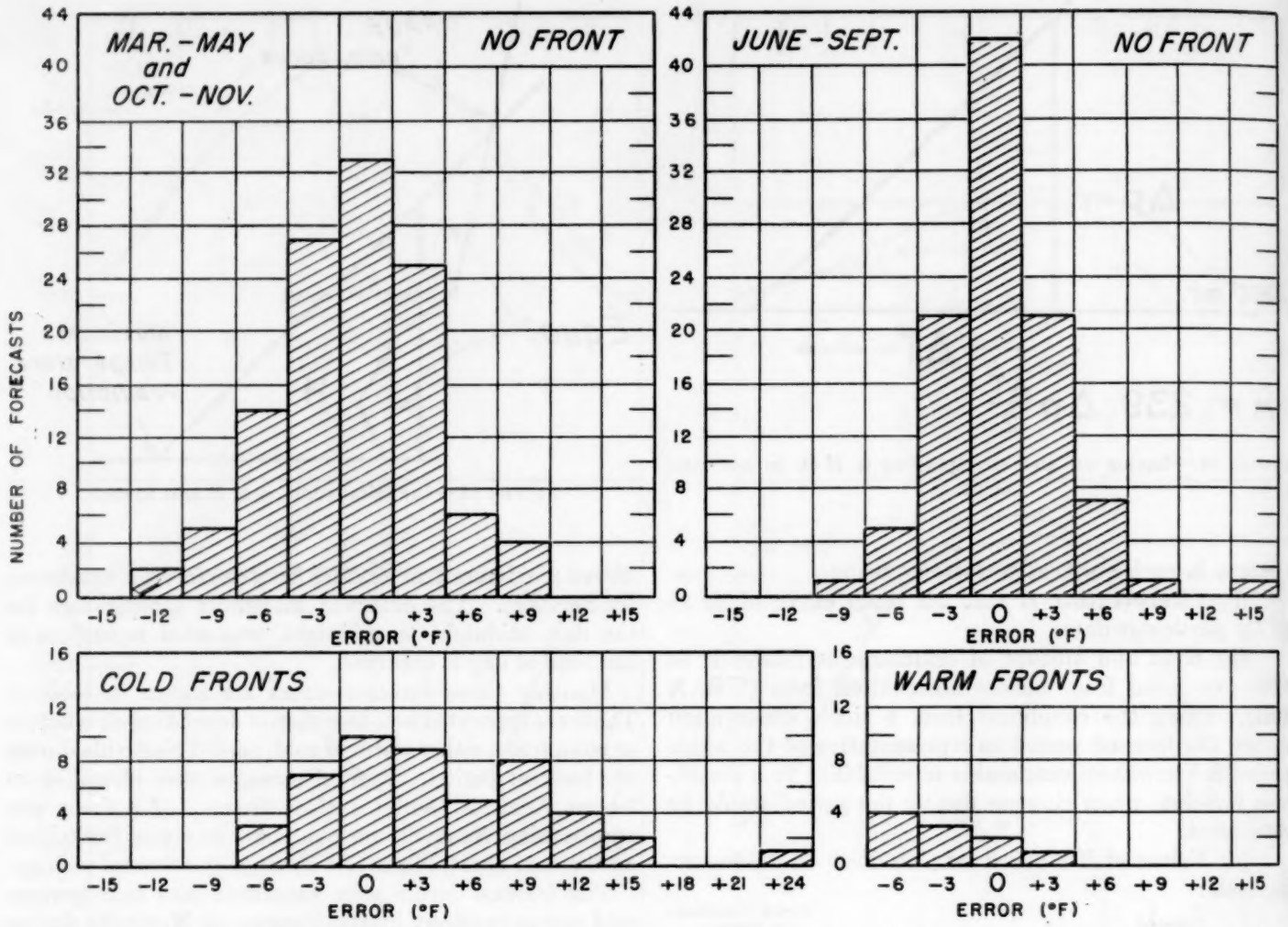
MAR.-MAY and OCT.-NOV.
NO FRONT
JUNE-SEPT.
NO FRONT
COLD FRONTS
WARM FRONTS
NUMBER OF FORECASTS
ERROR (°F)
-15 -12 -9 -6 -3 0 +3 +6 +9 +12 +15
-15 -12 -9 -6 -3 0 +3 +6 +9 +12 +15
-15 -12 -9 -6 -3 0 +3 +6 +9 +12 +15 +18 +21 +24
-6 -3 0 +3 +6 +9 +12 +15

FIGURE 15.—Frequency distributions of errors in Nashville maximum temperature forecasts made using the curve labeled "mean" in lower right panel of figure 12. March through November 1954.

too high or too low. For the cold-season forecasts without frontal passages 33 of 116 forecasts were in the $-1°$ to $+1°$ class interval. That frequency distribution shows a slight skewness toward forecasts that are too low. This could be due to bias in the forecast curve, or possibly to warm advection exceeding cold advection on days of no frontal passages rather than canceling it out. The distributions on days of frontal passage are skewed in the directions one would expect.

Practical application to forecasting.—For a number of years the method described in this paper has been used in conjunction with other methods for maximum temperature forecasts prepared by the Weather Bureau Office at Knoxville, Tenn., for Knoxville and other cities. This is described by Kleinsasser and Younkin [10]. The practice is to predict the clear-weather maximum temperature from the 2200 CST raobs at all raob stations in and around the forecast area and to plot these values on a map. Isopleths of equal values are constructed. The forecaster then makes a subjective allowance for advection and for cloudiness. He also learns to make local allowances for particular stations that are consistently warmer or colder than neighboring stations.

6. NET DAILY HEATING

The net daily local heating of the air at Nashville in clear weather is obtained by adding together the H values for the day, evening, and night periods. Annual curves of these sums are shown in figure 16. Both curves clearly indicate that the net daily heating of the air in clear weather at the latitude of Nashville (36° N.) is sizable, except for a brief period in midwinter. In summer the net daily heating, if restricted to the lower 5,000 feet of the atmosphere, would produce a rise in temperature from 2° to more than 4° C. each day in clear weather. (In a column extending to 5,000 feet a 1° C. mean temperature rise is produced by each 36 langleys added.)

These curves suggest the following conclusions. First, a major factor in warming southward-moving air masses is the greater sunshine at lower latitudes. The heat storage of the ground is minor by comparison. Second, in summer nature invokes certain heat controls which prevent the temperature from rising indefinitely. These operate somewhat as follows: As the surface layers of air become warmer and warmer, the heating is convected to

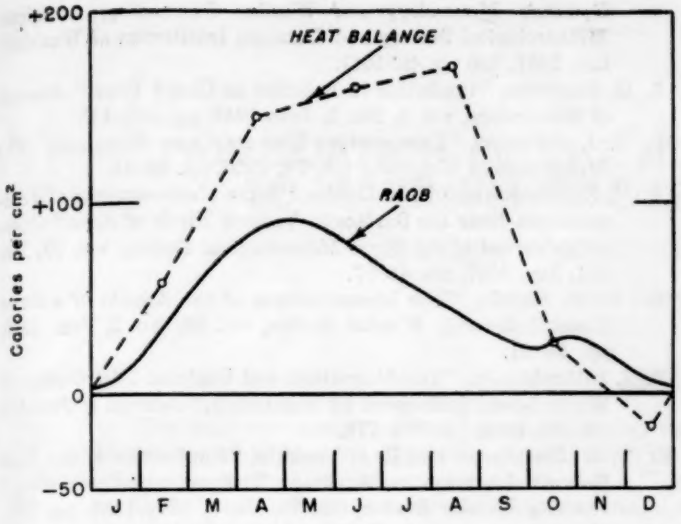

FIGURE 16.—Net daily heating of air in clear weather at Nashville.

higher and higher elevations. In a desert region of little cloudiness the heat must be carried off by the winds. In a more humid climate as the heating extends to higher and higher levels cumulus development automatically becomes greater, intercepting and reflecting some of the sunshine. The cumuli then typically dissipate at night allowing strong nocturnal cooling. The final stage is the development of cumulonimbus clouds. These clouds are an effective thermodynamic vehicle for transporting great quantities of heat from lower to higher layers. The upper layers are warmed by the release of latent heat of condensation while the lower layers are cooled by the evaporation of rain. The role of cumuliform clouds not only as rain producers but as effective summertime heat controls becomes apparent.

7. SUMMARY

The local daily clear-weather heating or cooling is a climatological parameter. This parameter was evaluated on an hourly basis for clear weather at Nashville, Tenn., by an energy-balance technique. Observed temperature changes from raobs agreed well with computed changes on the average for two periods of the day. For the period from 1600 to 2100 CST the mean observed cooling exceeded the computed cooling.

It was shown that the heating parameter is useful in forecasting the daily maximum temperature from the raob of the night before. Mean errors in an objective forecast test, in which advection was neglected but days with front passages were excluded, ranged from 4.6° F. for March to 1.6° F. for July. (An index of cloudiness observed after the other initial conditions was admitted in this test.)

It was shown that at the latitude of Nashville the net daily heating in clear weather is a factor that must be taken into account in explaining summer weather. An appreciable amount of cloudiness is required to maintain a temperature balance in the absence of air mass changes. If subsidence suppresses cloudiness a heat wave is inevitable.

8. SUGGESTIONS FOR FURTHER WORK

Climatological studies to evaluate the local heat balance, similar to the one presented here for Nashville and that by Williams for the Las Vegas-Phoenix area, should be made for other regions. Some of the more recent microclimatological studies, not available at the time this work was begun, should be reviewed in connection with such studies for basic data on ground temperatures, evaporation, etc. The direct absorption of insolation by clear air, which may range up to an equivalent of about 0.7° C. per day [4], and which was neglected in developing the heat-balance diagrams of the present study, should be considered.

There are many other fruitful tasks that could be carried out in organizing, adapting, and bringing to the forecaster's desk available micrometeorological data that have a bearing on the local heat balance. As examples, information is needed on the difference in heat absorption by the ground when dry, wet, frozen, and snow covered. More quantitative work is needed on the effects of clouds on the local heat balance.

The author believes that it would now be feasible to attack the problem of minimum temperature forecasting on an energy-balance basis. This is admittedly more complex than maximum temperatures. The return long-wave radiation from air to ground would have to be taken into account in a more precise fashion than by monthly means. Wind speed would be important but possibly would not prove unduly troublesome. Nights with strong turbulence throughout the night are the exception. The distribution of moisture in the air might possibly have predictive value as to what the night anemometer-level speed will be; the smaller the radiative cooling of the air in comparison with cooling by conduction of heat into the ground, the more stabilizing the situation.

TABLE 10.—*Net cooling of air in clear weather from 1800 to 2115* CST *at Nashville, Tenn.*

Month	Langleys/hour	Total langleys
February	8.4	27
April	13.1	43
June	14.6	47.5
August	12.8	41.5
October	11.9	39
December	8.0	26

ACKNOWLEDGMENT

The work reported here, except for the forecast test, is taken from a Thesis prepared at the Massachusetts Institute of Technology under the supervision of Prof. H. G. Houghton.

APPENDIX

The standard raob times were changed on June 1, 1957. A curve for forecasting the maximum temperature from

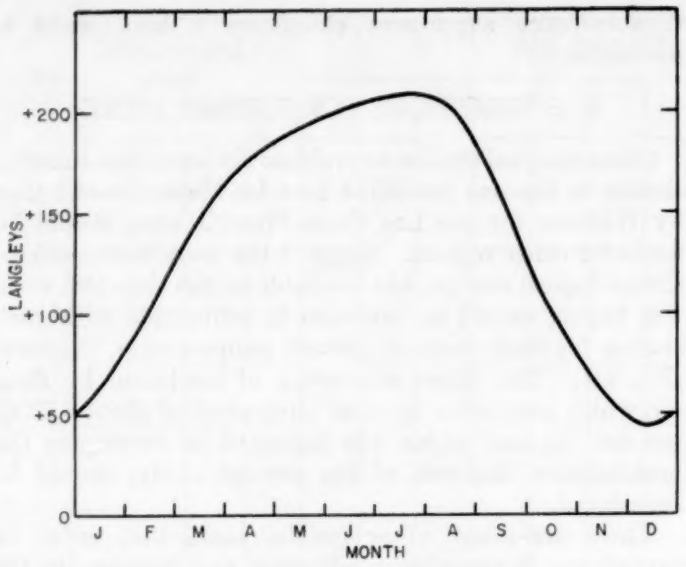

FIGURE 17.—Heating of air in clear weather Nashville. This curve corresponds to the "mean" curve in figure 12 but has been adjusted for use with 1800 CST raob data.

the 1800 CST raob of the evening before is shown in figure 17. This was constructed by measuring the cooling on the air curves of figures 1–6 between 1800 and 2115 CST (1812 to 2127 mean local time) and subtracting this amount of cooling from the mean curve of figure 12. These additional cooling increments are listed in table 10. No verifications have been performed with the curve for the new time.

REFERENCES

1. D. Brunt, *Physical and Dynamical Meteorology*, 2d Ed. University Press, Cambridge, England, 1939, 428 pp. (p. 136).
2. W. M. Elsasser, "Heat Transfer by Infrared Radiation in the Atmosphere," *Harvard Meteorological Studies* No. 6, Harvard University Press, 1942, 107 pp. (p. 21).
3. S. Fritz, "The Albedo of the Ground and Atmosphere," *Bulletin of the American Meteorological Society*, vol. 29, No. 6, June 1948, pp. 303–312.
4. C. L. Godske, T. Bergeron, J. Bjerknes, and R. C. Bundgaard, *Dynamic Meteorology and Weather Forecasting*, American Meteorological Society and Carnegie Institution of Washington, 1957, 800 pp. (p. 101).
5. B. Haurwitz, "Insolation in Relation to Cloud Type," *Journal of Meteorology*, vol. 5, No. 3, June 1948, pp. 110–113.
6. G. J. Jefferson, "Temperature Rise on Clear Mornings," *The Meteorological Magazine*, vol. 79, 1950, pp. 33–41.
7. N. K. Johnson and E. L. Davies, "Some Measurements of Temperatures Near the Surface in Various Kinds of Soils," *Quarterly Journal of the Royal Meteorological Society*, vol. 53, No. 221, Jan. 1927, pp. 45–57.
8. N. N. Kalitin, "The Measurements of the Albedo of a Snow Cover," *Monthly Weather Review*, vol. 58, No. 2, Feb. 1930, pp. 59–61.
9. J. Kittredge, Jr., "The Magnitude and Regional Distribution of Water Losses Influenced by Vegetation," *Journal of Forestry*, vol. 36, 1938, pp. 775–778.
10. T. W. Kleinsasser and R. J. Younkin, "Application of the Heat Balance Approach to Maximum Temperature Forecasting," *Monthly Weather Review*, vol. 86, No. 5, May 1958, pp. 165–170.
11. R. J. List, "Smithsonian Meteorological Tables," 6th revised ed., *Smithsonian Miscellaneous Collections*, vol. 114, Washington, D. C., 1951.
12. M. Neiburger, "Insolation and the Prediction of Maximum Temperatures," *Bulletin of the American Meteorological Society*, vol. 22, No. 3, Mar. 1941, pp. 95–102.
13. H. L. Penman, "Daily and Seasonal Changes in the Surface Temperature of Fallow Soil at Rothamsted," *Quarterly Journal of the Royal Meteorological Society*, vol. 69, No. 296, Jan. 1943, pp. 1–16.
14. J. H. Perry, Ed., *Chemical Engineer's Handbook*, McGraw-Hill Book Co. Inc., New York, 1941, p. 454.
15. N. Shaw, *Manual of Meteorology*, vol. III, University Press, Cambridge, England, 1930, 445 pp. (p. 144).
16. C. W. Thornthwaite and B. Holzman, "The Determination of Evaporation from Land and Water Surfaces," *Monthly Weather Review*, vol. 67, No. 1, Jan. 1939, pp. 4–11.
17. C. W. Thornthwaite, and B. Holzman, "Measurement of Evaporation from Land and Water Surfaces," U. S. Department of Agriculture *Technical Bulletin*, No. 817, 1942, 143 pp.
18. U. S. Weather Bureau, Monthly Meteorological Summary, Nashville, Tennessee, mimeographed.
19. T. L. Williams, "The Use of Insolation in Forecasting Temperatures," *Bulletin of the American Meteorological Society*, vol. 34, No. 6, June 1953, pp. 245–249.
20. H. G. Wilm and C. W. Thornthwaite, "Report of the Committee on Transpiration and Evaporation, 1943–44," *Transactions, American Geophysical Union*, 1944, Part V, p. 690.

APPLICATION OF THE HEAT BALANCE APPROACH TO MAXIMUM TEMPERATURE FORECASTING

THEODORE W. KLEINSASSER AND RUSSELL J. YOUNKIN

Weather Bureau Airport Station, Knoxville, Tenn.

[Manuscript received June 24, 1957; revised April 14, 1958]

ABSTRACT

The daily net energy available for heating the air from 0300 GMT to the following afternoon, as determined by Myers, is used to compute objectively the maximum temperature expected under static, clear-sky conditions at 12 cities in the power distribution area of the Tennessee Valley Authority. The maximum temperatures thus obtained are plotted and analyzed to resolve irregular features of the isotherm patterns. The analysis is then adjusted subjectively primarily for the effect of temperature advection but also for cloudiness, precipitational cooling, and vertical motion—to take account of changes expected by mid-afternoon of the current day and also of the following day. Verification results for seven cities in the TVA area during 1954 and 1955 are presented. The current-day forecast errors are approximately 50 percent less than persistence forecast errors.

1. INTRODUCTION

Myers [1, 2] investigated the local heat balance under clear-sky conditions at Nashville, Tenn., for the five energy transfer processes, insolation, long-wave radiation, ground heating, reflection, and evaporation. His results included a computation of the annual march of the net energy available for heating the air from the time of the 0300 GMT raob to the average time of occurrence of the maximum temperature during the following afternoon.

As a check against these values, Myers made independent estimates of the clear-sky heat balance directly from the Nashville raob data. This was done by first constructing a hypothetical midafternoon sounding based on the maximum temperature for the day and upon the previous 1500 GMT raob and then measuring the heating or cooling from one raob to the next.

The heat-balance values that Myers thus obtained by two different methods showed satisfactory agreement for the period 0300 to 2100 GMT, and particularly for the period 1500 GMT to 2100 GMT, the period of greatest heating during the day. As a final refinement, mean values of the data obtained by the two methods were computed. (See Myers' [2] figure 12 in the preceding article.)

Since these values represent the daily net energy available for heating the air between the time of the 0300 GMT raob and the following afternoon, they can be utilized in determining objectively the maximum temperature that would occur under static, clear-sky conditions. Subjective adjustments for expected thermal changes in the lower atmospheric air column are then applied in making the actual maximum temperature forecast. The Weather Bureau Airport Station at Knoxville has used this approach since 1948 in the preparation of its 12- and 36-hour maximum temperature forecasts for 12 cities in the TVA power distribution area. This paper describes the procedure used in this application of the heat-balance method to maximum temperature forecasting and summarizes the results obtained over a period of 2 years.

It is emphasized that the procedure described represents an actual forecasting operation subject to both time and personnel limitations. Obviously, refinements of the application could be achieved if these limitations were relaxed.

2. DESCRIPTION OF FORECASTING PROCEDURE

The first step in the maximum temperature forecasting procedure is to plot on a pseudoadiabatic chart (WB Form 1147) the 0300 GMT soundings for all raob stations in and around the TVA power distribution area. The appropriate heat energy, as determined by Myers, then is added graphically as a triangular area to the lower portion of each sounding (fig. 1). A transparent overlay (fig. 2), developed by Myers and slightly modified by this office, is used to make the graphical addition. The permanent lines on the overlay are marked lightly, while the line in current use is heavily overwritten with ink to stand out distinctly and prevent confusion. Dates for change in areas, to the nearest fifth day, are shown on the overlay. With the overlay applied to the sounding, as illustrated in figure 1, the clear-sky maximum temperature is determined.

The maximum temperatures thus obtained are plotted on a convenient map base and isotherms drawn at 2° F. intervals. Considerable care is taken to make the isotherm analysis consistent with the 850-mb. constant pressure chart, and the 1,000–850-mb. thickness chart, which is prepared locally for other uses. In addition, past winds at all levels through the heating layer and the maximum temperatures observed the previous day are considered in resolving irregular and unusual isotherm patterns.

470451—58——2

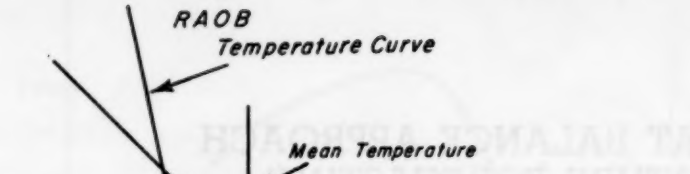

FIGURE 1.—Method used in determining the clear-sky maximum temperature from the raob. (After Myers [2].)

The resulting analysis is a mapped forecast of the maximum temperature that may reasonably be expected under static clear-sky conditions. The next step is to forecast the changes that will take place in the isotherm pattern by midafternoon of the current day and also of the following day.

Expected advection accounts for most of the changes in the forecast isotherm pattern, although cloudiness, precipitational cooling, and vertical stretching and sinking are recognized as important. The advective adjustment is principally subjective in application but is based primarily on the wind expected at gradient level during the forecast period. As a general rule, the isotherms are moved a distance equal to approximately 60 to 80 percent of the wind component normal to the isotherms.

Linear extrapolation of 24-hour thickness change centers on the 1,000–850-mb. chart serves as a check on the logicality of the advective adjustment. A thickness change of 8.7 gpft. in the 1,000–850-mb. layer is equal to a change of 1° F. Disagreement between location of the isotherms by extrapolation and location by the advective method usually indicates that vertical motion will be of considerable importance and that the 60-to 80-percent normal wind advective component will not be reliable. In such cases, an attempt to evaluate the effect of vertical motion is made by compromising the isotherm location between that indicated by advection and by extrapolation. As the advected isotherm pattern location becomes less and less reliable, the greater becomes the anticipated vertical motion.

No general rules can be stated for isotherm adjustments made for cloudiness, and precipitational cooling. Application of adjustments for these factors varies considerably from forecaster to forecaster and is almost completely subjective, although the ratios of insolation with overcast sky to insolation with cloudless sky presented by Haurwitz

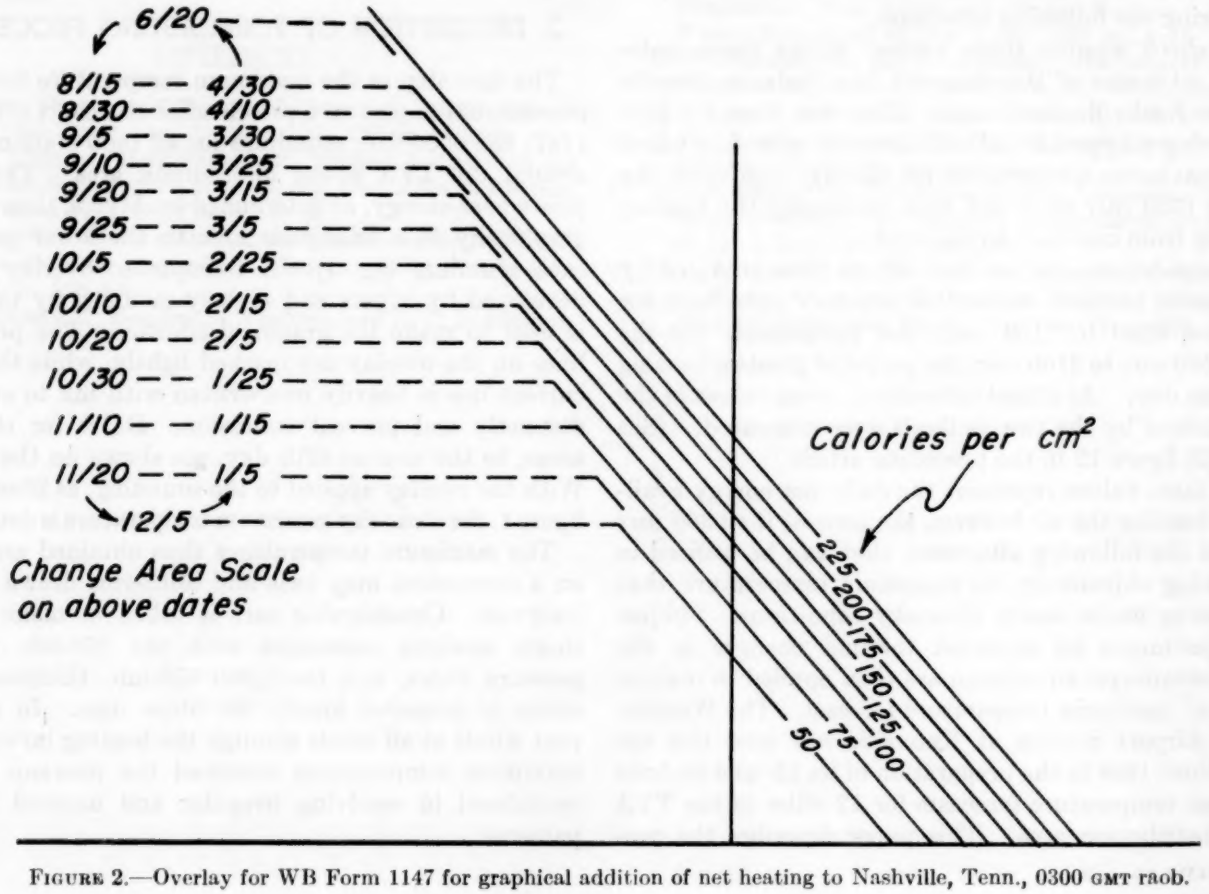

FIGURE 2.—Overlay for WB Form 1147 for graphical addition of net heating to Nashville, Tenn., 0300 GMT raob.

TABLE 1.—*Mean absolute error (° F.) in current-day maximum temperature forecasts and comparison with errors in persistence forecasts, by months. Data period 1954 and 1955*

Station (WBAS)	Mean error in ° F.											
	January	February	March	April	May	June	July	August	September	October	November	December
Birmingham, Ala.:												
Actual	4.2	3.5	3.1	3.0	2.2	2.3	1.9	1.9	2.5	2.6	2.6	3.8
Persistence	7.8	8.3	7.7	5.3	3.7	3.1	2.6	2.4	3.4	5.3	7.2	6.9
Bowling Green, Ky.:												
Actual	4.1	3.8	3.2	3.2	3.0	2.5	1.9	2.6	3.0	2.7	3.0	2.9
Persistence	8.0	9.1	8.1	7.1	5.1	4.4	3.3	5.0	4.4	5.0	7.7	7.0
Bristol, Tenn.:												
Actual	3.4	3.8	3.6	3.0	2.7	2.3	1.7	2.3	2.5	2.1	3.2	3.4
Persistence	6.4	9.9	8.5	5.9	4.8	4.0	2.7	3.5	4.1	4.9	6.7	7.3
Chattanooga, Tenn.:												
Actual	3.8	3.5	3.5	3.1	2.5	2.0	2.0	2.3	2.6	2.5	3.3	3.8
Persistence	6.3	7.1	7.3	6.2	4.6	3.6	3.0	3.0	4.0	5.1	6.7	5.4
Knoxville, Tenn.:												
Actual	3.8	3.3	2.9	2.8	2.8	2.6	1.9	2.7	2.4	2.4	2.7	3.5
Persistence	6.0	8.2	8.4	5.7	4.6	4.3	3.2	3.5	3.7	5.1	6.9	6.2
Memphis, Tenn.:												
Actual	3.6	3.7	3.3	4.0	2.9	2.2	1.9	2.0	2.3	3.2	3.3	3.3
Persistence	7.6	8.3	8.2	6.0	4.5	3.3	2.6	2.8	3.8	5.0	7.2	7.7
Nashville, Tenn.:												
Actual	3.9	3.8	3.4	3.7	2.5	1.7	1.9	2.4	2.7	2.6	3.1	2.8
Persistence	8.5	9.5	8.7	6.3	4.8	3.7	3.1	4.6	4.5	5.4	7.5	7.5
All stations:												
Actual	3.8	3.6	3.3	3.3	2.7	2.2	1.9	2.3	2.6	2.6	3.0	3.4
Persistence	7.2	8.6	8.1	6.1	4.6	3.8	2.9	3.5	4.0	5.1	7.1	6.9

[3] have been helpful in making adjustments for cloudiness. A more objective determination of the alterations to be made to the isotherm pattern resulting from these influences is desirable, but, in general, subjective forecast adjustments seem to be as successful and far less time consuming than any objective methods that we know of.

3. VERIFICATION RESULTS

Monthly verification results of current-day maximum temperature forecasts for seven Weather Bureau Airport Stations are given in table 1. Verification records were not available for the other five cities included in the forecast service.

Table 2 presents the verification results by seasons. The seasonal grouping of months is based on error frequency distributions. While this paper deals primarily with current-day maximum temperature forecasting, second-day maximum temperature forecast verification data in table 3 are given for general informational purposes.

Maximum temperature forecasts for both the current-day and second-day were made at approximately 1230 GMT. Due to TVA operational requirements and procedures, maximum temperature forecasts were not made for a station when the highest temperature was expected to occur early in the day with generally falling temperatures throughout the remainder of the day. All such cases were omitted from the maximum temperature verification data. There was no opportunity for the forecasters to "play the verification system" as the verification system was devised after the basic-data period. Lack of com-

TABLE 2.—*Mean absolute error in current-day maximum temperature forecasts and comparison with errors in persistence forecasts by seasons [1] and year. Data period 1954 and 1955.*

Forecasts for:	Source	Mean Error in ° F.				
		Winter	Spring	Summer	Fall	Year
Birmingham	Actual	3.6	2.6	2.2	3.0	2.8
	Persistence	7.9	4.5	2.9	6.4	5.3
Bowling Green	Actual	3.7	3.1	2.5	2.9	3.0
	Persistence	8.4	6.1	4.3	6.5	6.2
Bristol	Actual	3.6	2.9	2.2	2.9	2.8
	Persistence	8.3	5.3	3.6	6.3	5.7
Chattanooga	Actual	3.6	2.8	2.2	3.2	2.9
	Persistence	6.9	5.4	3.4	5.7	5.2
Knoxville	Actual	3.4	2.8	2.4	2.8	2.8
	Persistence	7.6	5.1	3.7	6.0	5.5
Memphis	Actual	3.5	3.5	2.0	3.3	2.9
	Persistence	8.0	5.2	3.2	6.6	5.6
Nashville	Actual	3.7	3.1	2.2	2.8	2.9
	Persistence	8.9	5.5	4.0	6.8	6.2
All Stations	Actual	3.6	3.0	2.2	3.0	2.9
	Persistence	8.0	5.3	3.6	6.4	5.7
		Percent improvement of actual over persistence				
All Stations		55	43	39	53	49

[1] Winter: December–March; Spring: April–May; Summer: June–September; Fall: October–November.

TABLE 3.—*Mean absolute error in second-day maximum temperature forecasts and also a comparison with errors in 2-day persistence forecasts for Knoxville, Tenn. Data period 1954 and 1955.*

Station	Mean error in ° F.												
	January	February	March	April	May	June	July	August	September	October	November	December	Year
Birmingham	6.3	7.0	5.8	4.3	3.7	3.5	2.6	2.9	3.6	4.6	5.6	6.2	4.6
Bowling Green	6.4	7.0	6.6	5.1	4.5	3.7	3.3	4.3	5.2	5.5	6.2	4.5	5.2
Bristol	5.5	7.1	5.7	4.9	4.6	4.1	2.9	3.1	4.1	4.0	4.8	6.2	4.7
Chattanooga	5.2	6.7	4.9	4.8	3.9	3.2	3.0	3.3	3.9	4.6	4.9	5.3	4.4
Knoxville	4.6	5.6	4.9	4.8	4.3	3.5	3.3	3.7	3.9	4.6	4.9	6.1	4.5
2-day persistence	9.3	11.4	11.7	7.7	6.5	5.3	4.1	4.3	5.5	8.0	9.5	9.1	7.7
Memphis	5.9	7.0	6.0	6.0	4.0	3.6	3.0	2.8	4.4	4.9	6.4	5.6	5.0
Nashville	6.7	6.8	6.1	4.9	4.6	3.4	3.1	4.2	4.8	5.6	5.3	5.1	5.0
All stations	5.8	6.7	5.7	5.0	4.2	3.6	3.0	3.5	4.3	4.8	5.4	5.6	4.8

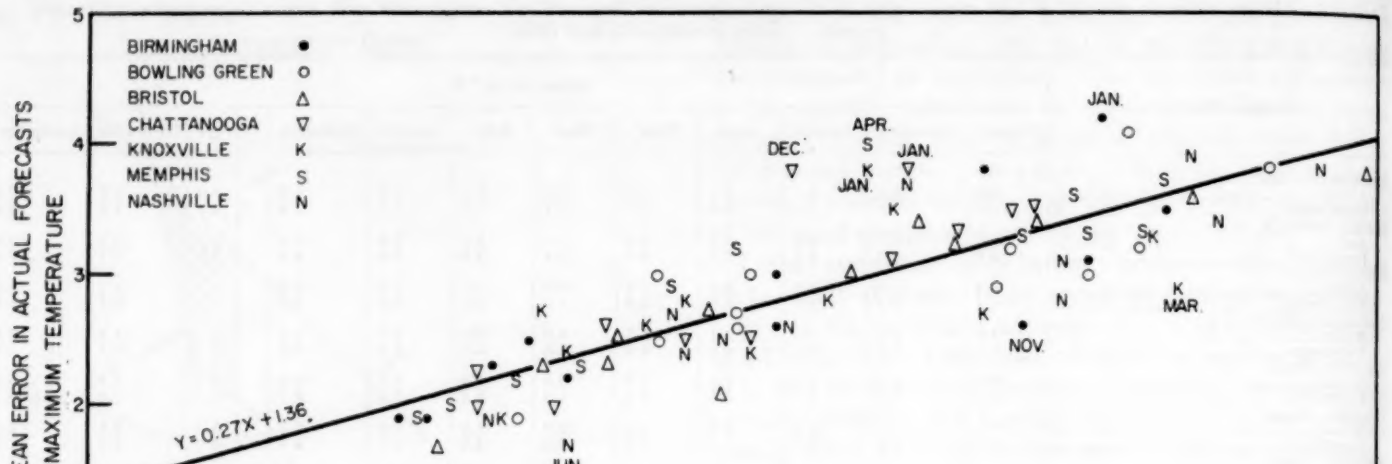

FIGURE 3.—Monthly mean error in actual current-day maximum temperature forecasts plotted against monthly mean error in persistence forecasts for each station, and the regression line for all stations. Data period 1954 and 1955.

parable data arrived at by other practical methods of forecasting maximum temperatures prevented relative evaluation of results. It would have been desirable to compare the actual forecasts with purely objective forecasts based on certain meteorological factors, or combinations of factors, physically related to maximum temperature. However, the preparation of an objective control system would have required considerably more data and time than were available. Therefore, a persistence forecast-control system which required no additional data and which required a minimum of time was selected as most suitable for comparative verification. Under this system, the maximum temperature observed on one day is used as the forecast maximum temperature for the following day. This "blind" persistence forecast system has no forecasting skill. For comparative purposes and to make the absolute error in actual forecasts more meaningful persistence forecast verifications are included in the actual forecast verification in tables 1, 2, and 3.

Several measures of the correspondence between forecast and observed maximum temperatures were computed. These are described here to assist in interpreting the forecast results. The mean or average error was computed for both the actual and persistence forecasts. This is the mean difference between forecast and observed maximum temperature, without regard to sign.

Examination of the monthly mean error in table 1 shows that the actual forecasts were superior to the persistence forecasts in all cases. Percent improvement for all stations combined (table 2) ranged from 39 in the summer season to 55 in the winter season. Table 1 shows that actual forecast errors tend to be large when persistence forecast errors are large. This is an expected characteristic and has been examined in more detail through computation of correlation and regression coefficients (see table 4).

Figure 3 compares the actual forecasts with the persistence forecasts and identifies some months that appear to be unusually poor and unusually good. Birmingham–January, Chattanooga–January and December, Knoxville–January, and Memphis–April appear to be exceptionally poor; while Birmingham–November, Knoxville–March, and Nashville–June appear to be exceptionally good. Examination of both the exceptionally poor and good months showed that the subjective adjustments, especially the timing element for advection, cloudiness, and precipitation were of paramount importance in the overall monthly average forecast accuracy. There was no indication of unreliability of the objectively determined clear-sky maximum temperature.

TABLE 4.—*Mean error of actual maximum temperature forecasts as a function of mean error of persistence forecasts. The 12 pairs of mean errors for each station given in table 1 were used to compute the regression coefficients* a *and* b, *and the correlation coefficient* r. *The regression equation is* $E=a+bP$, *where* E *is the mean error of the actual forecasts and* P *is the mean error of the persistence forecasts for the same station and month.*

Station	*a*	*b*	*r*
Birmingham	1.31	+0.28	0.85
Bowling Green	1.38	+0.26	.83
Bristol	1.17	+0.29	.94
Chattanooga	0.99	+0.37	.85
Knoxville	1.83	+0.18	.60
Memphis	1.22	+0.30	.84
Nashville	1.02	+0.30	.88
All Stations	1.36	+0.27	.83

TABLE 5.—*Frequency distribution of errors in actual current-day maximum temperature forecasts for Birmingham, Bowling Green, Bristol, Nashville, and Memphis combined. Data period 1954 and 1955*

		°F.													Total cases
		−19 to −17	−16 to −14	−13 to −11	−10 to −8	−7 to −5	−4 to −2	−1 to +1	+2 to +4	+5 to +7	+8 to +10	+11 to +13	+14 to +16	+17 to +19	
December	No. cases	1		2	5	25	56	85	72	32	13	6	3		300
	Percent	(*)		1	4	9	21	28	20	10	4	2	1		
January	No. cases		2	4	12	33	65	65	48	30	10	2			271
	Percent		1	1	4	12	24	24	18	11	4	1			
February	No. cases			3	17	21	45	78	53	33	16	1			267
	Percent			1	6	8	17	29	20	12	6	(*)			
March	No. cases			3	13	28	74	87	57	22	6	3	2	1	296
	Percent			1	4	9	25	29	19	7	2	1	1	(*)	
Winter	No. cases	1	2	12	47	107	240	315	230	117	45	12	5	1	1, 134
	Percent	(*)	(*)	1	4	9	21	28	20	10	4	1	(*)	(*)	
April	No. cases			1	8	22	67	93	66	18	18	5		2	300
	Percent			(*)	3	7	22	31	22	6	6	2		1	
May	No. cases			1	4	16	99	109	44	22	10	1			306
	Percent			(*)	1	5	32	36	14	7	3	(*)			
Spring	No. cases			2	12	38	166	202	110	40	28	6		2	606
	Percent			(*)	2	6	27	33	18	7	5	1		(*)	
June	No. cases				1	5	52	140	73	23	6				300
	Percent				(*)	2	17	47	24	8	2				
July	No. cases					10	52	157	74	9	2			1	305
	Percent					3	17	51	24	3	1			(*)	
August	No. cases					14	79	123	73	17	2		1	1	310
	Percent					5	25	40	24	5	1		(*)	(*)	
September	No. cases				9	32	91	108	40	9	5	4	2		300
	Percent				3	11	30	36	13	3	2	1	1		
Summer	No. cases				10	61	274	328	260	58	15	4	3	2	1, 215
	Percent				1	5	23	43	21	5	1	(*)	(*)	(*)	
October	No. cases				4	27	62	111	72	17	6		1		300
	Percent				1	9	21	37	24	6	2		(*)		
November	No. cases			1	6	30	73	78	62	21	7				278
	Percent			(*)	2	11	26	28	22	8	3				
Fall	No. cases			1	10	57	135	189	134	38	13		1		578
	Percent			(*)	2	10	23	33	23	7	2		(*)		
Annual	No. cases	1	2	15	79	263	815	1, 234	734	253	101	22	9	5	3, 533
	Percent	(*)	(*)	(*)	2	7	23	35	21	7	3	1	(*)	(*)	

*Less than 0.5 percent.

Second-day maximum temperature forecast verification data in table 3 show that on the average the mean error in the actual forecasts for the second day was about 1½ times that for the current day. On the average, the mean error for 2-day persistence forecasts (Knoxville only) was about 1⅓ times that for the simple persistence forecasts. Percent improvement of actual second-day forecasts over 2-day persistence forecasts for Knoxville was 42. This compares with an improvement of 49 percent for the actual current-day forecasts over simple persistence forecasts at Knoxville.

The root mean square error was another statistic computed in addition to the mean or average error. In the present study, the forecast errors were approximately

TABLE 6.—*Frequency distribution of errors in actual current-day maximum temperature forecasts for all stations combined. Data period 1954 and 1955*

		°F.													Total cases
		−19 to −17	−16 to −14	−13 to −11	−10 to −8	−7 to −5	−4 to −2	−1 to +1	+2 to +4	+5 to +7	+8 to +10	+11 to +13	+14 to +16	+17 to +19	
December	No. Cases	1		3	8	37	82	131	89	41	16	10	2		420
	Percent	(*)		1	2	9	20	31	21	10	4	2	(*)		
January	No. Cases		2	5	18	45	80	91	74	42	16	2			375
	Percent		1	1	5	12	21	24	20	11	4	1			
February	No. Cases			3	21	33	66	115	68	41	20	3	1		371
	Percent			1	6	9	18	31	18	11	5	1	(*)		
March	No. Cases			5	13	36	105	121	79	35	10	3	2	1	410
	Percent			1	3	9	26	30	19	9	2	1	(*)	(*)	
Winter	No. Cases	1	2	16	60	151	333	458	310	159	62	18	5	1	1, 576
	Percent	(*)	(*)	1	4	10	21	29	20	10	4	1	(*)	(*)	
April	No. Cases			1	11	31	98	133	87	29	23	5		2	420
	Percent			(*)	3	7	23	32	21	7	5	1		(*)	
May	No. Cases			1	2	14	113	157	88	37	13	2		1	428
	Percent			(*)	(*)	3	26	37	21	9	3	(*)		(*)	
Spring	No. Cases			2	13	45	211	290	175	66	36	7		3	848
	Percent			(*)	2	5	25	34	21	8	4	1		(*)	
June	No. Cases				1	5	76	194	102	33	8	1			420
	Percent				(*)	1	18	46	24	8	2	(*)			
July	No. Cases					12	74	221	99	15	5			1	427
	Percent					3	17	52	23	4	1			(*)	
August	No. Cases					18	114	171	95	28	5		2	1	434
	Percent					4	26	39	22	6	1		(*)	(*)	
September	No. Cases				5	25	123	165	71	16	6	4	5		420
	Percent				1	6	29	39	17	4	1	1	1		
Summer	No. Cases				6	60	387	751	367	92	24	5	7	2	1, 701
	Percent				(*)	4	23	44	22	5	1	(*)	(*)	(*)	
October	No. Cases			1	4	31	86	165	101	23	9	1	1		422
	Percent			(*)	1	7	20	39	24	5	2	(*)	(*)		
November	No. Cases			2	9	43	98	110	89	31	8				390
	Percent			1	2	11	25	28	23	8	2				
Fall	No. Cases			3	13	74	184	275	190	54	17	1	1		812
	Percent			(*)	2	9	23	34	23	7	2	(*)	(*)		
Annual	No. Cases	1	2	21	92	330	1, 115	1, 774	1, 042	371	139	31	13	6	4, 937
	Percent	(*)	(*)	(*)	2	7	23	36	21	7	3	1	(*)	(*)	

*Less than 0.5 percent.

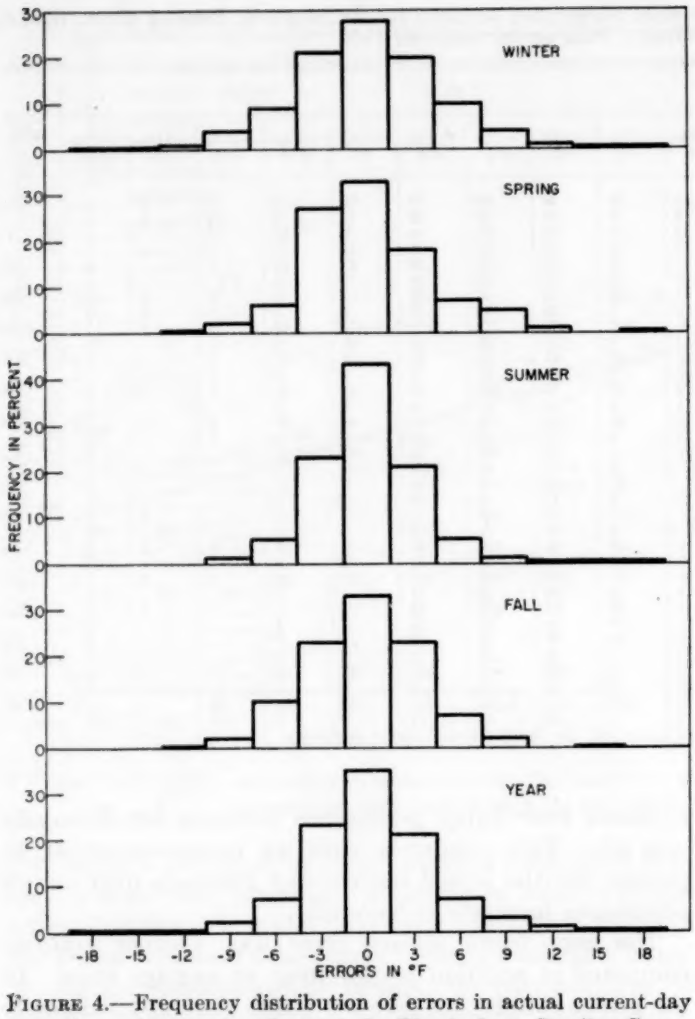

FIGURE 4.—Frequency distribution of errors in actual current-day maximum temperature forecasts for Birmingham, Bowling Green, Bristol, Nashville, and Memphis combined. Data period 1954 and 1955.

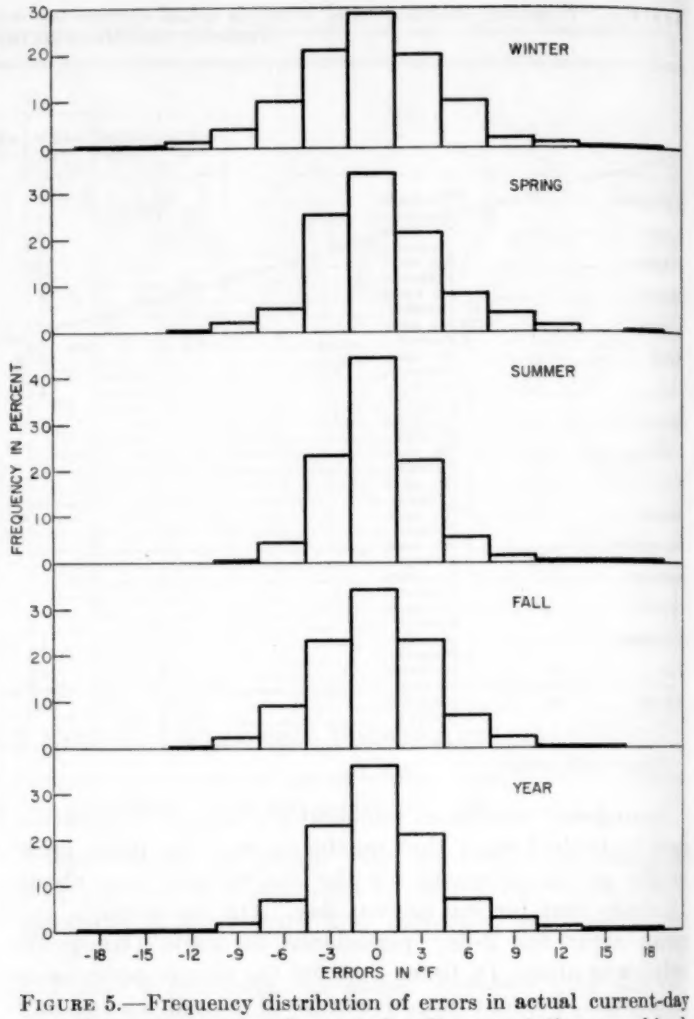

FIGURE 5.—Frequency distribution of errors in actual current-day maximum temperature forecasts for all seven stations combined. Data period 1954 and 1955.

normally distributed and the mean error and root mean square error were highly correlated. Graphical relations between the two statistics suggested that no additional information for ranking purposes could be gained from the use of the root mean square error in addition to the mean error. Graphs of monthly mean error in actual forecasts versus monthly mean error in persistence forecasts indicated that Birmingham, Bowling Green, Bristol, Memphis, and Nashville could be combined in error frequency distributions (table 5 and fig. 4) without appreciable loss of information. All stations were combined in error frequency distributions (table 6 and fig. 5) to provide information of a more general nature to forecasters interested in overall results for all seven stations.

4. SUMMARY

The use of the heat-balance method of maximum temperature forecasting does not require an intimate knowledge of the previous day's weather at each station as does the conventional method of using observed maximum temperatures for the previous day as the forecasting base. In addition, the heat-balance maximum temperature chart with isotherms at 2° F. intervals provides an excellent tool for multiple-station maximum temperature forecasting.

ACKNOWLEDGMENTS

We express our thanks and appreciation to Roger A. Allen, Office of Meteorological Research, U. S. Weather Bureau, Washington, D. C., for preparation of the persistence-control system and many suggestions regarding statistical analysis of results; to Vance A. Myers, Hydrometeorological Section, U. S. Weather Bureau, Washington, D. C., for review of method and procedure; and to Lowell R. Semans, U. S. Weather Bureau Airport Station, Knoxville, Tenn. for considerable work on data computation.

REFERENCES

1. V. A. Myers, "An Investigation of Diurnal Temperature Changes," M. S. Thesis, Massachusetts Institute of Technology, 1947 (unpublished). (Available from Library, U. S. Weather Bureau, Washington, D. C.)
2. V. A. Myers, "Application of Radiation Data to Maximum Temperature Forecasting," *Monthly Weather Review*, vol. 86, No. 5, May 1958, pp. 149–164.
3. B. Haurwitz, "Insolation in Relation to Cloud Type," *Journal of Meteorology*, vol. 5, No. 3, June 1948, pp. 110–113.

EFFECT OF THE STATE OF THE GROUND ON THE LOCAL HEAT BALANCE

G. DANIEL HEMBREE

U. S. Weather Bureau, Oklahoma City, Okla.[1]

[Manuscript received November 29, 1956; revised March 3, 1958]

ABSTRACT

The heat absorbed by the air during the diurnal temperature rise is computed for Oklahoma City. Insolation measurements are recorded for each day, and the energy that is not used in raising the temperature is assumed to represent an empirical integration of the other terms of the local energy balance. With this empirical value taken to be the sum of energy losses, computations are made to show the ratio of the energy loss to the total insolation. These ratios of energy loss are correlated to the observed states of the ground. The computations are made for 141 days taken at random during one year. Eight ground states are used in the analysis and significance tests. The results show that the state of the ground affects the energy balance to such an extent that errors of 4° F. or more in maximum temperature forecasts may be due entirely to the effect of the state of the ground.

1. INTRODUCTION

Neiburger [1] calculated the part of the total solar energy received at the ground that is available to raise the air temperature (near the surface) to the afternoon maximum and to increase the lapse rate of the heated layer to dry adiabatic. He did this by computing and estimating average values for each term in the energy balance equation with the residue considered to be effective in heating the layer. The verification cases listed by Neiburger were restricted to cloudless days in the summer season when wind was light. In view of these nearly ideal conditions, good results might be expected, but, of course, Neiburger's purpose was to demonstrate what could be done with calculations of a local energy balance. It follows from Neiburger's energy balance and energy-area equations that similar results should be expected for widely varying conditions. The fact that less success is sometimes encountered under varying conditions suggests that more study is needed. Neiburger suggested that the energy absorbed by the heated layer should be established empirically and that the balance of the insolation could then be considered a physical integration of the other terms in the energy balance equation.

Myers [2, 3] calculated an empirical curve for the effective absorption of the heated layer for Nashville. He also discussed the variability of the other terms of the energy balance equation, but these variabilities did not affect the empirical curve which was a smoothed annual march of the effective absorption.

Williams [4] described a technique for application of heat-balance computations to short-range temperature forecasting and obtained an impressive verification on test forecasts. His computations were similar to Neiburger's, although he used more recent tables to obtain values of albedo and insolation. Kleinsasser and Younkin [5] have used Myers' approach to forecast maximum temperatures in the TVA power distribution area.

This present paper is a study of local heat balance computations for Oklahoma City and, in a sense, is a continuation of the work of Neiburger, Myers, and Williams. The objective here is to evaluate the effect of the state of ground on the energy loss that does not contribute to raising the air temperature. The procedure is to determine empirically the sum of the energy losses and to correlate the state of the ground with the ratio of energy loss to total insolation.

2. DATA AND COMPUTATIONS

The local energy balance at the ground is represented by the following equation:

$$I_0 = RI_0 + B_0 + LE + S + H_0 \tag{1}$$

where I_0 is the total incident solar radiation per unit surface, R is the surface albedo, B_0 is the net long-wave radiation (positive upward), E is the amount of water evaporated or transpired, L is the latent heat of evaporation, S is the heat used in raising the temperature of the ground, and H_0 is the heat available from the ground surface to raise the temperature of the lower atmosphere and to offset advective and radiative changes in the energy of the heated layer. It follows, then, that the energy ϕ not available to the air of the heated layer is

$$\phi = I_0 - H_0 = RI_0 + B_0 + LE + S \tag{2}$$

In this survey values of ϕ were determined from meas-

[1] Present address: Washington, D. C.

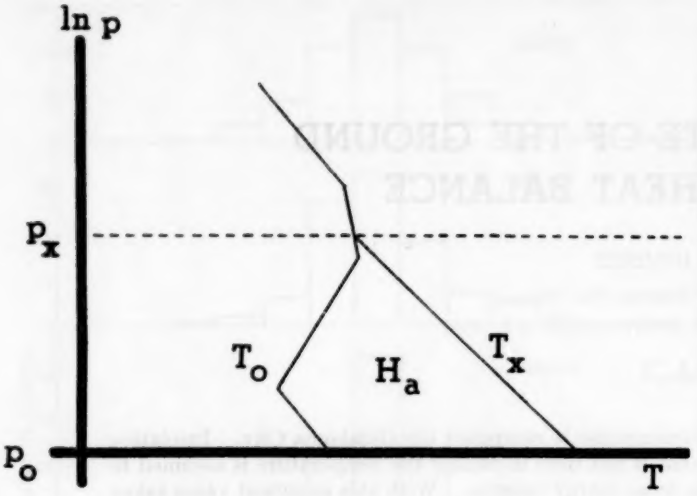

FIGURE 1.—Emagram of a typical case of heating H_a of layer of air from initial temperature T_0 to assumed afternoon maximum temperature T_x. After correction for advective and radiative effects in the layer, the energy H_a is taken as a measure of H_0, the heat available from the surface to the heated layer

urements of I_0 and estimations of H_0. The data for I_0 were taken from an Eppley pyrheliometer. H_0 was estimated from the temperature change on an emagram as illustrated in figure 1.

The quantity of heat H_a used in raising the temperature of the layer is given by:

$$H_a=\frac{c_p}{g}(p_0-p_x)(\overline{T}_x-\overline{T}_0) \tag{3}$$

where c_p is the specific heat at constant pressure, g is the acceleration due to gravity, p_0 is the surface pressure, p_x is the pressure at the top of the layer affected by surface heating, $\overline{T}_0$ is the initial mean temperature of the layer, and $\overline{T}_x$ is the maximum mean temperature of the layer. Assuming $c_p=.2417$ cal. gm.$^{-1}$(° C.)$^{-1}$ for moist air, $g=$ 980 cm. sec.$^{-2}$, and converting pressure units to millibars and temperature units to degrees Fahrenheit:

$$H_a=.1372(p_0-p_x)(\overline{T}_x-\overline{T}_0) \tag{4}$$

where H_a is in langleys.

Figure 1 presents an emagram of a typical case in which heat H_0 from the surface increases the lapse rate until it is presumably near dry-adiabatic at the time of the afternoon maximum temperature. The area between the curves is proportional to the change in energy H_a. Therefore, the difference in the means of the temperature curves, T_0 and T_x, may be taken as a measure of the temperature change $(\overline{T}_x-\overline{T}_0)$, to be used in equation (4). In general however, $H_a\neq H_0$ because of advective temperature changes and short-wave and long-wave radiation effects on the energy balance of the layer. (See for example Myers' [3] equation (2).) Therefore corrections, to be explained later, were applied to T_0 to offset these effects. With these corrections taken into account, equation (4) yields $H'_a\simeq H_0$.

Data for 141 days were tabulated during a 1-year period beginning February 11, 1953, and ending February 10, 1954. The data were recorded from the observation forms of the Weather Bureau Airport Station, Oklahoma City, each time the writer verified the forms as a routine office duty. Since verification duty was rotated, the selection of data for the survey was assumed to be random, except for a leave period during July and August in which no data were recorded.

The selected data were believed to be unbiased because weather conditions were not a determining factor in the selection. Daily cloudiness varied from clear to overcast. Variations in cloudiness were not believed to influence the correlation significantly, first, because the selection of days was random, and second, because cloudiness subtracts from the insolation total, I_0 and its effect is therefore reflected in the pyrheliometer measurement.

The data for the initial temperature curve, T_0, were taken from the 1500 GMT radiosonde observations to which advection corrections were applied. The amount of the correction was arbitrarily taken to be one-half of the difference between the mean temperature of the layer at 1500 GMT and the mean temperature of the same layer 12 hours later. This difference, however, is also affected by short-wave and long-wave radiation, so it was necessary to make adjustments to the mean 0300 GMT temperatures based on the diurnal temperature variation of the layer. For these radiation adjustments to the advection corrections, monthly means of the differences between the mean-layer temperatures at 1500 and 0300 GMT were computed. The monthly mean differences were between 1° F. and 4° F.

The maximum-temperature curve, T_x, for each case was assumed to be the potential temperature line corresponding to the observed surface afternoon maximum temperature. These curves were not the precise limits of the diurnal energy areas, but they were sufficiently representative to show the correlation required.

From the values of I_0 and H_0, ϕ was determined from equation (2) and the ratio $100\phi/I_0$ was computed. This ratio was used as the dependent variable in the statistical analysis.

The data for the independent variable, the state of the ground, were taken from the observation forms (WBAN 10B, Col. 50, 1200 GMT) at the Weather Bureau Airport Station, Oklahoma City. The observations were adjusted in cases where the state of the ground changed abruptly soon after the observation. The classifications dry ground, wet ground, and puddles are identical to codes 0, 1, and 2 of the international synoptic code (Weather Bureau *Circular* N, table 11–2). These classifications contain 91 percent of the total data. The remaining data were cases in which fusion may have been a factor. Because there were only 13 of these cases, they were classified into only two categories: Surface of snow or slush, and frozen ground or heavy frost. For the same reason, conclusions as to the effects of fusion are possibly less reliable than other results.

TABLE 1.—Relation between the ratio $100\,\phi/I_0$ and the state of the ground as shown by frequency of contingent categories of the variables Bars show the mean of each column.

$\frac{100\,\phi}{I_0}$ (%)	d	Barren Season					Growing Season			Class frequency
		Sfc. of snow or slush	Frzn gnd or hvy frost	Puddles	Wet gnd	Dry gnd	Puddles	Wet gnd	Dry gnd	
96 to 100	5	3								3
91 to 95	4									
86 to 90	3	1	1		1	3	1	1	1	9
81 to 85	2		2	1		4	1	4	8	20
76 to 80	1	1	2	3	1	6	2	7	15	37
71 to 75	0		3	2	8	7		5	18	43
66 to 70	-1					5		1	7	13
61 to 65	-2				1	5			5	11
56 to 60	-3					1			1	2
51 to 55	-4					1				1
46 to 50	-5					1				1
41 to 45	-6									
36 to 40	-7								1	1
Col freq		5	8	6	11	33	4	18	56	141
Mean (%)		93	79	77	74	72	83	78	73	75
Variance		64	19	8	47	92	17	23	62	79
Sum of squares		320	222	71	341	3088	71	424	3503	10269

Separate tabulations were used for ground states during the barren season and the growing season which began April 4, 1953, and ended November 8, 1953. Although a freeze occurred at Oklahoma City on April 18, most plants, especially the pastures, turned green again almost immediately and the growing season was virtually uninterrupted.

The tabulation of the data according to the value of the ratio $100\phi/I_0$ and the state of the ground is given in table 1. The results were analyzed statistically by the technique of analysis of variance and the significance determined by the F-ratio and appropriate tables (c. f. Panofsky and Brier [6]). The results of this analysis are given in table 2. The F-ratio of 5.3 exceeds the F-table value of 2.8 at the 1 percent level of significance.

Seasonal variations of insolation and variation in time

TABLE 2.—*Analysis of variance of the data in table 1.*

Source of variance	Degrees of freedom	Sum of squares	Mean square	F-ratio
Between columns	7	2229	319	5.3
Within columns	133	8040	60	
Totals	140	10269		

Note: F-table value at 1 percent level of significance = 2.8.

TABLE 3.—*Seasonal variation of insolation and absorption (after Myers [2]). Insolation and heat values are in langleys.*

	Jan.	Feb.	Mar.	Apr.	May	June	July	Aug.	Sept.	Oct.	Nov.	Dec.
Insolation (Daily totals) (I_0)		369		614		716		647		395		251
Insolation (Sunrise to 4 p. m., T. S. T.) (I_0')		360		574		652		597		383		248
Heat from surface absorbed by lower atmos. (H_0)		108		190		212		215		115		50
Sum of heat losses ($\phi' = I_0' - H_0$)		252		384		440		382		268		198
$\frac{100\ \phi'}{I_0'}$, Sunrise to 4 p. m., (T. S. T.)	75	70	69	67	67	67	66	64	67	70	75	80
Deviation from mean	+5	0	−1	−3	−3	−3	−4	−6	−3	0	+5	+10
Seasonal correction	−5	0	+1	+3	+3	+3	+4	+6	+3	0	−5	−10

of sunset also affected the ratio 100 ϕ/I_0. Myers' [2] curves for the annual march of daily insolation and daily heating (table 3) were used to evaluate these effects on the ratio. Monthly deviations from the annual mean value of 70 percent were added to each value of the ratio for the 141 cases, and the variance-ratio was recomputed (tables 4 and 5) in the same manner as in tables 1 and 2. Myers' data were assumed to be applicable at Oklahoma City because Oklahoma City and Nashville are very near the same latitude. Some error may be introduced by this assumption because cloudiness is a factor and the seasonal variation in cloudiness is not identical at the two stations.

Means were not computed in table 4 because the data were not completely empirical. The means of table 1 resulted directly from measurements and were, therefore, the empirical results sought. The increase in the variance-ratio (F) as shown by table 5 suggests that it would be desirable to compute means for the ratio 100 ϕ/I_0 for each month, but a great deal more data would be needed. The increase in the variance-ratio (F) in table 5 indicates further that the decrease in the effectiveness of insolation in raising temperature during the growing season is even more pronounced than indicated in table 1.

TABLE 4.—*Relation between the ratio 100 ϕ/I_0 and the state of the ground after applying seasonal corrections as shown by frequency of contingent categories.*

100 ϕ/I_0 (percent)	d	Barren season					Growing season			Class freq.
		Sfc of snw or slush	Frzn gnd or hvy frost	Puddles	Wet gnd	Dry gnd	Puddles	Wet gnd	Dry gnd	
91/95	4	3					1	1	1	6
86/90	3						1	2	3	6
81/85	2	1	1	1	1	3	1	4	10	22
76/80	1	1	4	3	3	4	1	7	18	41
71/75	0		2	2	4	11		4	13	36
66/70	−1				2	7			6	15
61/65	−2		1		1	2			4	8
56/60	−3					2				2
51/55	−4					2				2
46/50	−5					2				2
41/45	−6									
36/40	−7								1	1
Col. freq		5	8	6	11	33	4	18	56	141
Sum of sqrs		200	250	71	323	2,802	125	557	3,898	11,127

TABLE 5.—*Analysis of variance of the data in table 4*

Source of variance	Degrees of freedom	Sum of squares	Mean square	F-ratio
Between columns	7	2,901	414	6.7
Within columns	133	8,226	62	
Totals	140	11,127		

Note: F-table value at 1 percent level of significance = 2.8

Table 6 is a comparison of data used in this paper with data used by Myers [2] and Williams [4]. The data shown were average values for the month of June with adjustments made so that values of insolation and absorption between sunrise and 4:00 p. m. (True Solar Time) were comparable. Corrections for latitude were not necessary since the three stations, Nashville, Oklahoma City, and Las Vegas, are all near the 36th parallel. No corrections were made for the differences in longitude even though the differences in solar time of radiosonde observations may have been a factor in the comparisons. Values for H_0 were affected by local differences in terrain, soil, and vegetation. Insolation reaching the ground was greatest at Las Vegas—a result which conforms to altitude and humidity considerations. In addition to this a greater part of the insolation was used to increase air temperature at Las Vegas. Williams makes note of this fact in describing the extremely dry, sandy soil conditions. Hembree's averages for I_0 and H_0 were smallest as one may expect since data for days with cloudiness were included.

Since the data used in this paper for I_0 and H_0 have not been included in the tables, a brief summary is included here. The mean of the insolation measurements, I_0, was 431 langleys; the monthly means ranged from 256 to 615; the absolute range was from 121 to 701. The mean of the computed values of H_0 was 107 ly.; the monthly means ranged from 49 to 151; the absolute range was from 2 to 273.

3. DISCUSSION

According to Neiburger [1], we may assume that inso-

lation is reflected, reradiated, absorbed by the ground, or lost in evaporation, and that the balance is effective in changing air temperature. The quantity ϕ was computed as an empirical integration of the energy loss terms and its variations appear to be the result of variations in surface albedo, evaporation losses, and surface conduction.

The within-column variance (table 2) of the data in table 1 was due partly to the effect of the long-wave radiation, partly to the arbitrary limits chosen for the diurnal energy area, and partly to the arbitrary manner in which advection corrections were made, and to variations in static stability and relative humidity.

From the statistical analysis, the F-test indicates that the correlation between $100\ \phi/I_0$ and state of the ground is significant. The F-ratio of 5.3 in table 2 is nearly twice the F-table value of 2.8 at the 1 percent level of significance. The correlation can be applied in short-range forecasting to estimate the effect of insolation in temperature forecasting.

Objective methods for forecasting temperatures by the use of radiation data have been discussed in detail by Myers [3], Williams [4], and Kleinsasser and Younkin [5]. As with any objective technique, accuracy is dependent entirely on the validity of the assumptions and the representativeness of the data used. If the assumptions are accurate and if all the data are representative to within fractions of units, objective temperature forecasts that are accurate to within a fraction of a degree should be routine.

Often empirical data uncover errors in assumptions. For example, there is an equation used by Williams [4], and by many other writers, that assumes a linear relationship between amount of cloud cover and the albedo of the clouds. Measurements show that the relationship is nonlinear. Kimball [7] gives the following measurements of insolation at Washington for days without cloudiness ranging from 0 to 10 tenths:

Cloudiness (tenths)	0	1	2	3	4	5	6	7	8	9	10
Insolation (percent of clear day value)	100	99	96	90	85	79	73	67	57	48	26

These figures show that the assumption of linearity may cause appreciable error. Scattered cloudiness has but slight effect on insolation, broken cloudiness permits most of the insolation to penetrate, yet an overcast reflects a large fraction of the energy (c. f. Fritz [8])—a fact well known to temperature forecasters.

The ellipse,

$$y=1.18\sqrt{1-\frac{(x+0.3)^2}{(1.4)^2}}-0.15,$$

where y is the fraction of clear-day insolation received and x is the fraction of the sky covered with clouds, is a good fit for Kimball's results. This equation may be used to estimate the effect of cloud cover on insolation with better results than the more popular linear equation, but the eccentricity may vary with locality. Fritz [9] discussed the nonlinearity of this relation, but he found that the relation between I_0 and the duration of sunshine was linear. He suggested that the difference may lie in the fact that a sunshine recorder is sensitive to insolation passing through thin clouds. Accordingly, the curvature of a statistical relation between I_0 and sky cover may be a function of the station's cloud regime. At the present time there are more that 5 years of data punched on the "solar cards" from the stations equipped with pyrheliometers. Each card contains the average daily cloud cover, duration of sunshine, and the data necessary to compute the fraction of clear-day insolation received. A group of empirical curves, showing any desired degree of detail, can be computed for any of the stations in about 8 minutes time by the computers currently being used for this type of problem.

TABLE 6.—*A comparison of the June data of three authors. (Period: Sunrise to 4:00 p. m., true solar time)*

	Unit	Williams [4]	Myers [2]	Hembree
Insolation (I_0')	ly.	759	652	503
Heat from surface absorbed by lower atmosphere (H_0)	ly.	512	212	128
Sum of heat losses (ϕ')	ly.	247	440	375
$100\ \phi'/I_0'$		33	67	75

A simple solution to the temperature forecasting problem by statistical analysis is not possible due to the number of variables and lack of observations. Therefore, the quantity ϕ, the sum of energy losses, is a convenient parameter, although it is not entirely satisfactory due to the interrelation of some of the variables.

Table 1 gives the relationship between the ratio $100\ \phi/I_0$ and the state of the ground as a column mean regression, and the regression may be used to estimate the effect of the state of the ground in forecasting an element, such as maximum temperature, for which the effectiveness of insolation is an important argument.

Consider, for example, a simple maximum temperature forecast in which the effectiveness of the insolation in warming the air is the only argument. Suppose that the ground is dry and that a temperature rise of 20° F. is forecast (a change of 10° F. in the mean of the heated layer). T_0 is known. Therefore, the forecasting of T_x and the lapse rate of T_x (which is usually dry-adiabatic) is equivalent to forecasting the pressure interval and the area H_0. It follows, then, from equation (4) and table 1 that 612 ly. of insolation are forecast and that 27 percent of the incident energy will be used in warming the air. But, if a hard shower during the night has left puddles of water on the ground, an effectiveness of 17 percent may be expected, or a temperature rise of only 16°.

Accordingly, the state of the ground should be considered as an independent variable in the formulation of any scheme for forecasting an element, such as maximum

temperature, that depends on the effectiveness of insolation. This is especially true if very small error is desired. However, attention would have to be given to the large within-column variance of table 2 and to the sources of this variance. The most obvious sources of the variance are listed above.

To suggest merely that additional study is needed is to greatly deemphasize the problem of forecasting temperatures. It is extremely desirable to forecast temperatures with errors less than 1°. To do this, however, it is necessary to formulate the interrelationships of the variables as they occur in the available measurements of observed conditions. The regression in table 1 between the state of the ground and the effectiveness of the insolation in heating the air is a portion of this larger problem and demonstrates how a single variable, the state of the ground, acts independently on three terms, RI_0, LE, and S, to disturb the energy balance.

ACKNOWLEDGMENTS

The writer wishes to express his gratitude to John W. Hamilton for valuable aid and encouragement and to Donald M. Hanson who reviewed the paper and made important contributions. He is also indebted to Dr. Sigmund Fritz, Miss Eula Ann Depuy, and Mr. Dansy T. Williams.

REFERENCES

1. M. Neiburger, "Insolation and the Prediction of Maximum Temperatures," *Bulletin of the American Meteorological Society*, vol. 22, No. 3, Mar. 1941, pp. 95–102.
2. V. A. Myers, "An Investigation of Diurnal Temperature Changes," M. S. Thesis, Massachusetts Institute of Technology, 1947 (Unpublished), (Available from Library, U. S. Weather Bureau, Washington, D. C.).
3. V. A. Myers, "Application of Radiation Data to Maximum Temperature Forecasting," *Monthly Weather Review*, vol. 86, No. 5, May 1958, pp. 149–164.
4. T. L. Williams, "The Use of Insolation in Forecasting Temperatures," *Bulletin of the American Meteorological Society*, vol. 34, No. 6, June 1953, pp. 245–249.
5. T. W. Kleinsasser and R. J. Younkin, "Application of the Heat Balance Approach to Maximum Temperature Forecasting," *Monthly Weather Review*, vol. 86, No. 5, May 1958, pp. 165–170.
6. H. A. Panofsky and G. W. Brier, *Some Applications of Statistics to Meteorology*, The Pennsylvanian State University, University Park, Pa., 1958, 224 pp.
7. H. H. Kimball, "Variations in the Total and Luminous Solar Radiation with Geographical Position in the United States," *Monthly Weather Review*, vol. 47, No. 11, Nov. 1919, pp. 769–793.
8. S. Fritz, "Measurements of the Albedo of Clouds," *Bulletin of the American Meteorological Society*, vol. 31, No. 1, Jan. 1950, pp. 25–27.
9. S. Fritz, "Solar Energy on Clear and Cloudy Days," *The Scientific Monthly*, vol. 84, No. 2, Feb. 1957, pp. 55–65.

THE WEATHER AND CIRCULATION OF MAY 1958[1]

Reversal from a Long-Period Regime

JAMES F. ANDREWS

Extended Forecast Section, U. S. Weather Bureau, Washington, D. C.

1. INTRODUCTION

May 1958 was characterized by reversal from a weather and circulation regime which had persisted since January 1958. Such persistent regimes, lasting for a period of several months, are not uncommon and have been treated in previous articles of this series. The transition from a weather pattern more characteristic of winter than spring actually began during April and was completely effected by May. This article describes the transition which occurred, treating in more detail the reversal from April to May. The average monthly weather and its relation to the mean circulation are then discussed, followed by a comparison of tornado activity with May of 1957 and a discussion of intramonthly changes in circulation and weather.

2. CIRCULATION REVERSAL FOLLOWING LONG-PERIOD PERSISTENCE

The evolution of recent long-period circulation regimes is well illustrated by the westerly wind profile of the general circulation. In figure 1 is shown a time-latitude section of zonal wind speed at 700 mb. averaged over the Western Hemisphere on a series of overlapping 30-day mean charts prepared twice monthly. Late in 1957 the primary axis of westerly wind speed, or jet stream, shown in the illustration as a heavy solid curve, was some 5° north of its normal position (dashed curve). This was followed by an abrupt southward displacement of the maximum westerly wind belt to a position well south of normal with minimum latitude reached during the mean monthly period January–February 1958. This pronounced southward shift of the westerlies was related to an extensive index cycle which has been described in detail by Klein [1]. The 700-mb. jet remained well south of normal until late March when a steady progression northward began. From April to May the recovery was very rapid, and the jet during May reached a position 8° north of its normal location. Thus, from January to April the primary westerly wind jet at 700 mb. remained well south of its normal position, and the long index cycle which began during December 1957 was not finally completed until May of 1958.

During the period January to April 1958 the zonal index, a measure of the mean geostrophic westerly flow between latitudes 55° N. and 35° N. in the Western Hemisphere, remained well below normal at both 700 mb. and sea level, as shown in table 1. As a matter of fact the minimum values reached by both these indices during March were the lowest ever observed on monthly mean charts during a period of record dating back to 1942. The sea level value did, however, equal that observed for the monthly period from mid-February to mid-March during the abnormal winter of 1946–47 [2]. By considering shorter time periods it can be seen that the zonal index during its current recovery reached a peak value at 700 mb. of 10.0 m. p. s., 2.4 m. p. s. above normal, during the 5-day period May 8–12. This represents the greatest positive anomaly of this index since December 19–23, 1957, when the value reached was 14.3 m. p. s., 2.9 m. p. s. above the monthly normal.

The rapid migration northward of the maximum westerly wind belt from April to May is further illustrated by comparing the zonal wind speed profiles at 700 mb. for these months (fig. 2). It is seen that on a mean monthly basis the west-wind maximum was displaced northward some 12° of latitude, a considerably greater displacement than normally occurs between these two months. The mean 700-mb. isotachs and their departure from normal, as derived from the average 700-mb. map for May, are portrayed in figure 3. Superimposed on the isotach chart are the primary jet stream positions for May and April. The marked northward shift of the primary jet from the eastern Pacific to the central Atlantic was very striking, averaging about 20° of latitude in the

TABLE 1.—*Monthly mean values of zonal indices in the Western Hemisphere (in meters per second)*

Month	700 mb.			Sea level		
	Index	Normal	Anomaly	Index	Normal	Anomaly
December 1957	12.7	11.3	+1.4	5.7	4.3	+1.4
January 1958	9.1	11.8	−2.7	3.0	4.1	−1.1
February 1958	7.0	10.2	−3.2	1.2	3.4	−2.2
March 1958	5.3	9.1	−3.8	[1] −0.1	2.8	−2.9
April 1958	7.9	8.3	−0.4	2.4	2.5	−0.1
May 1958	8.0	7.7	+0.3	2.5	2.5	0.0

[1] See Charts I–XVII following p. 196 for analyzed climatological data for the month.

[1] Represents net easterly flow.

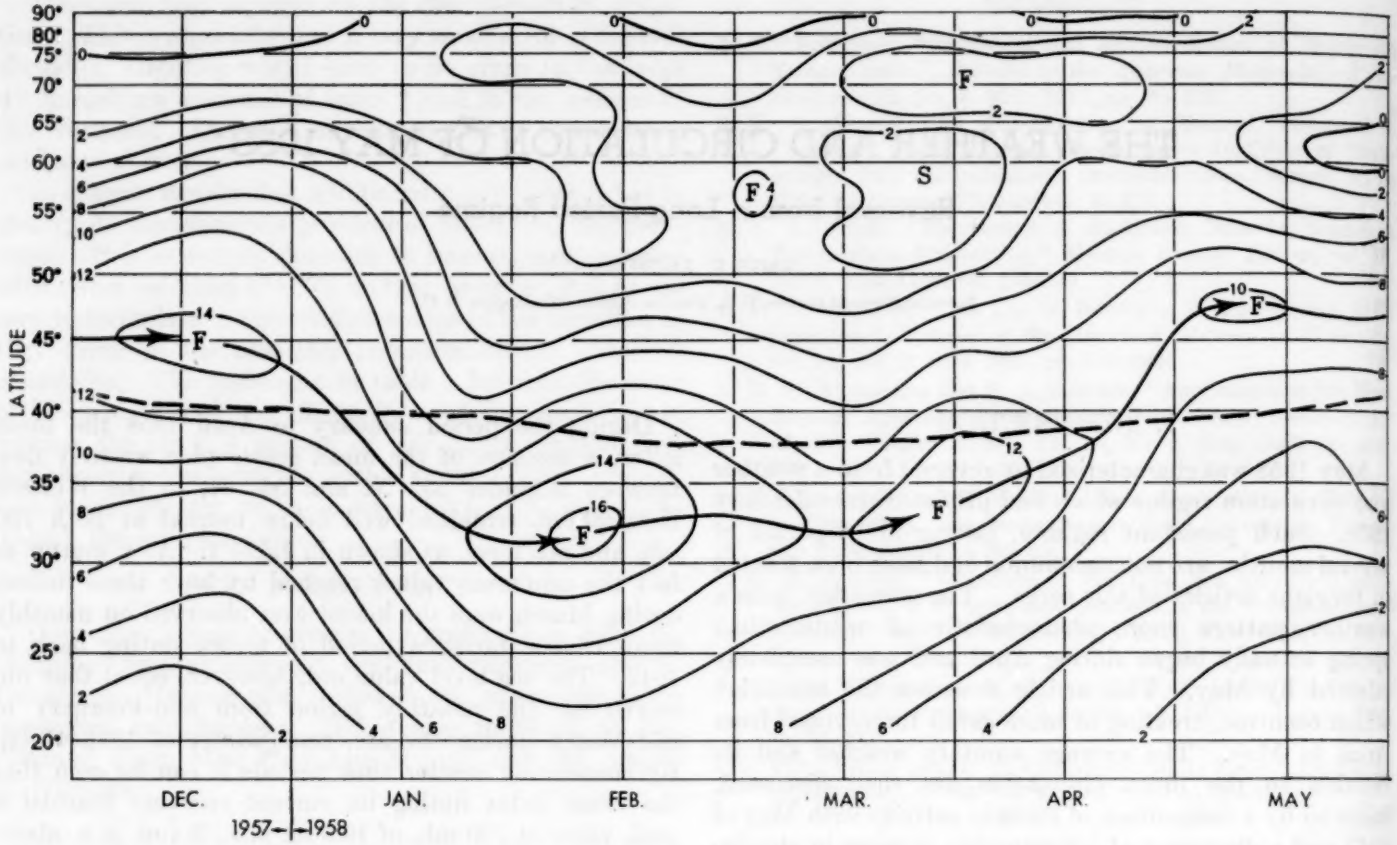

FIGURE 1.—Time-latitude section of 30-day mean zonal wind components averaged over the Western Hemisphere at 700 mb. Wind speeds were computed twice-monthly in 5° latitude belts from the period mid-November to mid-December 1957 until the period mid-May to mid-June 1958. Isotachs are in meters per second with easterly winds negative. Centers of maximum and minimum west wind speed are labeled F and S respectively. Evolution of the axis of maximum westerlies (heavy solid curve) and its position relative to normal (broken line) was closely related to changing weather regimes.

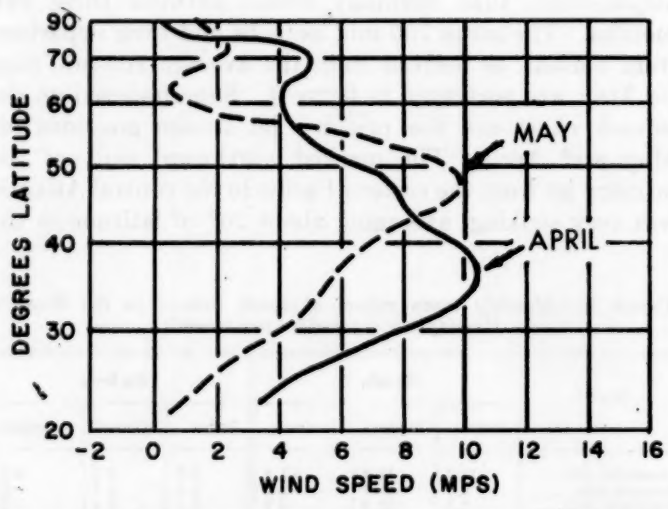

FIGURE 2.—Mean 700-mb. zonal wind speed profiles in the Western Hemisphere for April (solid line) and May 1958 (dashed line). Rapid northward shift of the belt of maximum westerlies is evident.

United States. During April [3] maximum wind speeds were centered over the Gulf States, while in May the strongest winds were over the Great Lakes where speeds were as much as 6 m. p. s. above the normal (fig. 3B).

A similar change occurred in the high-level wind pattern, but with some differences. For instance, at 200 mb. the jet axis during April (not shown) was well established and slightly south of its 700-mb. counterpart from the eastern Pacific to the western Atlantic. This jet axis persisted in low latitudes during May (fig. 4), although much weaker, while a new, higher-latitude jet appeared near the location of the 700-mb. wind maxima. The low-latitude jet axis now extended across the entire Western Hemisphere, its only complement at 700 mb. being a weak speed maximum in the eastern Pacific. In this area wind speeds in the 200-mb. jet reached 30 m. p. s. at the base of a pronounced trough in the westerlies (fig. 4).

The April–May reversal in the general circulation is also illustrated by figure 5, which represents the change in 700-mb. height anomaly from April to May 1958. In North America the greatest anomalous height change was the fall of 320 ft. centered over southern Hudson Bay. Here persistent blocking since January finally gave way

to an abnormally deep cyclonic vortex in May (fig. 6). The band of height falls from eastern Canada to Alaska, in conjunction with a band of middle-latitude height rises from the western Atlantic to the central Pacific, were intimately related to the abrupt northward shift of the mid-latitude westerlies. In the eastern Pacific the anomalous height change pattern of rises in the middle latitudes and falls at low latitudes was associated with a strongly difluent circulation, not only at 700 mb. (fig. 6) but also at 200 mb. (fig. 4) and a related split in the westerlies (figs. 3 and 4).

3. TEMPERATURE REVERSAL IN THE UNITED STATES

The reversal in circulation from April to May was accompanied by an equally pronounced change in temperature. This is best seen by comparing the monthly mean temperature anomalies observed in the United States during the two months, as shown in figure 7. Northeast of a line from the Dakotas to Virginia the above norma temperatures of April gave way to subnormal temperatures during May, while to the southwest of this line most of the Nation experienced a change to warmer weather. The area of greatest change occurred in the Rocky Mountain States and the eastern portions of Washington and Oregon where temperatures rose as much as 9° F. (relative to normal) (fig. 7C). In the Northeast and Upper Lakes region the anomalous temperature change was as much as 7° to 8° F. cooler. In terms of temperature class change only 46 cities out of a possible 100 remained in the same or adjacent class (out of five) from April to May. This is considerably less persistence than that expected either by chance (59) or the 1942–57 average (62). Such abrupt transitions in large-scale weather regimes are quite common during this season of the year [4], other recent examples of April-May temperature reversals having occurred in 1954 and 1956 [5, 6].

4. AVERAGE UNITED STATES WEATHER AND ITS RELATION TO THE MEAN CIRCULATION

TEMPERATURE

May temperatures averaged below seasonal normals in the northeastern quarter of the Nation and along the Atlantic coastal plain to Florida (fig. 7B and Chart I–B). Greatest departures, 3° F. or more, were observed in parts of New York and New England. At Columbus, Ga., a temperature of 40° F. on the 8th was the lowest ever observed during May in a station record which dates back to 1889. New daily minimum temperature records were established at several cities, including Portland, Maine, Toledo, Ohio, and Erie, Pa., on the 26th; Sault St. Marie, Mich., on the 2d and 29th; and Albany, N. Y., on the 10th.

This unseasonable coolness can be related quite readily to the mean circulation patterns. For instance, stronger than normal northwesterly flow prevailed between the

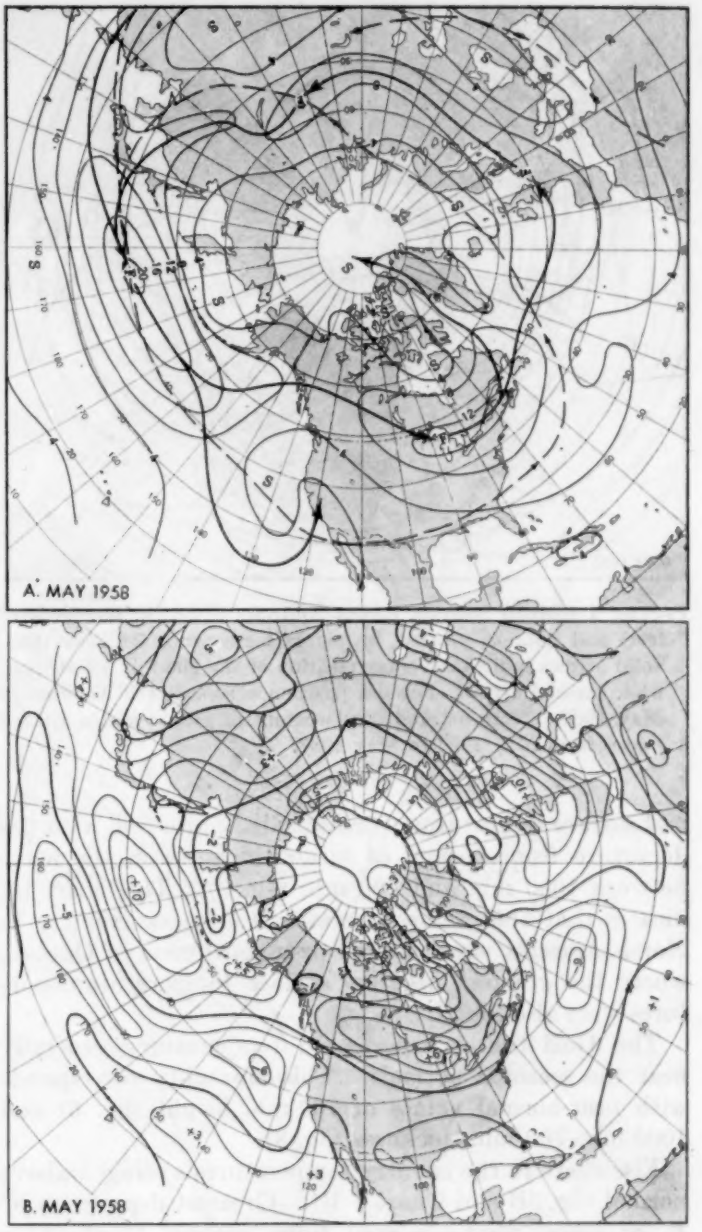

FIGURE 3.—(A) Mean 700-mb. isotachs and (B) departure from normal wind speed (both in meters per second) for May 1958. Solid arrows in (A) indicate major axis of westerly jet during May 1958, while dashed arrows show mean position of corresponding jet during April 1958. Difluence in eastern Pacific and northward displacement of jet stream from April to May are notable features.

ridge in western North America and the trough in eastern North America (figs. 4, 6). Wind speeds in the principal axis of this flow were higher than normal, as much as 6 m. p. s. greater over the Great Lakes at 700 mb. (fig. 3B). At sea level polar continental anticyclones were steered into the Northeast from central Canada by this controlling current, each anticyclone bringing with it a fresh outbreak of cold air. Tracks of these anticyclones are shown in Chart IX. As might be expected, the area of subnor-

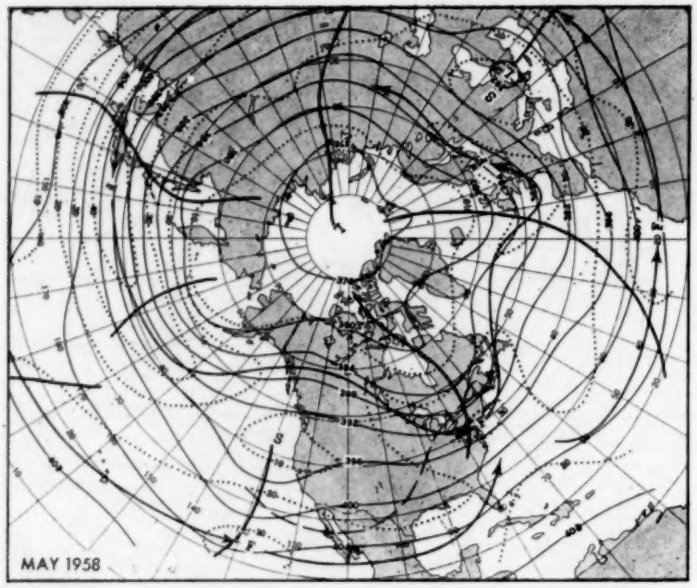

FIGURE 4.—Mean 200-mb. height contours (solid, in hundreds of feet) and isotachs (dotted, in meters per second) for May 1958. Solid arrows indicate average position of the 200-mb. jet stream, while dashed arrows show its position across North America in May 1957. Note marked displacement of jet stream in United States from May 1957 to May 1958.

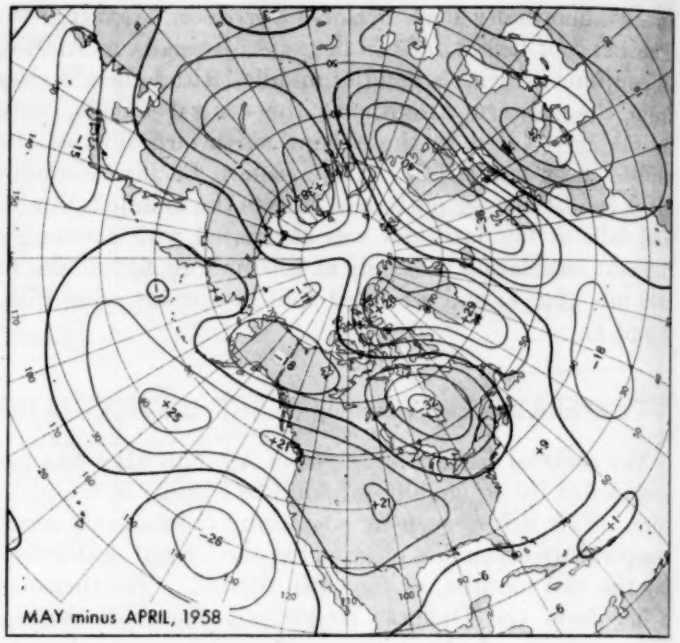

FIGURE 5.—Mean 700-mb. anomalous height change (in tens of feet) from April to May 1958. Areas of large change were related to marked reversal of the planetary circulation.

mal surface temperature corresponded quite well with the departure from normal of mean thickness in the layer between 1000 mb. and 700 mb. (fig. 8). This chart indicates that the greatest negative thickness anomaly in North America was centered over southwestern Quebec, where the greatest negative surface temperature departures were also found.

The Gulf States experienced temperatures generally near the seasonal normals. This normality corresponds with near-normal values of 700-mb. height (fig. 6) and 1000 mb.–700 mb. thickness (fig. 8).

Elsewhere in the country temperatures averaged above normal (fig. 3B and Chart I–B). Greatest departures, 8° F. or more, were observed from western Montana to northeastern Washington, but the +6° F. isotherm embraced a large area of the Far West (Chart I–B). Many monthly mean temperature records for May were established, some of which are listed in table 2. In addition, daily maximum temperature records for individual dates were set, but these are too numerous to mention.

TABLE 2.—*Selected cities reporting warmest May on record during 1958*

Station	Mean temperature (°F.)	Anomaly	Years of record
Tucson, Ariz.	79.1	+6.0	67
Winslow, Ariz.	67.8	+5.8	69
Yuma, Ariz.	84.9	+4.5	81
Los Angeles, Calif.	68.0	+3.2	80
Helena, Mont.	60.7	+8.4	78
Kalispell, Mont.	60.3	+7.9	59
Seattle, Wash.	62.3	+5.0	66
Walla Wal[1]a, Wash.	66.5	+5.3	86

This extensive area of abnormal warmth was associated with a generally anticyclonic circulation pattern that extended well into upper levels of the atmosphere (fig. 4 and Charts XII to XVII). Accompanying factors were above normal values of height (fig. 6), thickness (fig. 8), and sunshine (Chart VII); while at sea level a somewhat stronger than normal southwesterly flow also contributed to the warming (Chart XI, inset).

PRECIPITATION

Because precipitation is discontinuous and the physical processes relating to its production are much more complex than those for temperature, this element is more difficult to relate to time-averaged charts for periods as long as a month. During May 1958 perhaps the easiest to explain are the heavy amounts which fell from the Lower Mississippi Valley to southern New England (Chart II). These were related to the mean troughs near the Atlantic coast and in the Gulf of Mexico (figs. 4 and 6). Two storm systems moving across the Southeast early in the month (Chart X) brought sufficient precipitation to result in flooding in many areas. Most serious flooding developed in southwestern Virginia, eastern Kentucky, and southern West Virginia. Streams also ran high in portions of Pennsylvania, Ohio, and Indiana. As a result of these floods the Ohio River at Cincinnati, Ohio, reached a record crest for May of 58.0 ft. on the 10th. In North Carolina the Neuse and Tar Rivers reached their highest stages in several years. Continuing rains after mid-month in the Lower Mississippi Valley caused the Ouachita River in Louisiana to crest at near record levels.

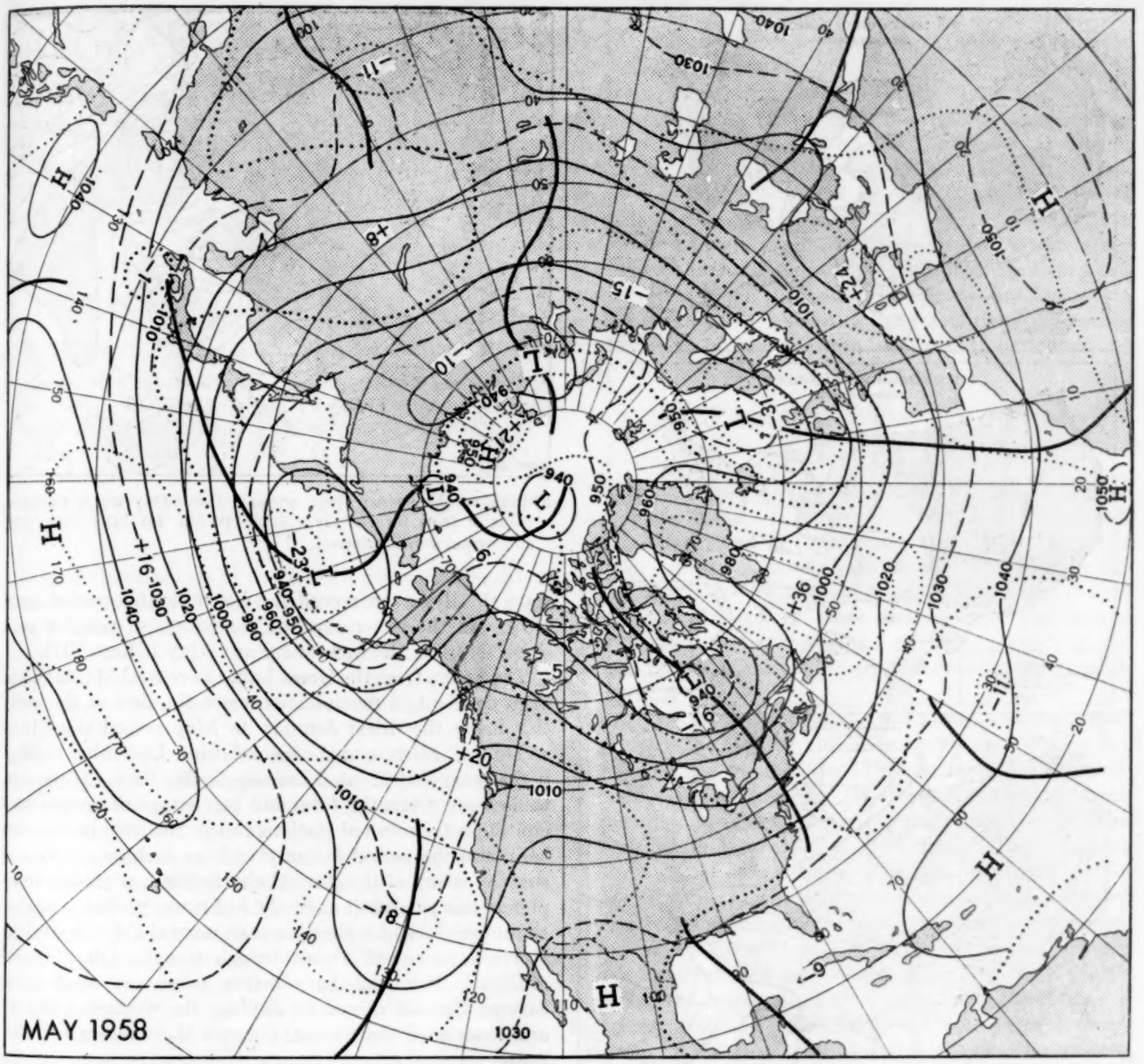

FIGURE 6.—Mean 700-mb. height contours (solid) and departure from normal (dotted) (both in tens of feet) for May 1958. Principal circulation features in North America were stronger than normal ridge in the West and deeper than normal trough in the East.

At Boston, Mass., the period January through May was the second wettest for any comparable period since observations began in 1872. Of interest also is the fact that no thunderstorms occurred there for the first time in the last 35 Mays. This was the second wettest May since records began in 1911 at Miami, Fla., more than half the month's total precipitation falling in connection with a tropical depression that developed in the Caribbean Sea and moved northward off the Atlantic coast (Chart X). A detailed treatment of this storm appears elsewhere in this issue.

Heavier than normal amounts of precipitation also fell from central Wyoming to western Texas and in California and western Arizona (Chart III-B). Much of this can be attributed to the eastward passage of several short-wave troughs from the Pacific. Precipitation along the immediate Pacific coast was associated with the deep trough in the eastern Pacific (figs. 4, 6).

From the Great Lakes westward, precipitation was generally light with May totals averaging about 50 percent of normal (Chart III-B). This deficiency can be related to anticyclonic flow with above normal heights and to

470451—58——3

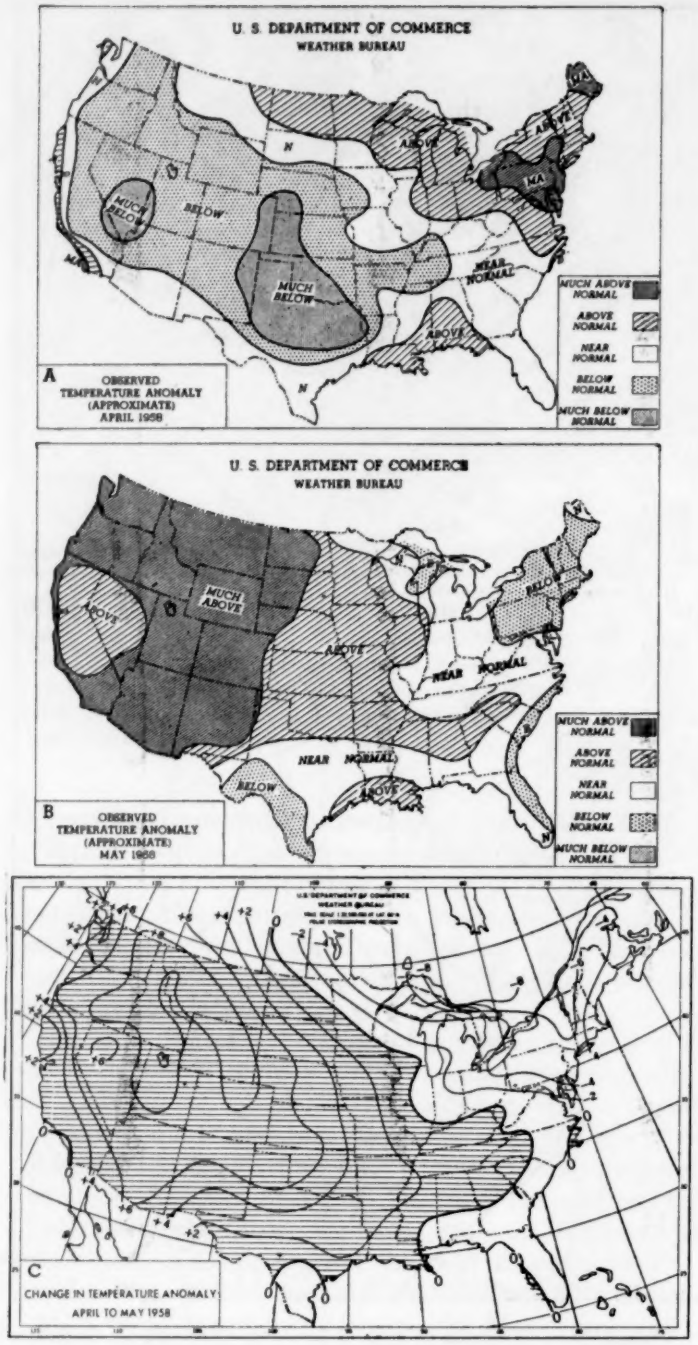

FIGURE 7.—Monthly mean surface temperature anomalies for (A) April 1958 and (B) May 1958. (The classes above, below, and near normal occur on the average one-fourth of the time; much below and much above each normally occur one-eighth of the time.) (C) Change in temperature anomaly (° F.) from April 1958 to May 1958. Note pronounced warming throughout most of the West and cooling in the Northeast.

stronger than normal northwesterly flow (fig. 6). In addition, in the Far Northwest, displacement northward of the 700-mb. jet stream (fig. 3A), plus lack of migratory cyclones (Chart X), reduced the normal orographic effect. Glasgow, Mont. experienced its driest May since 1911, while at Milwaukee, Wis., the first 29 days of the month

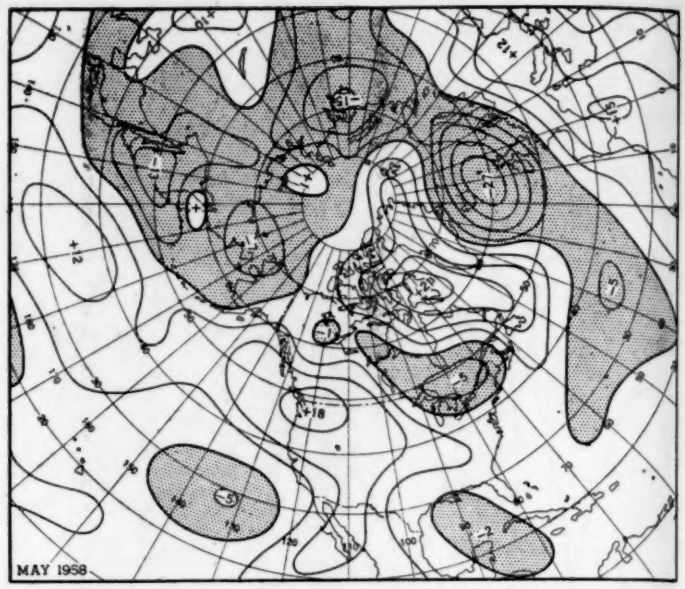

FIGURE 8.—Departure from normal of monthly mean thickness (tens of feet) for the layer 1000–700-mb. for May 1958, with subnormal values stippled.

were the driest on record for a comparable period since 1870. In the latter city the percentage of possible sunshine (88) was the highest for any May (Chart VII).

The region from the Great Lakes to central Montana has been deficient in precipitation since the first of the year, this being the driest January to May period since 1871 at Detroit, Mich. and the second driest December to May period since 1891 at Minneapolis-St. Paul, Minn. In table 3 are given the total and percentage of normal precipitation for selected stations in the northern interior for May and the period January to May inclusive. No one simple feature of the general circulation can explain completely this persistent anomaly, but it was probably related to the presence of a stronger than normal ridge in western North America and a mean trough near the Atlantic coast of North America. In addition, persistent blocking in eastern Canada served to displace the westerlies (fig. 1) and associated storm tracks across the southern United States.

TABLE 3.—*Total (inches) and percentage of normal precipitation for selected stations in northern interior United States* [1]

Station	May 1958		January to May 1958	
	Total	Percent	Total	Percent
Chicago, Ill.	3.12	85	6.54	
Fort Wayne, Ind.	1.88	55	7.37	
Alpena, Mich.	1.14	43	4.22	
Detroit, Mich.	1.16	32	4.79	
Minneapolis, Minn.	1.39	45	4.15	
Glasgow, Mont.	.03	2	1.36	
Devils Lake, N. Dak.	1.02	48	2.57	
Williston, N. Dak.	.06	4	1.95	
Sioux Falls, S. Dak.	.81	24	6.13	
Green Bay, Wis.	1.27	50	4.91	
La Crosse, Wis.	1.07	33	4.37	
Milwaukee, Wis.	2.07	69	5.93	

[1] Data from *Weekly Weather and Crop Bulletin, National Summary*, vol. XLV, No. 22, June 2, 1958.

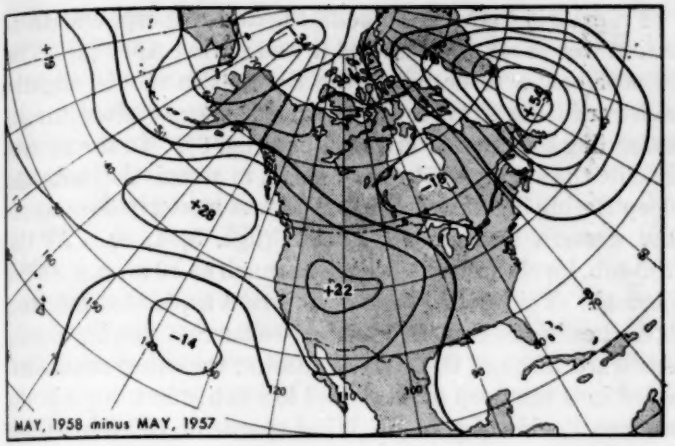

FIGURE 9.—Difference in mean monthly 700-mb. height from May 1957 to May 1958 (in tens of feet). Contrasting weather regimes accompanied change in the general circulation.

5. TORNADO ACTIVITY—A COMPARISON WITH MAY 1957

Tornado occurrences in the United States during May 1958 were considerably less frequent and severe than they were in May 1957. This continues a trend begun in March of this year [3]. Comparative data on the number of tornadoes show that there was a 60 percent reduction in the number reported between May 1957 and May 1958 (see table 4).

Much of this decrease in tornado activity can be attributed to marked differences in the general circulation between the two months. During May 1957 [7] synoptic, thermodynamic, and dynamic considerations were all, on the average, more favorable for tornado development than they were during May of 1958. For instance, the mean trough in the West and ridge in the East in May 1957 were replaced by a ridge-trough system in May 1958. Figure 9, the mean monthly 700-mb. height change between these two months, shows increased flow of dry air from the north which inhibited tornado development.

The thermal field associated with this circulation reversal also underwent a sharp transition—from temperatures well below normal in the Southwest last May to temperatures much above normal this May. Furthermore, the strong horizontal temperature gradient in the central and southern Plains in May 1957 was absent in May 1958. In addition, the average position of the jet stream in May 1957 [7] (fig. 4) was over the central and southern Plains States where tornadoes generally occur most frequently. In May 1958 both the mid-tropospheric jet (fig. 3A) and upper-level jets (fig. 4) were well removed from the Plains States.

TABLE 4.—*Number of tornadoes and funnel clouds observed in the United States during May 1957 and May 1958*

Period	Tornadoes	Funnels	Total
May 1957	230	253	483
May 1958	91	103	194

Examination of the mean monthly 700-mb. charts for all Mays back to 1933 reveals that the full-latitude ridge over western North America (fig. 6) was the strongest ridge ever observed in that area. A similar circulation pattern in May 1940 was associated with the fewest tornadoes in any May since 1933. Thus, while May 1957 produced a record number of tornadoes at a time when the general circulation was most favorable, May 1958 saw a sharp decrease in these storms when the circulation was highly unfavorable. There is little doubt that frequency of occurrence of tornadoes can be related to time-averaged charts for periods as long as a month.

6. CIRCULATION AND WEATHER FEATURES ELSEWHERE IN THE HEMISPHERE

A strong blocking-type ridge, with a large area of positive height anomaly centered off southern Greenland, featured the monthly mean circulation in the Atlantic (fig. 6). Pressures at sea level associated with this ridge were also well above normal, as much as 10 mb. (Chart XI, inset). An extensive area of subnormal wind speeds prevailed at 700 mb. over the southern portion of the Atlantic (fig. 3B), related in part to the low-latitude trough near 52° W.

The weather in northwestern Europe was controlled largely by the deep cyclon c center of action over the Norwegian Sea where 700-mb. heights were 310 ft. below the May normal (fig. 6). The trough emanating from this center extended southward to the African coast where 700-mb. heights were well above normal. This was part of an area of above normal heights extending across southern Europe which, in conjunction with negative anomaly to the north, combined to produce strong westerlies across central Europe. Wind speeds in this jet were as much as 10 m. p. s. above normal (fig. 3). As in North America, the circulation features discussed represented a sharp reversal from the April patterns. This is most apparent when one examines the anomalous 700-mb. height change for this area (fig. 5). In addition, the zone of strongest west winds over the Mediterranean in April was now displaced northward to central Europe (fig. 3A).

Frequent severe cyclones, moving along a path just north of the primary jet (fig. 3A), swept across northern Europe, and sea level pressures averaged 7 mb. below normal in Norway. An abnormally strong northerly flow between the Atlantic ridge and the Norwegian Sea Low brought subnormal temperatures to northern Europe. The lowest temperatures, relative to normal, were observed just north of the British Isles where temperatures in the layer from 1,000 mb. to 700 mb. averaged 9° C. below normal (fig. 8). Over southern Europe, where the flow was generally anticyclonic and pressure above normal, temperatures averaged well above the May normal.

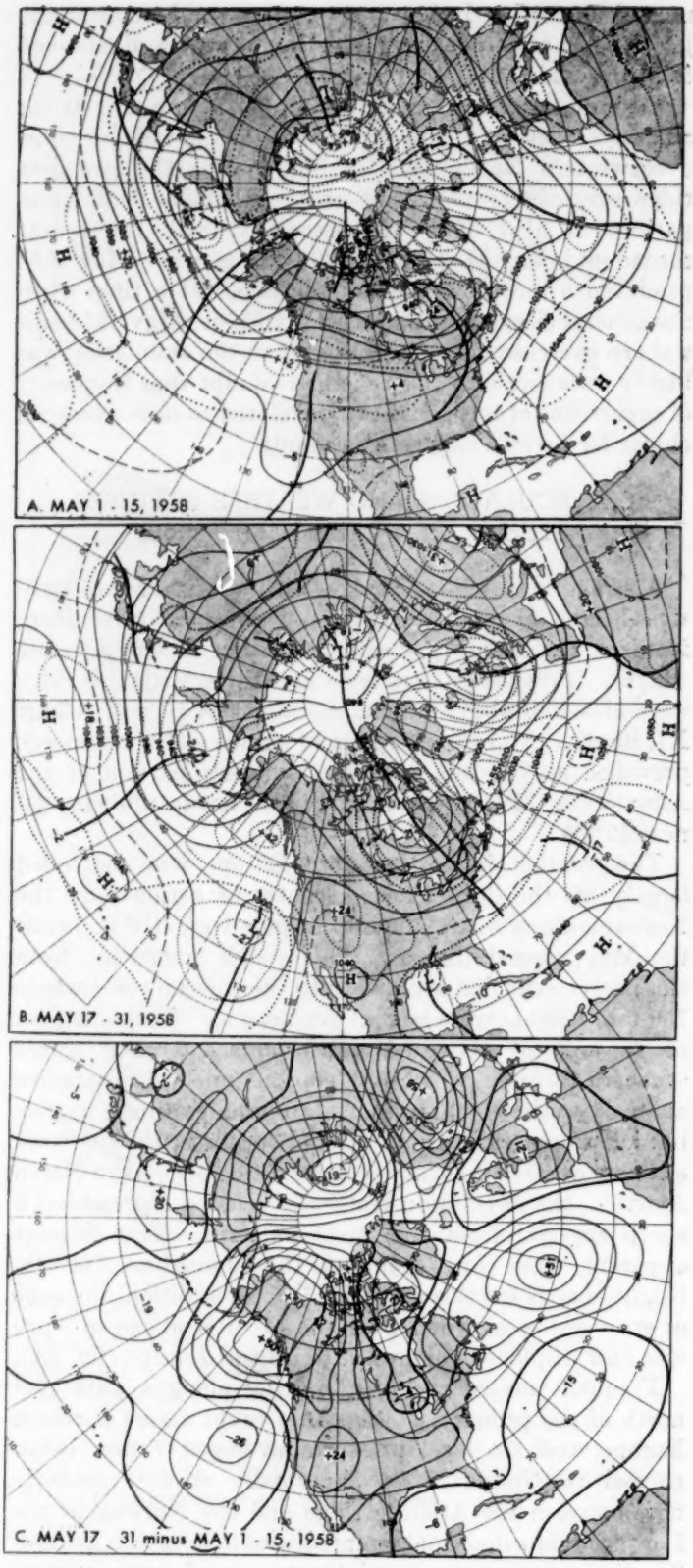

FIGURE 10.—Fifteen-day mean 700-mb. height contours (solid) and departures from normal (dotted) (both in tens of feet) for (A) May 1–15, 1958 and (B) May 17–31, 1958. (C) Difference in height between (A) and (B). Zonal circulation during the first half of May was replaced by a more meridional pattern during the latter half of the month.

From Asia to the mid-Pacific the mid-tropospheric circulation was much the same as it was during April [3]. The intense center of action in the Bering Sea moved slightly eastward from April to May with its sharply tilted trough extending southwestward to Japan (fig. 6). In the central Pacific the strong subtropical ridge, in association with the deep Bering Sea Low, maintained fast westerly flow across the western and central Pacific (figs. 3, 4, 6). At the 700-mb. level these winds were as much as 10 m. p. s. above normal. This strong westerly current separated into two branches in the eastern Pacific, one current flowing northeastward through the Gulf of Alaska, the other southeastward into the deep middle- and low-latitude trough in the eastern Pacific (fig. 3A). Wind speeds at 700 mb. in this latter area were much below normal (fig. 3B) as a result of the difluent circulation pattern.

One typhoon, named Phyllis, was observed in the Pacific during May. This storm, with sustained winds of 160 kt. and gusts to 200 kt., was first located on the 26th near 7° N., 150° E. Moving slowly northward in a weak low-latitude trough (fig. 6), the storm caused little damage before becoming extra-tropical on June 1.

7. INTRA-MONTHLY TRANSITION

Significant changes occurred in the general circulation between the first and second halves of May. These are best seen by reference to figure 10 which shows the mean 700-mb. maps for both halves of the month along with the height change between these charts. Areas of greatest change in the Western Hemisphere were found in northwestern North America and the central Atlantic (fig. 10C). The Pacific circulation during the first half of May was characterized by fast westerlies with two middle-latitude troughs and by difluence in the extreme eastern Pacific (fig. 10A). Amalgamation of these troughs during the latter half of the month increased the wavelength downstream, resulting in retrogression of the trough located near the Pacific coast of North America early in the month (fig. 10B). At the same time strong ridging occurred in western North America, the westerlies were displaced northward, difluence became more pronounced, and the eastern Pacific trough deepened and developed a closed center. These changes were accompanied by displacement northwestward of the High over Yucatan Peninsula to a position over northwestern Mexico (fig. 10A, B).

Of most direct influence upon the weather in the United States was the strengthening of the ridge and increase in heights from Mexico to Alaska (fig. 10C). The warmest weather in the West occurred during the latter half of May, with average temperatures for the week ending May 25 being as much as 15° F. above normal in northern Idaho [8]. Precipitation over the entire country averaged considerably less during the last half of May than it did during the first half. This is related directly to increased northerly flow components and to the rise in 700-mb. height anomaly over most of the Nation (fig. 10C).

Pronounced ridging also occurred in the central Atlantic where 700-mb. heights rose as much as 510 ft. from the first half to the last half of May (fig. 10C). The genesis of a new mean trough near 52° W., to the south of this ridging, was accompanied by forward motion of the major trough-ridge systems in Europe, with the trough over eastern Europe being replaced by a ridge (fig. 10 A, B). In the latter area 700-mb. heights rose over 500 ft. (fig. 10C).

Perhaps the most striking change occurred over the Kara Sea north of the Siberian Arctic. Here an extensive High cell early in May was replaced by a deep cyclonic vortex during the latter part of the month, as heights fell 610 ft. (fig. 10C).

REFERENCES

1. W. H. Klein, "The Weather and Circulation of February 1958—A Month with an Expanded Circumpolar Vortex of Record Intensity," *Monthly Weather Review*, vol. 86, No. 2, Feb. 1958, pp. 60–70.
2. J. Namias, "Characteristics of the General Circulation Over the Northern Hemisphere During the Abnormal Winter 1946–47," *Monthly Weather Review*, vol. 75, No. 8, Aug. 1947, pp. 145–152.
3. P. Stark, "The Weather and Circulation of April 1958," *Monthly Weather Review*, vol. 86, No. 4, Apr. 1958, pp. 132–140.
4. J. Namias, "The Annual Course of Month-to-Month Persistence in Climatic Anomalies," *Bulletin of the American Meteorological Society*, vol. 33, No. 7, Sept. 1952, pp. 279–285.
5. W. H. Klein, "The Weather and Circulation of May 1954—A Circulation Reversal Effected by a Retrogressive Anticyclone During an Index Cycle," *Monthly Weather Review*, vol. 82, No. 5, May 1954, pp. 123–130.
6. W. H. Klein, "The Weather and Circulation of May 1956—Another April-May Reversal," *Monthly Weather Review*, vol. 84, No. 5, May 1956, pp. 190–197.
7. C. R. Dunn, "The Weather and Circulation of May 1957—A Month with Severe Floods and Devastating Tornadoes in the Southern Plains of the United States," *Monthly Weather Review*, vol. 85, No. 5, May 1957, pp. 175–182.
8. U. S. Weather Bureau, *Weekly Weather and Crop Bulletin, National Summary*, vol. XLV, No. 21, May 26, 1958.

SOME INTERESTING ASPECTS OF A SUBTROPICAL DEPRESSION MAY 18–28, 1958

JOHN R. CLARK AND WILLIAM O. FRENCH

National Weather Analysis Center, U. S. Weather Bureau, Washington, D. C.

1. INTRODUCTION

During the period May 18–28, 1958 a subtropical depression formed in the Caribbean Sea and moved north-northeastward parallel to the east coast of the United States. The Low became extra-tropical and continued northward west of Greenland. This system had many interesting features. It gave heavy rains to the Miami area causing some local flooding. It had all the prospects of becoming a full scale hurricane but the winds never even reached storm speed (greater than 38 m. p. h.) until after the depression became extra-tropical. As this occurred the Low's vertical structure was peculiar. These points and others are discussed in this article.

2. ORIGIN OF DEPRESSION

The depression had its origin on the asymptote of an earlier vortex that originated on May 17, when Pacific air crossed over Panama at 0000 GMT. By 0000 GMT on the 18th the vortex was clearly fixed at San Andres near 13° 30′ N., 81° W.

The pibal from Maracaibo, Venezuela first showed westerly winds (at 6,000 to 7,000 ft.) at 1800 GMT on May 18, indicating the formation of a sink on the well-developed asymptote for the parent storm at San Andres. The original center was still near San Andres on May 19 with the new center, on the asymptote, clearly in evidence near Maracaibo. The 1200 GMT pibal from Maracaibo continued to show southwest winds at the top of the run, indicating the intensification of the vortex.

On May 20 at 0000 GMT, the new system began to revolve around the original vortex which was still located at San Andres. The new system continued to rotate on the 21st as it approached Jamaica, and by 0000 GMT on the 22d was nearing Grand Cayman, while the old center remained near San Andres. At 0000 GMT on May 23 the new center had become better organized and by 1200 GMT of that date a definite closed Low could be located at the surface at 20° N., 83° 30′ W. Thenceforth the depression slowly deepened and continued to move northward.

The Low formed over an area of warm water. Figure 2A shows that on May 21 the surface water temperatures

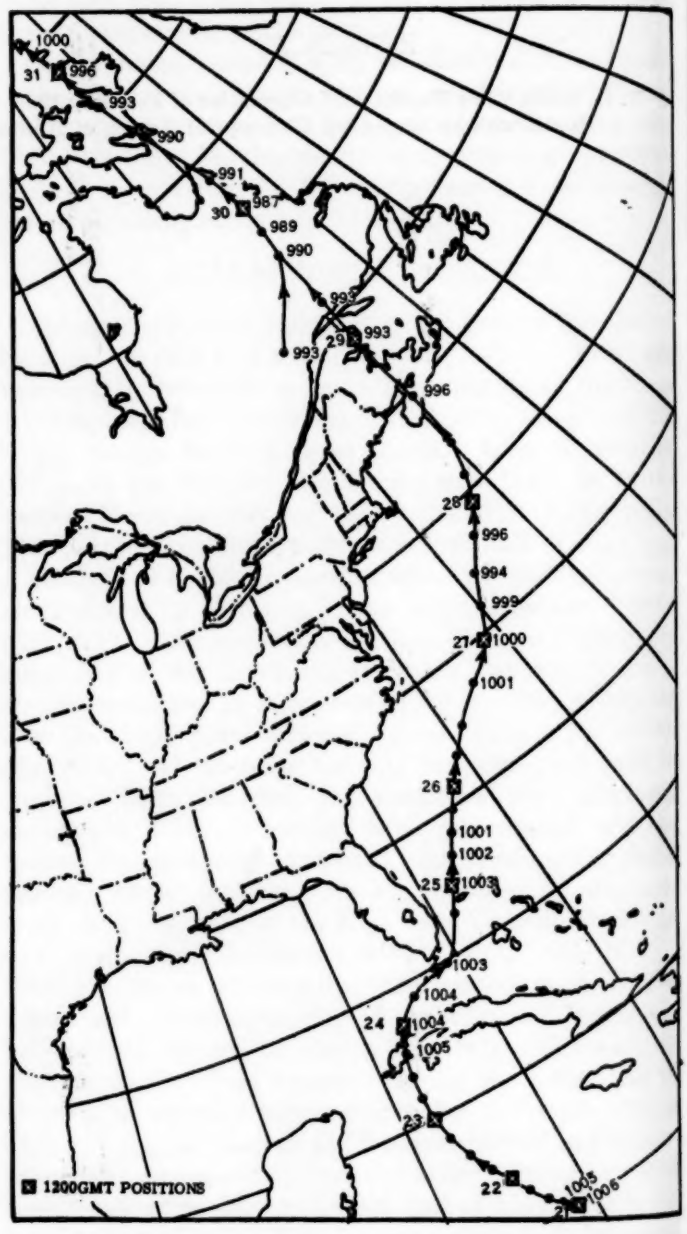

FIGURE 1.—Track of the depression including the track beyond the position when it became extra-tropical at 0000 GMT, May 27, 1958.

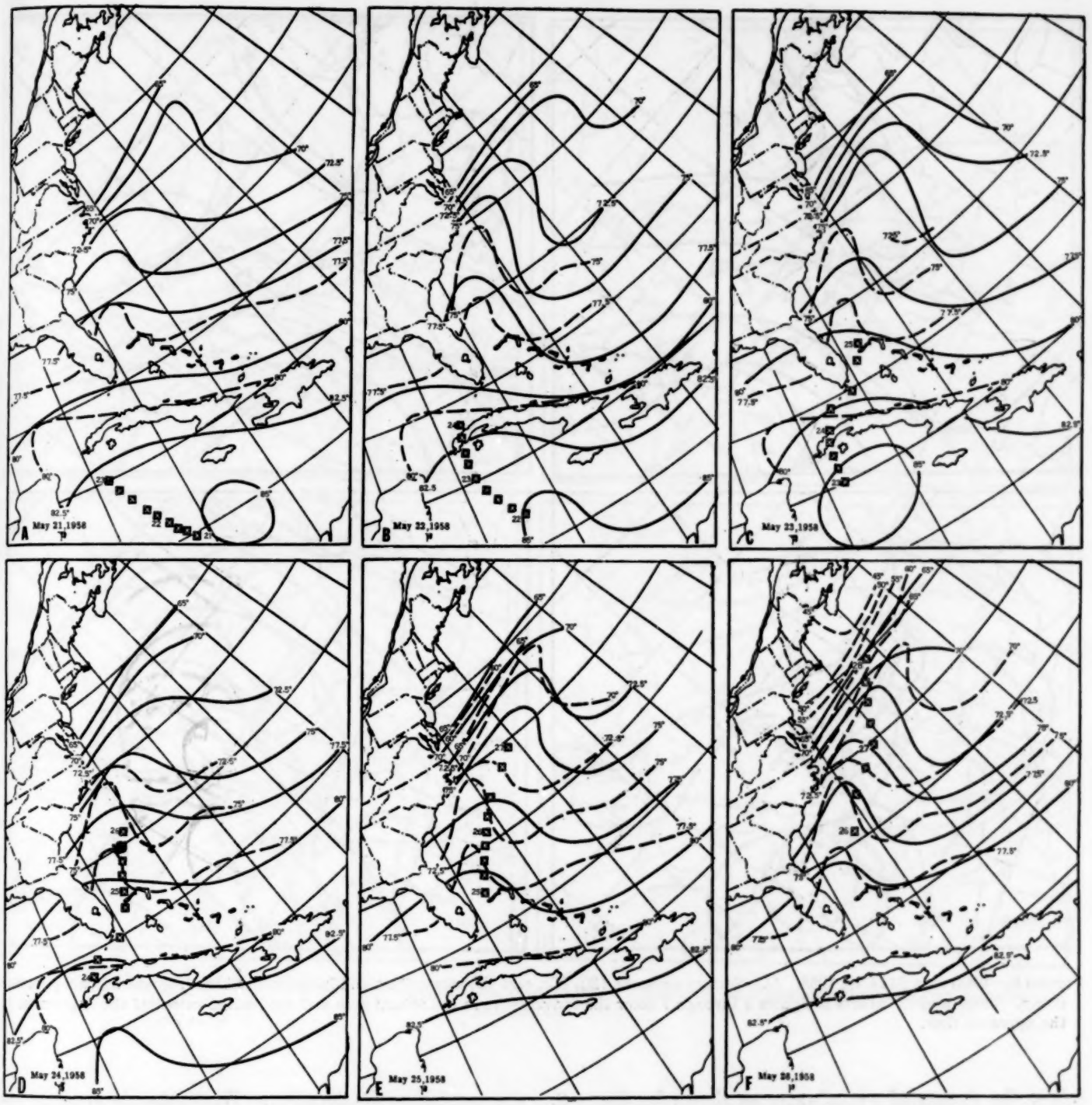

FIGURE 2.—Charts of the sea water temperature (solid lines) by days, for May 21–26. The normal sea water temperature for May is dashed. A portion of the storm track is superimposed to show the relationship between the direction of movement and the area of warm water.

were several degrees above normal in the area where the depression was forming.

3. TRACK OF DEPRESSION

After the circulation became well organized the depression moved northward and slightly eastward to a position at 24°30′ N., 82°30′ W. (fig. 1) by 1800 GMT, May 24. The system then took a more easterly direction as though trying to avoid the Florida peninsula or to follow the Gulf Stream between Cuba and Florida. After passing south of Florida the Low turned and began a northeasterly course on May 25.

As the depression moved northeastward it appeared to

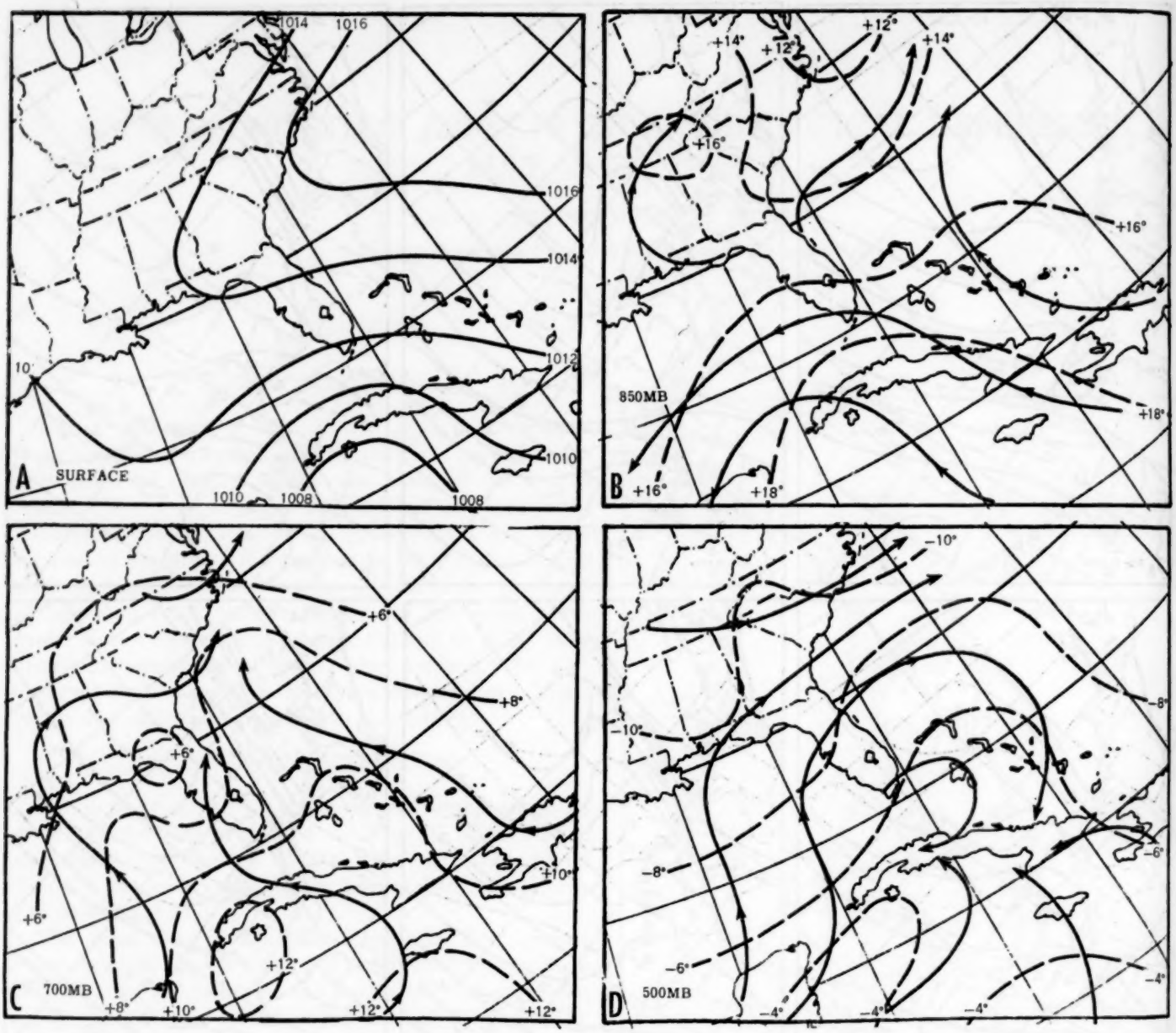

FIGURE 3.—0000 GMT, May 23, 1958. (A) Surface pressure, (B), (C), and (D) streamlines and isotherms at 850, 700, and 500 mb., respectively. These and the charts in figures 4 through 7 show the convergence in the Miami area and the limited extent of the depression in the upper-air flow.

follow the stream of warm water as shown by figure 2, where the track of the depression is superimposed on the surface water temperature charts as analyzed from ship reports. Reported water surface temperatures (solid lines in fig. 2) were above normal, consistent with the findings of Fisher [1]. The track shows that this depression continued to follow this warm stream of water through May 26.

4. PRECIPITATION IN THE MIAMI AREA

In a hurricane the northeast quadrant is expected to give the largest amounts of rainfall. While this depression never reached storm proportions the rainfall pattern fits the hurricane classification. When the depression was southwest of Miami the greatest area of convergence and curvature passed through Miami (figs. 3, 4, 5). This is evident on the 0000 GMT surface and 850-mb. charts of May 24 (fig. 4A, B). During the period of passage of the depression the total amounts of rainfall varied from 12.07 inches at Homestead, Fla. to 5.60 inches at Fort Lauderdale (fig. 8) with the greatest amounts concentrated in the Miami area. It can be concluded that the maximum curvature and convergence was concentrated in this location.

The upper-air soundings show almost complete saturation through 500 mb. for the 23d and 24th of May with

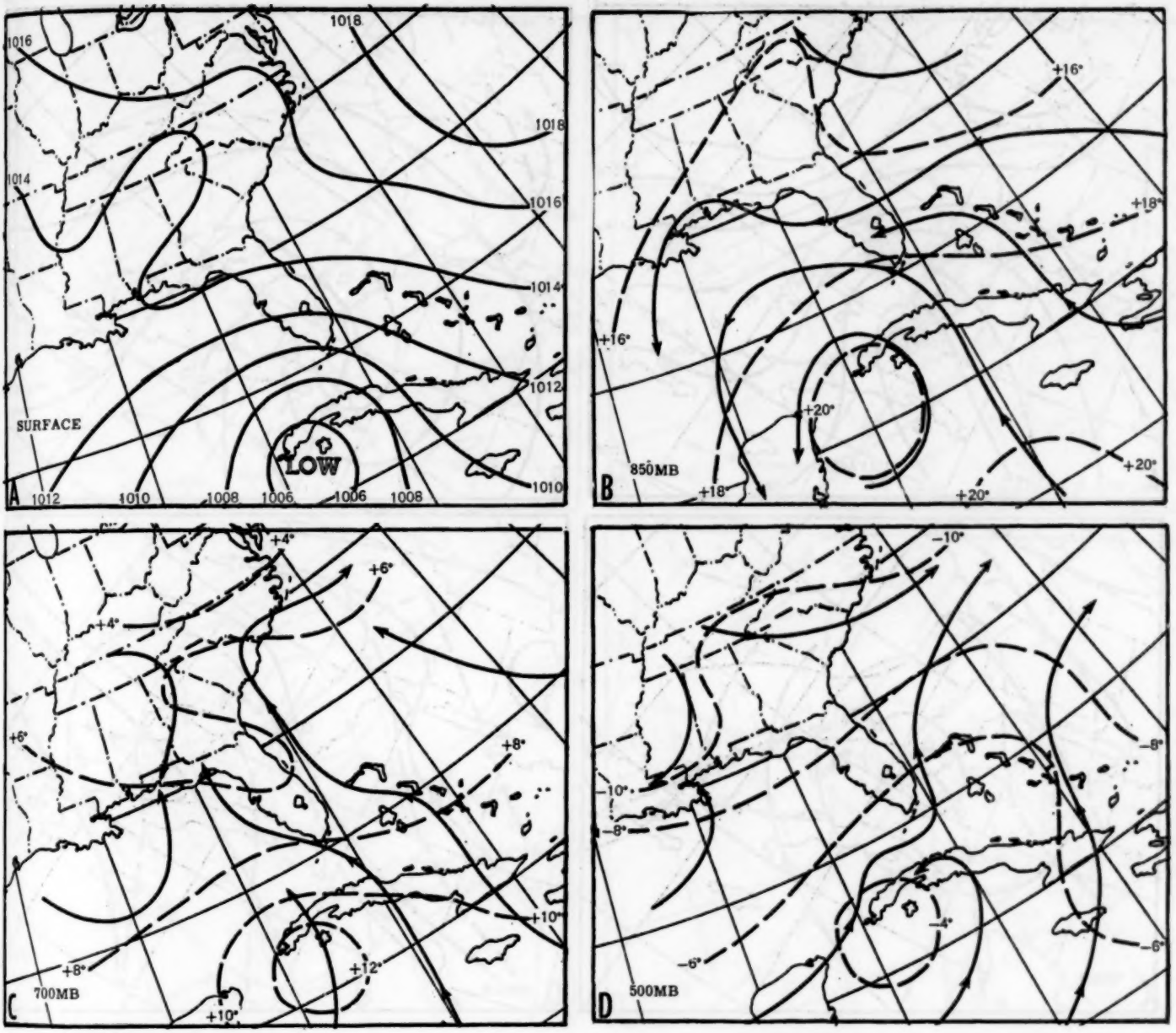

FIGURE 4.—0000 GMT, May 24, 1958. (A) Surface pressure, (B), (C), and (D) streamlines and isotherms for 850, 700, and 500 mb., respectively.

some drying out near 500 mb. at 1200 GMT, May 24 (fig. 9). The precipitable water values for these times were 1.65, 1.88, 1.80, and 1.57 inches, respectively. This compares with maximum precipitable water content of about 2.5 inches in hurricanes. As this area of convergence and curvature moved northeastward several island stations northeast and east of Miami reported large 6-hourly amounts of rainfall.

The rainfall of this system, when added to the rains of the month, gave WBO Miami 16.15 inches, the second wettest May since records began there in 1911 [2]. A total of 18.66 inches fell in 1925. Miami Airport recorded a monthly total of 18.14 inches, which was the greatest total fall for May during its 18 years of record. Miami Beach also broke its existing May record (since 1941) with a total fall of 11.70 inches. This period of heavy rain interrupted the harvesting of vegetables in Dade and Broward counties. Some crops showed a loss in production in the area of extremely heavy rains [3].

5. VERTICAL DEVELOPMENT

Throughout the Low's history as a depression its vertical structure never developed very much. As figures 3–7 show, while the Low deepened at the surface, the upper-air picture did not become well organized. Only during

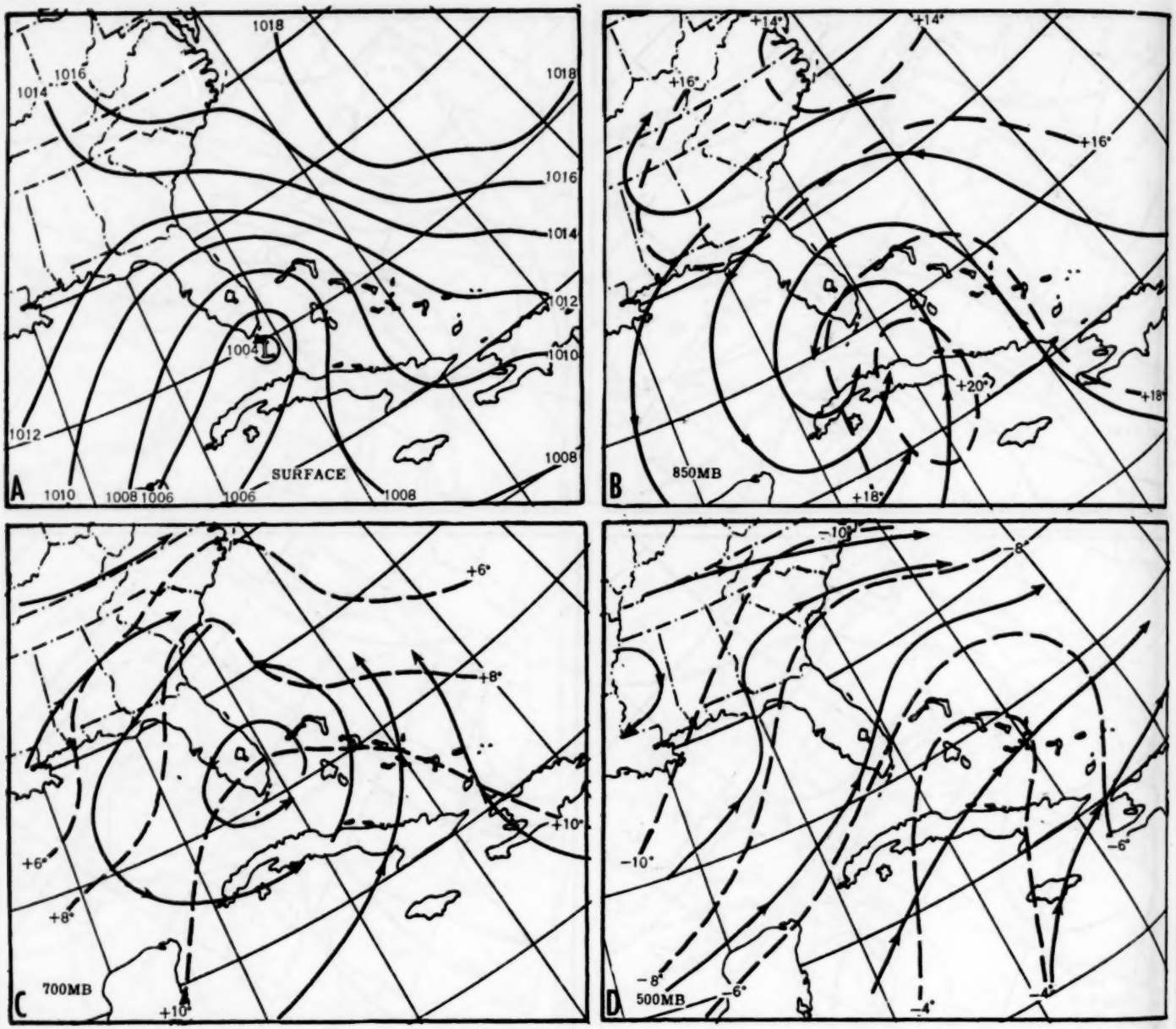

FIGURE 5.—0000 GMT, May 25, 1958. (A) Surface pressure, (B), (C), and (D) streamlines and isotherms for 850, 700, and 500 mb., respectively.

May 24, 25, and 26 did the Low build to any great height, and even on these days the structure developed only through the 700-mb. level, with the 500-mb. level never showing a closed circulation. Examination of the upper air through 200 mb. during the Low's history never shows any level of definite divergence.

Malkus [4] has set certain conditions for a depression to become a full grown hurricane. Although she refers to a depression formed on an easterly wave, it can be assumed that the requirements for development are applicable in this situation. This Low, although having a warm core, did not have the temperature discontinuity Malkus feels necessary for development. Without this temperature discontinuity or the more necessary upper-level divergence, this depression never reached the stage of forming an eye. The formation of an eye is referred to by Malkus as the point of no return.

Examination of the charts (fig. 5A, B) also shows some signs of a secondary circulation at the surface and at the 850-mb. level southwest of the main Low. This secondary Low may have robbed the primary system of enough energy to prohibit the main Low from becoming a major storm.

6. FORECASTING DIFFICULTIES

On May 26 the position and recent movement of the Low up the coast presented a forecasting problem as to its future movement. The forecaster who made the surface

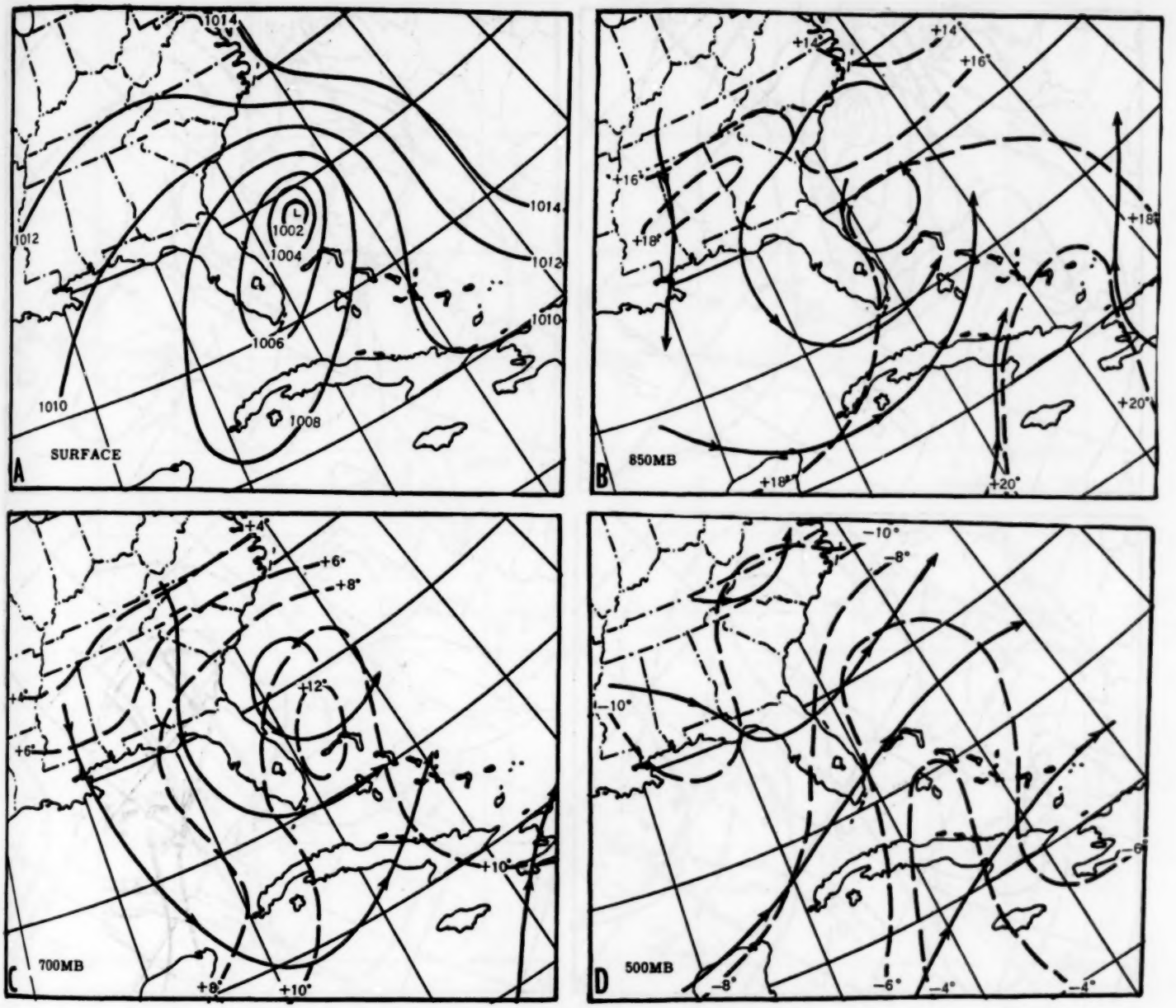

FIGURE 6.—0000 GMT, May 26, 1958. (A) Surface pressure, (B), (C), and (D) streamlines and isotherms at 850, 700, and 500 mb. respectively.

prognostic chart from the 1200 GMT chart used the 500-mb. flow to forecast the movement of the Low. This upper-air flow indicated the system would continue to move on its northeasterly course.

The succeeding forecaster had another problem to face. The surface High located over the eastern Great Lakes region appeared to be moving eastward across the path of the Low. Since the High appeared to be moving to the north or north-northeast of the current path of the Low, the forecaster expected the High to block the Low for a period of about 18 hours and force the system into a more northerly course. Using this reasoning the Low was forecast to hit the east coast near Wilmington, N. C. (fig. 10).

At the same time the District Forecaster at Washington, D. C., had used comparable reasoning to bring the Low to the coast. The District Forecast Office at Washington uses a rule in forecasting hurricanes and similar Lows, which briefly is as follows. When 12-hour pressure *rises* are in the path of a storm the Low will tend to turn to the left. Alternatively, when 12-hour pressure *falls* are in the path, the Low will tend to turn to the right. Using this forecast tool, the District Forecaster brought the storm into the coast and forecast cloudy skies with rain, the rain becoming heavy at times, for the coastal area from North Carolina to New England.

However, as sound as the reasoning was, these events

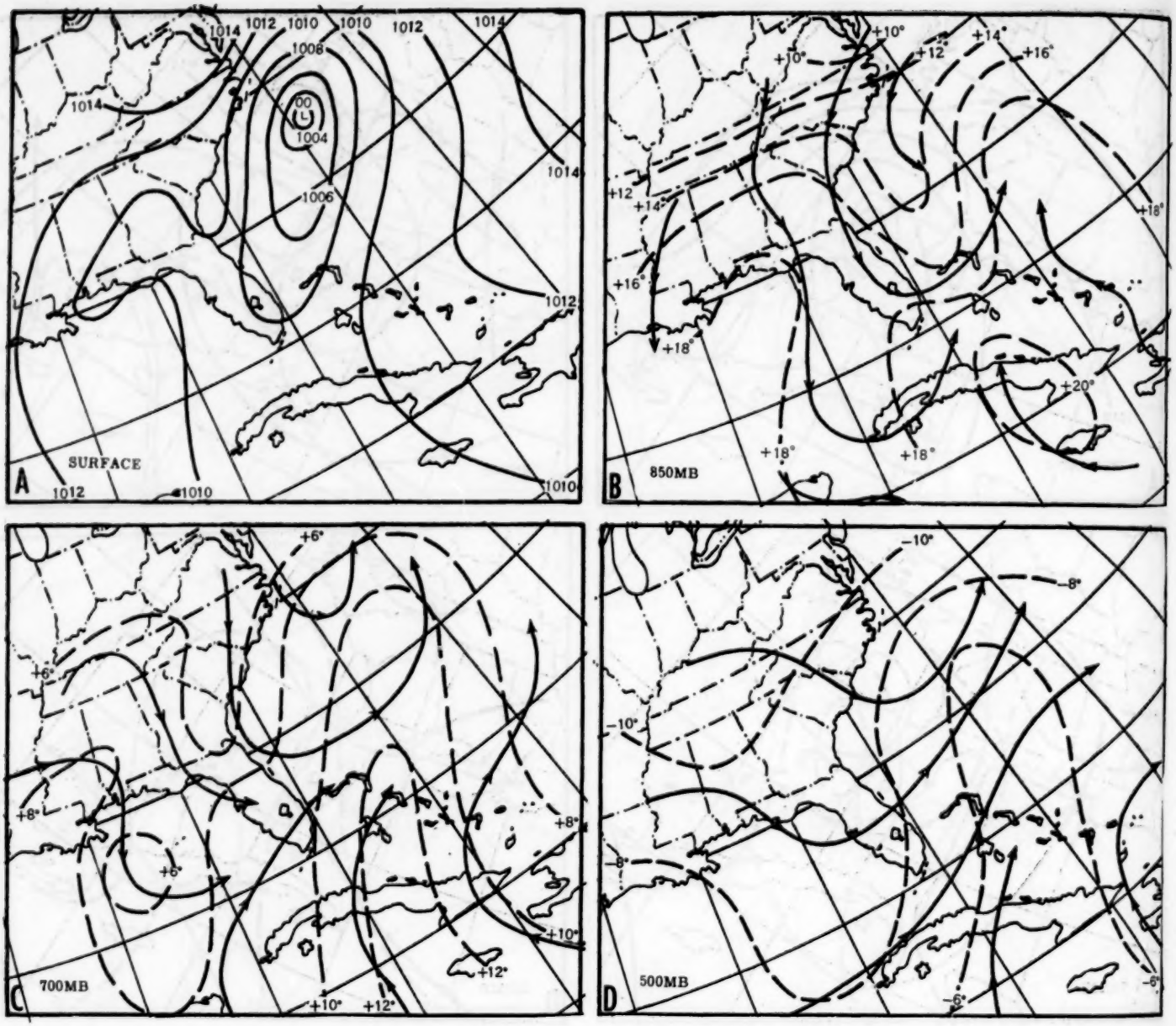

FIGURE 7.—0000 GMT, May 27, 1958. (A) Surface pressure, (B), (C), and (D) streamlines and isotherms at 850, 700, and 500 mb., respectively.

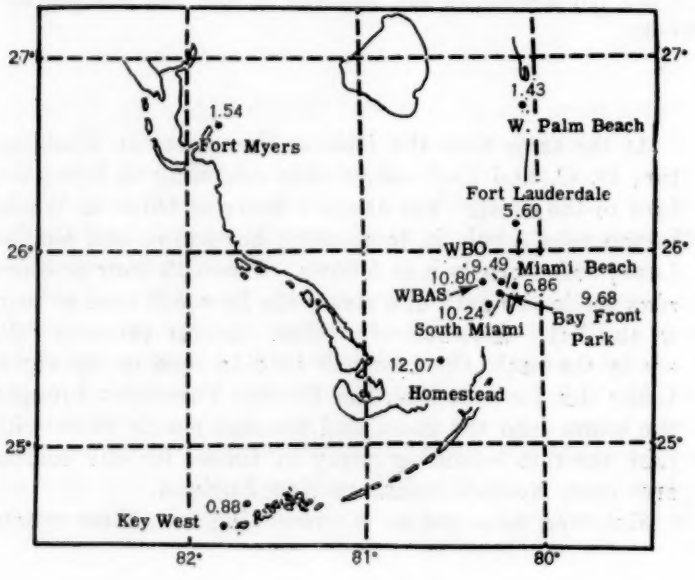

FIGURE 8.—Total amount of rainfall (inches) over central and southern Florida during the depression's passage.

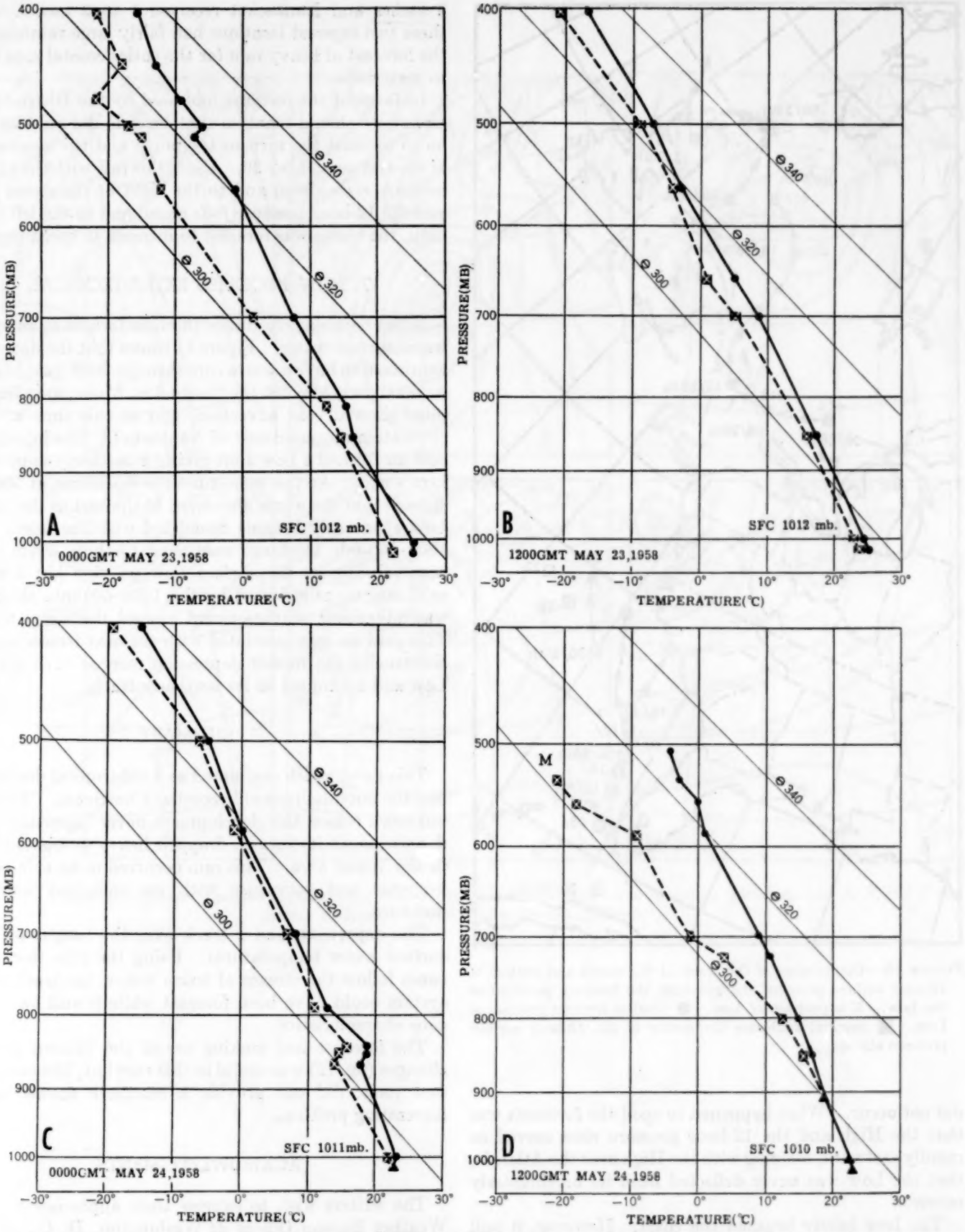

FIGURE 9.—Raob soundings for Miami for May 23–24, 1958 (solid lines=temperature, dashed lines=dew point). They show the large amount of moisture present in the atmosphere during the period of heavy rain. (A) 0000 GMT, May 23, (B) 1200 GMT, May 23, (C) 0000 GMT, May 24, and (D) 1200 GMT, May 24.

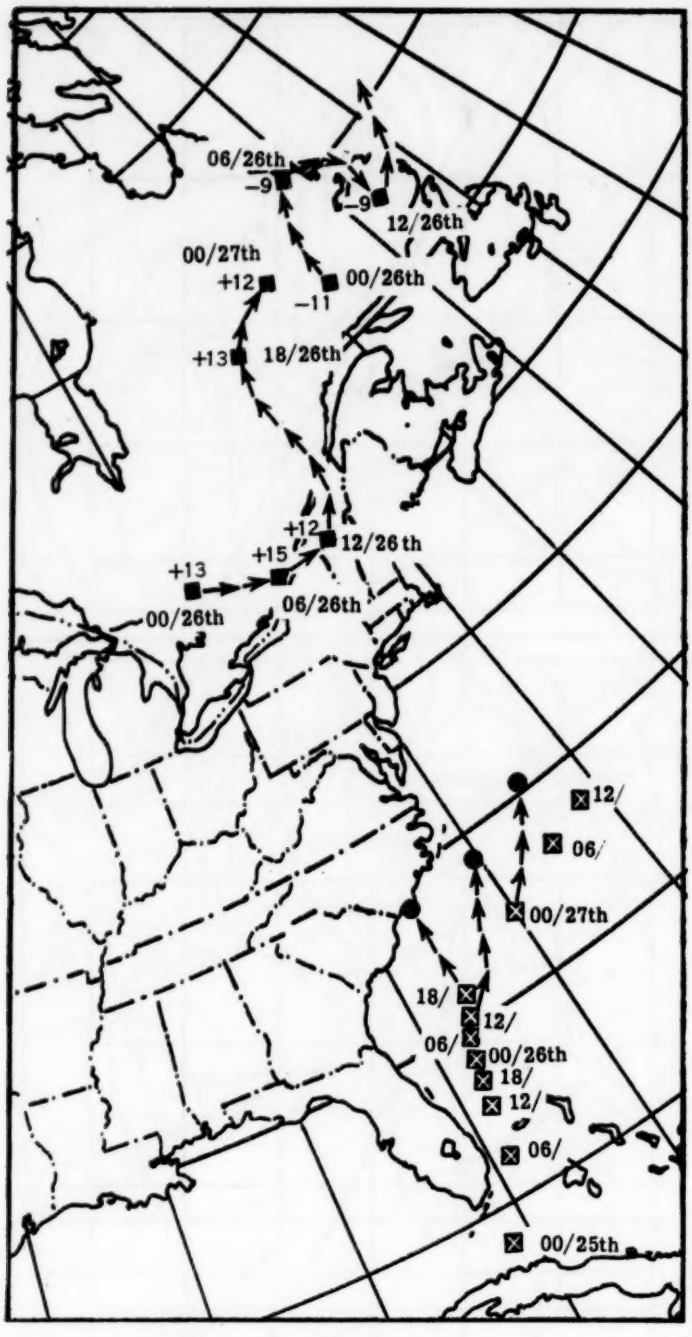

FIGURE 10.—Comparison of the track of the storm and centers of 12-hour surface pressure changes with the forecast positions of the Low. X is position of Low. ● (dot) is forecast position of Low. ■ (square) indicates the center of the 12-hour surface pressure change.

did not occur. What happened to spoil the forecasts was that the High and the 12-hour pressure rises moved so rapidly eastward, merging with the High over the Atlantic, that the Low was never deflected from its northeasterly course.

The Low barely brushed the coast. However, it still contained a large amount of moisture; Hatteras received 3 inches and Nantucket received 1 to 2 inches. Only these two exposed locations had fairly large rainfalls, and the forecast of heavy rain for the entire coastal area failed to materialize.

In favor of the forecast tool used by the District Forecaster, we should mention that his rule did aid him later on to forecast the turn to the north and the acceleration of the system on May 29. Using this rule with the 12-hour pressure *rises* ahead and to the right of the storm path, and the 12-hour pressure *falls* ahead and to the left of the path, the storm was forecast to increase in speed (fig. 12).

7. LOW BECOMES EXTRA-TROPICAL

It has been described how the Low formed in an area of warm surface water. Figure 11 shows that the depression continued to have a warm core through 0000 GMT, May 27. At 0000 GMT, May 28, the Nantucket, Mass., sounding and pibal showed cold advection, and at this time a closed circulation appeared east of Nantucket. The injection of cold air formed a Low aloft giving a northerly slope to the Low's axis. At the same time the isotherms at 500 mb. showed that the warm air veered to the east as the surface Low apparently became associated with the front. The 1000–500-mb. thickness continued to show warm thickness values over the surface Low position but a strong cold tongue, as reflected by the 1000–500-mb. thickness, was advancing southeastward around the warm tongue. This cold air was associated with the next frontal system. Eventually the former depression merged with the next Low and continued on its northerly track.

8. SUMMARY

This Low, which originated as a subtropical depression, had the potentialities of becoming a hurricane. For some unknown reason this development never happened. The depression, in its course, dropped heavy amounts of rain in the Miami area. This rain occurred in an area of convergence and curvature with an unlimited source of moisture.

The depression had a track over the tongue of warm surface water temperatures. Using the rule that hurricanes follow the stream of warm water, the track of this system could have been forecast while it still had hurricane characteristics.

The forecast tool making use of the 12-hour pressure changes (fig. 12) was useful in this case but, like most forecast tools, did not provide a complete answer to the forecasting problem.

ACKNOWLEDGMENTS

The writers wish to express their appreciation to the Weather Bureau Offices at Washington, D. C., Airport, at Miami, Fla., and at NHRP, West Palm Beach, Fla.,

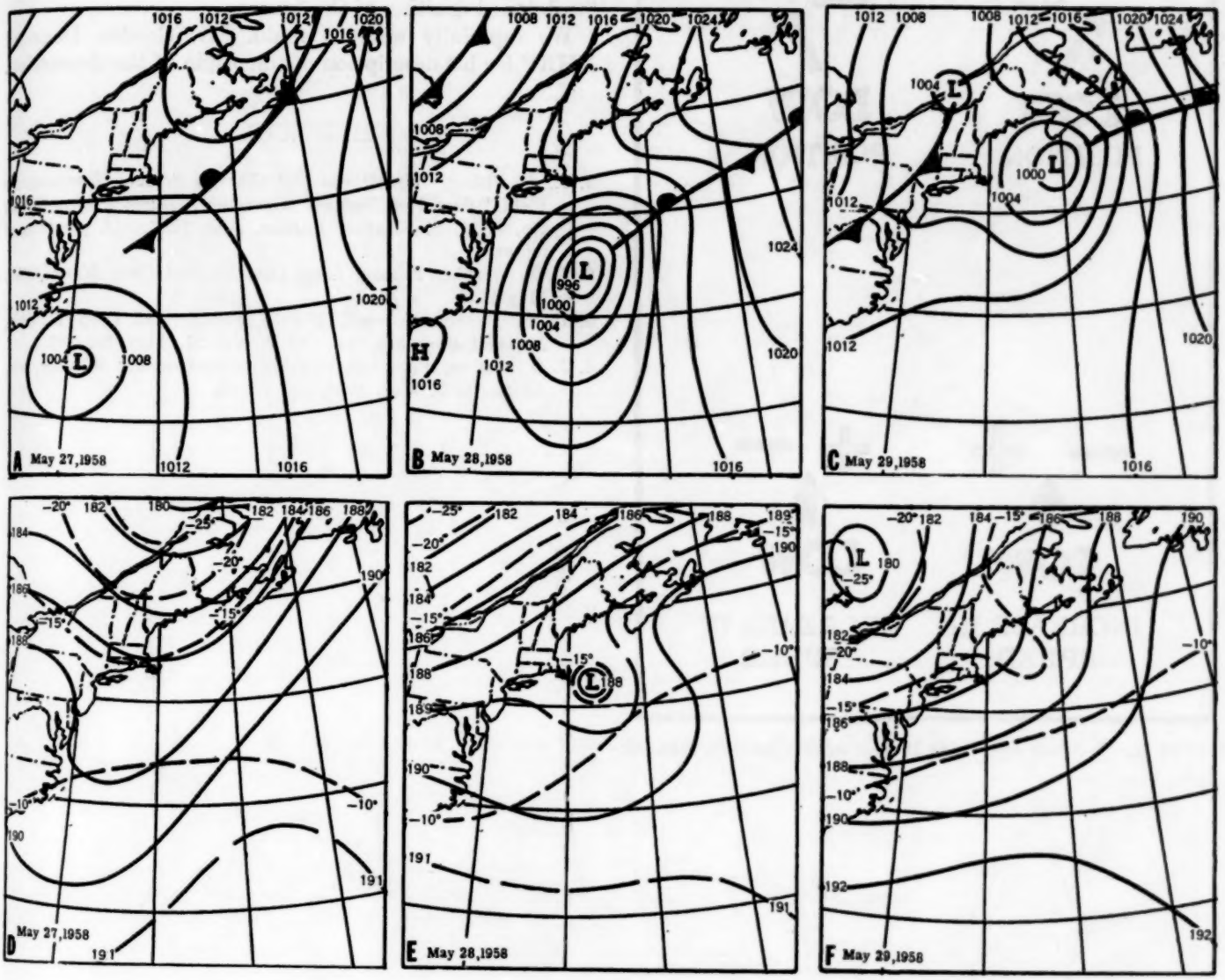

FIGURE 11.—Surface and 500-mb. analyses for 0000 GMT, May 27–29, showing the depression becoming extra-tropical. A, B, and C are surface analyses; D, E, and F are 500-mb. analyses.

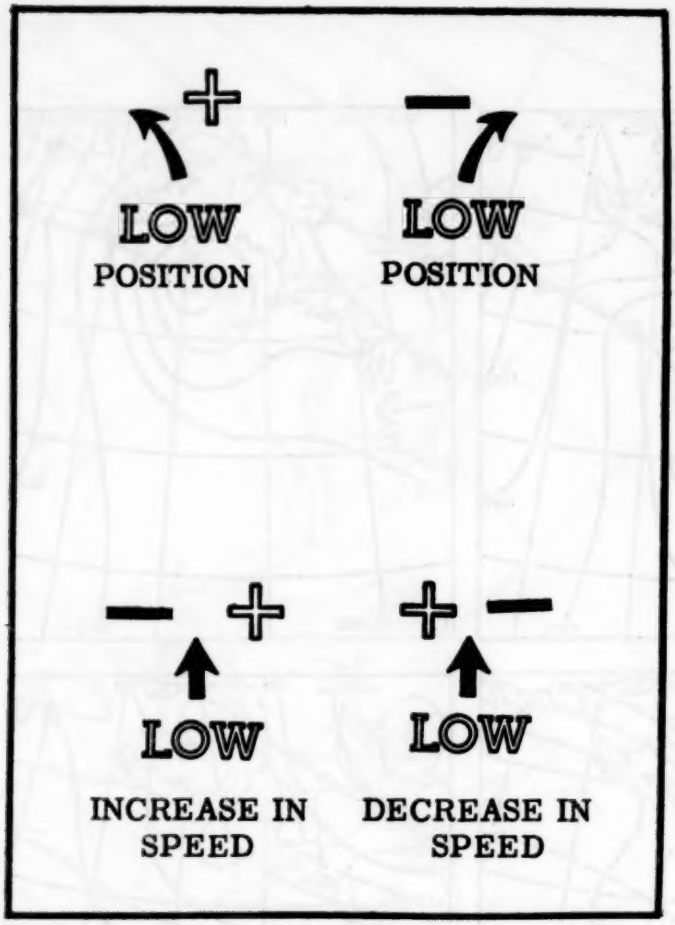

FIGURE 12.—Forecast rules using 12-hour surface pressure changes.

for information furnished; to the staff members of NAWAC for helpful suggestions and the reviewing of the article; and to the Daily Map Unit of the Weather Bureau for detailed drafting of the figures.

We especially wish to thank Mr. Gordon Dean of NHRP for his description of the origin of the depression.

REFERENCES

1. E. L. Fisher, "Hurricanes and the Sea Surface Temperature Field," Part I of *National Hurricane Research Project Report* No. 8, U. S. Weather Bureau, June 1957. (A pre-printed report.)
2. U. S. Weather Bureau, *Local Climatological Data, Miami, Fla.*, May 1958.
3. U. S. Weather Bureau, *Weekly Weather and Crop Bulletin, National Summary*, vol. XLV, No. 21, May 26, 1958.
4. J. S. Malkus, "Tropical Weather Disturbances," *Weather*, vol. XIII, No. 3, Mar. 1958, pp. 75–89.

U. S. GOVERNMENT PRINTING OFFICE: 1958

Chart I. A. Average Temperature (°F.) at Surface, May 1958

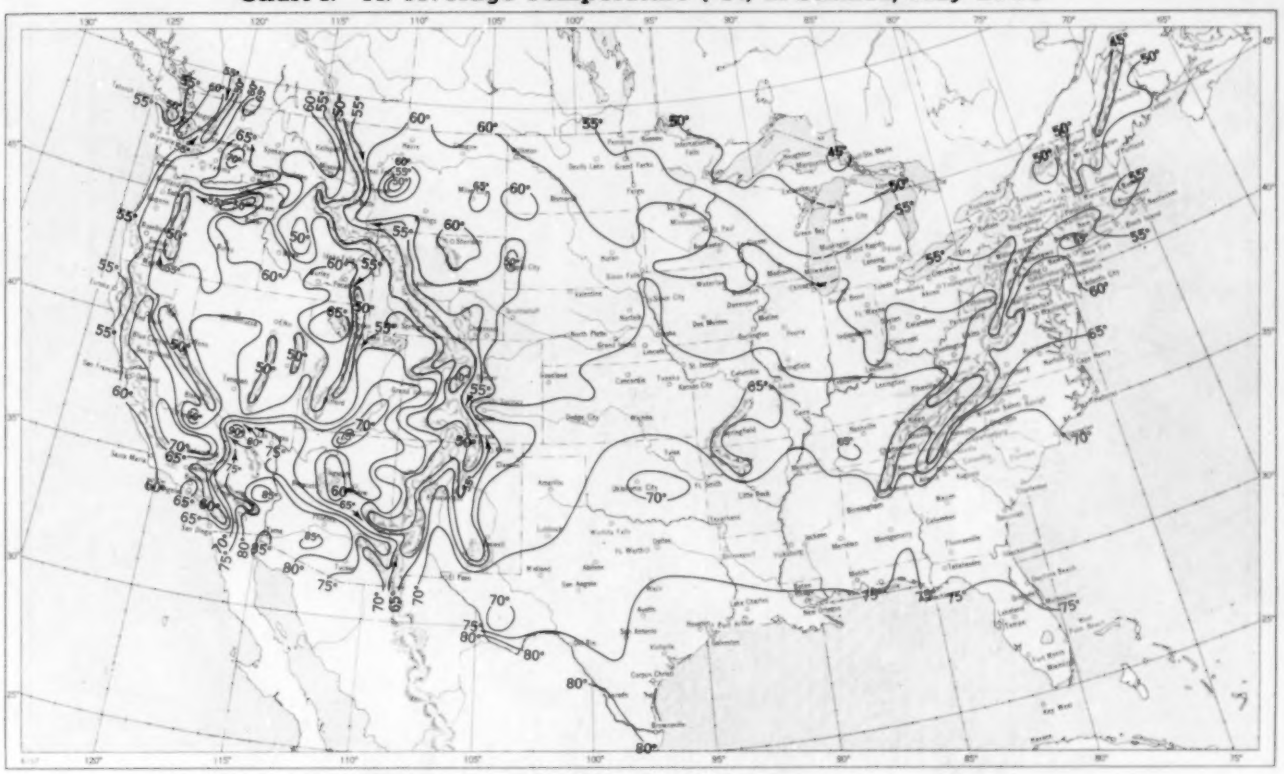

B. Departure of Average Temperature from Normal (°F.), May 1958.

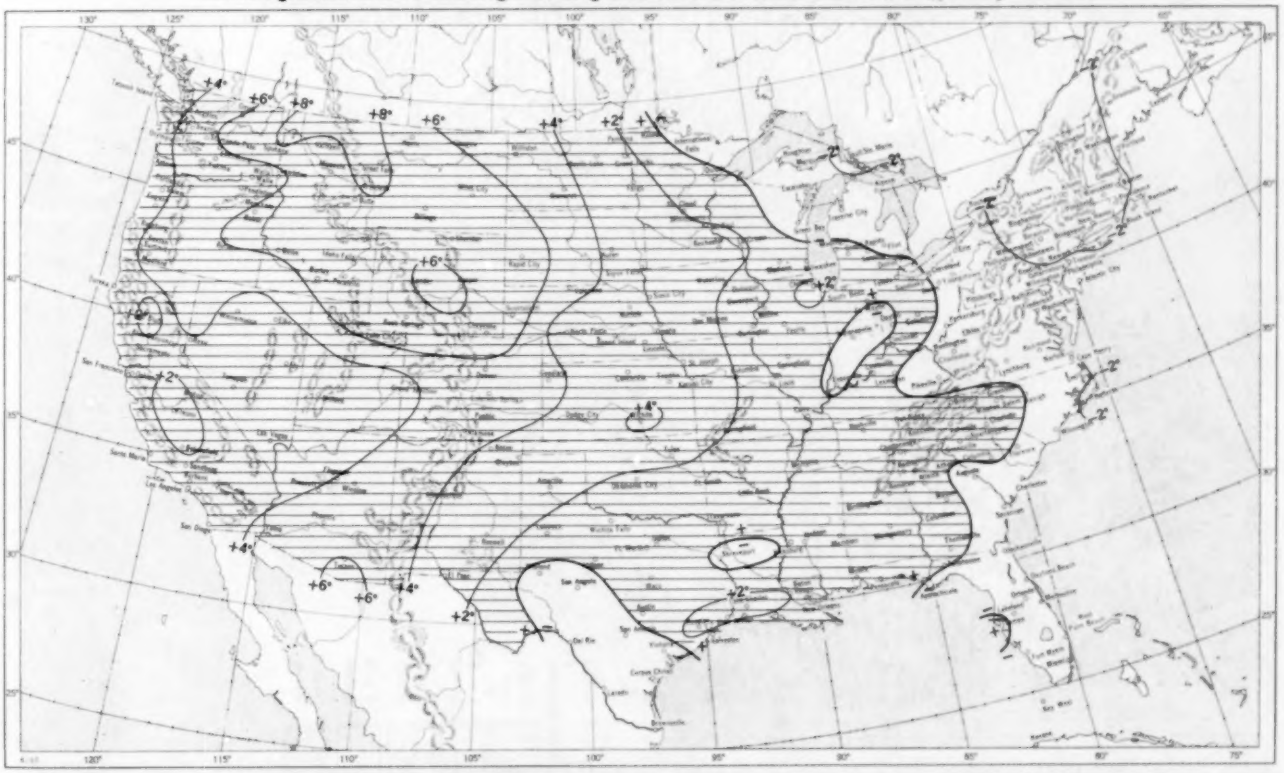

A. Based on reports from over 900 Weather Bureau and cooperative stations. The monthly average is half the sum of the monthly average maximum and monthly average minimum, which are the average of the daily maxima and daily minima, respectively.

B. Departures from normal are based on the 30-yr. normals (1921-50) for Weather Bureau stations and on means of 25 years or more (mostly 1931-55) for cooperative stations.

Chart II. Total Precipitation (Inches), May 1958.

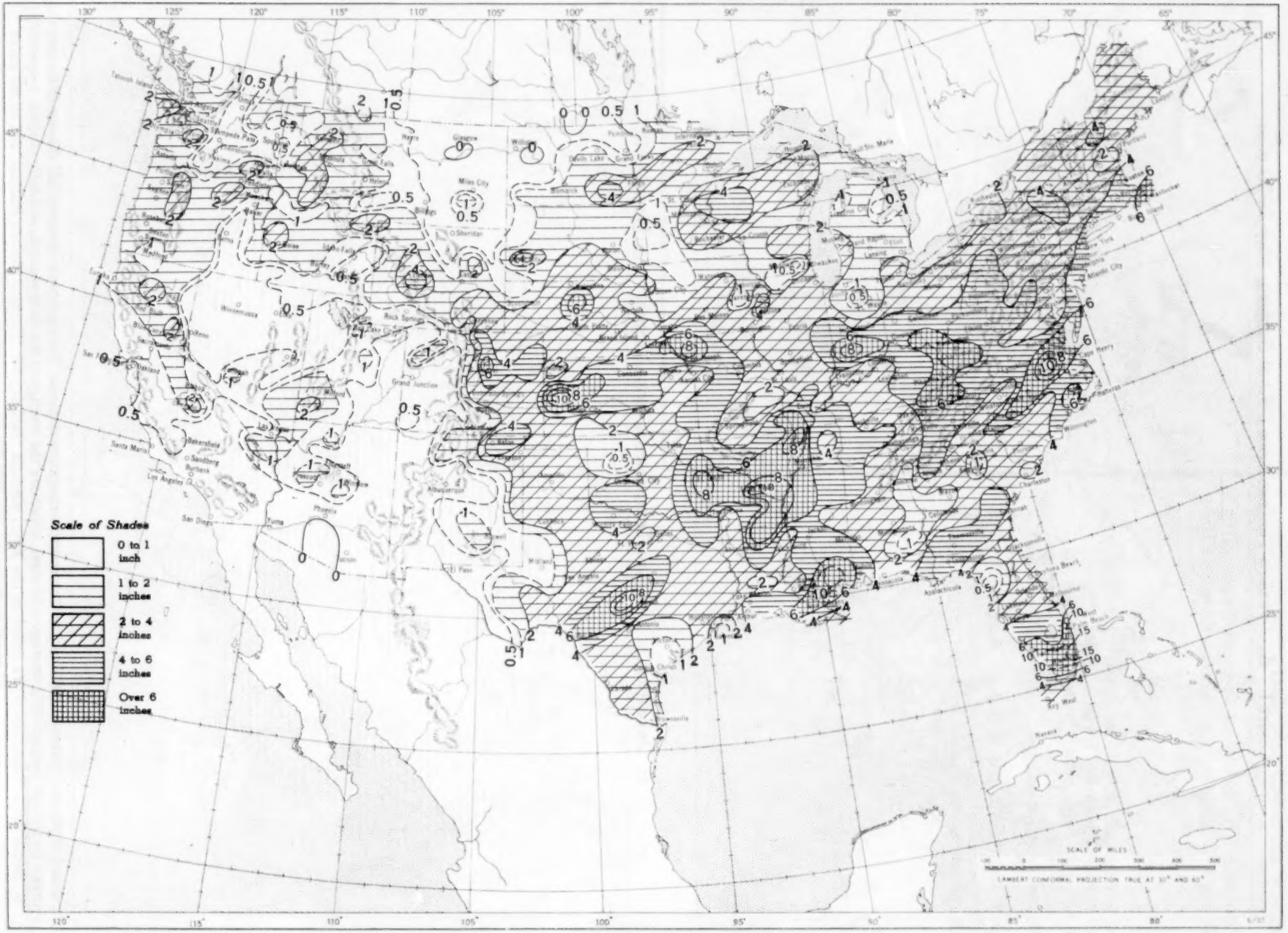
Scale of Shades
0 to 1 inch
1 to 2 inches
2 to 4 inches
4 to 6 inches
Over 6 inches
SCALE OF MILES
LAMBERT CONFORMAL PROJECTION TRUE AT 30° AND 60°

Based on daily precipitation records at about 800 Weather Bureau and cooperative stations.

Chart III. A. Departure of Precipitation from Normal (Inches), May 1958.

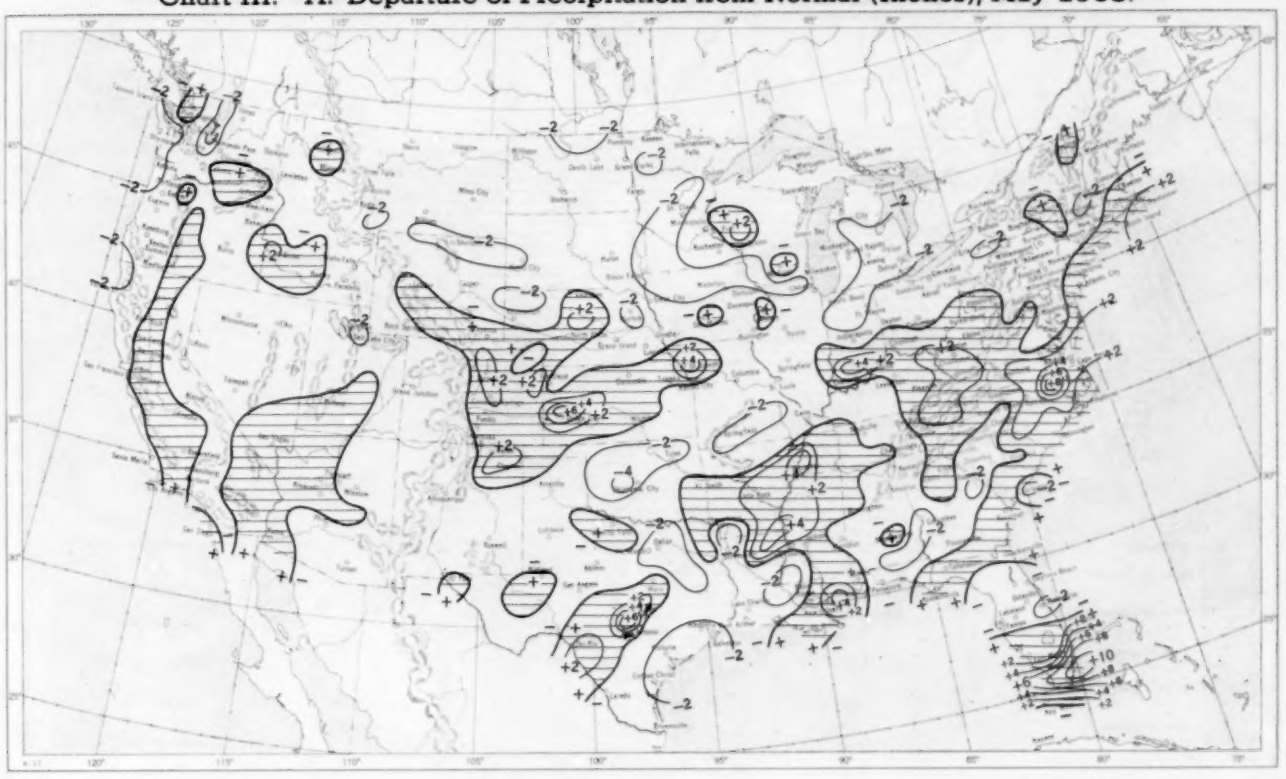

B. Percentage of Normal Precipitation, May 1958.

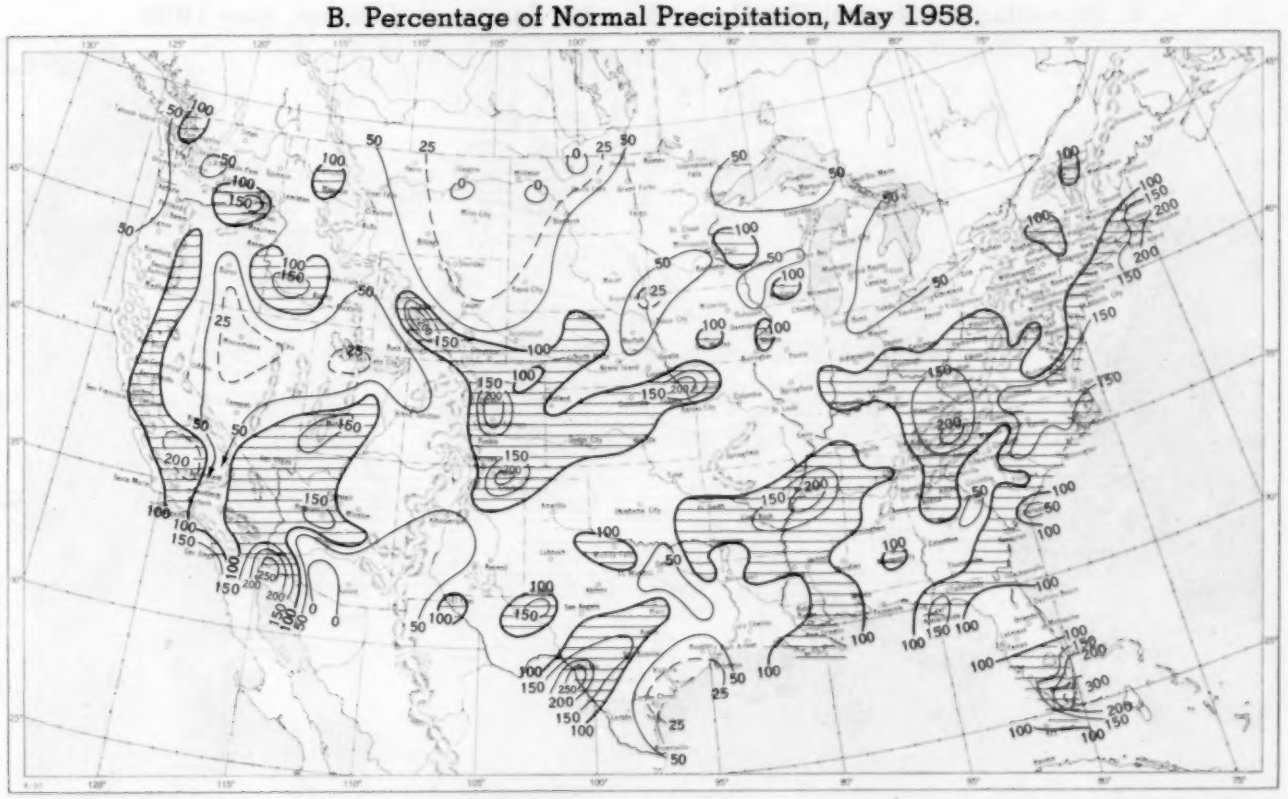

Normal monthly precipitation amounts are computed from the records for 1921-50 for Weather Bureau stations and from records of 25 years or more (mostly 1931-55) for cooperative stations.

Chart VI. A. Percentage of Sky Cover Between Sunrise and Sunset, May 1958.

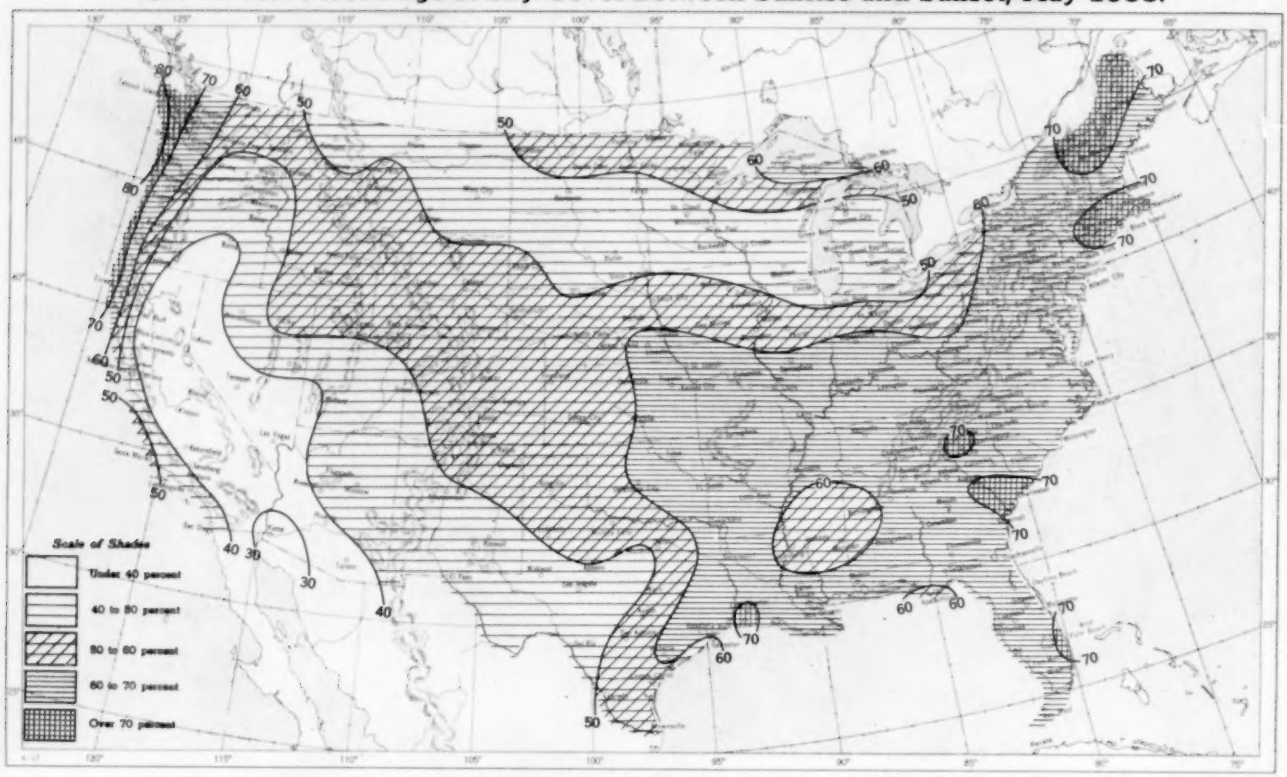

B. Percentage of Normal Sky Cover Between Sunrise and Sunset, May 1958.

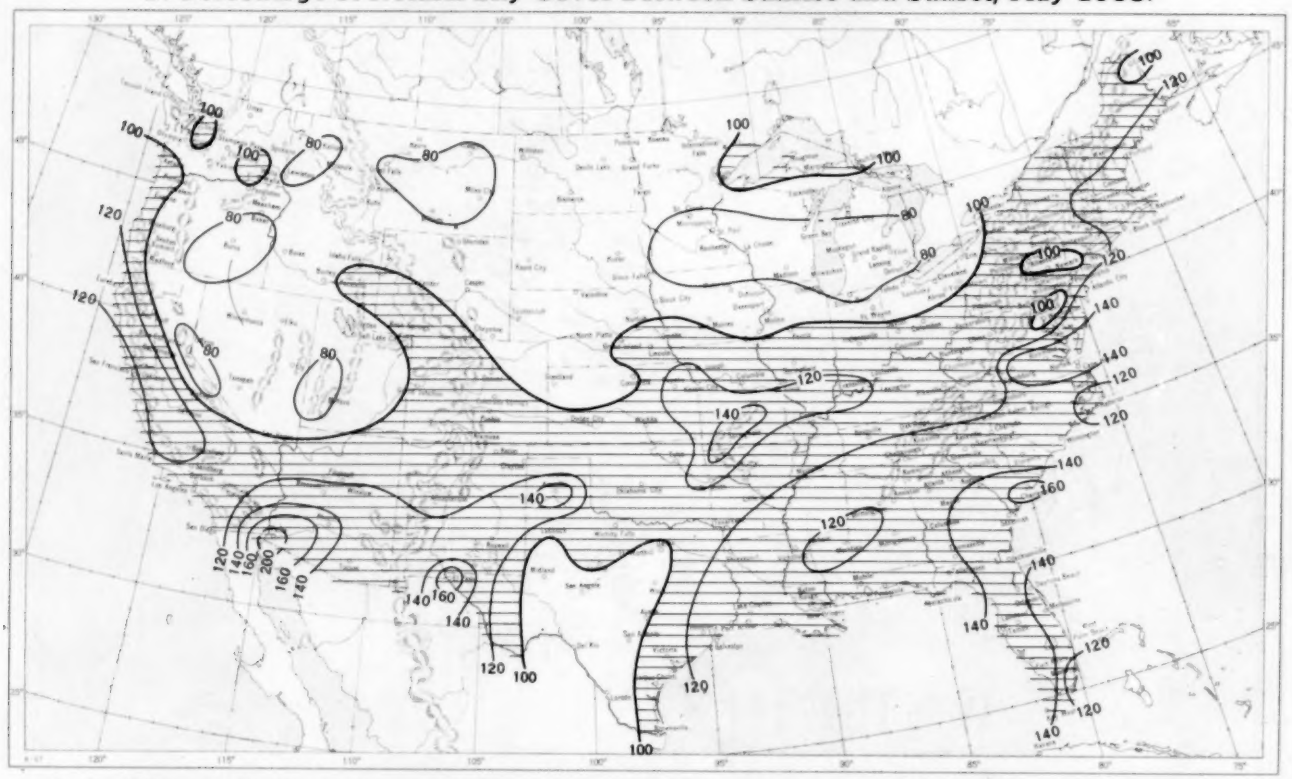

A. In addition to cloudiness, sky cover includes obscuration of the sky by fog, smoke, snow, etc. Chart based on visual observations made hourly at Weather Bureau stations and averaged over the month. B. Computations of normal amount of sky cover are made for stations having at least 10 years of record.

Chart VII. A. Percentage of Possible Sunshine, May 1958.

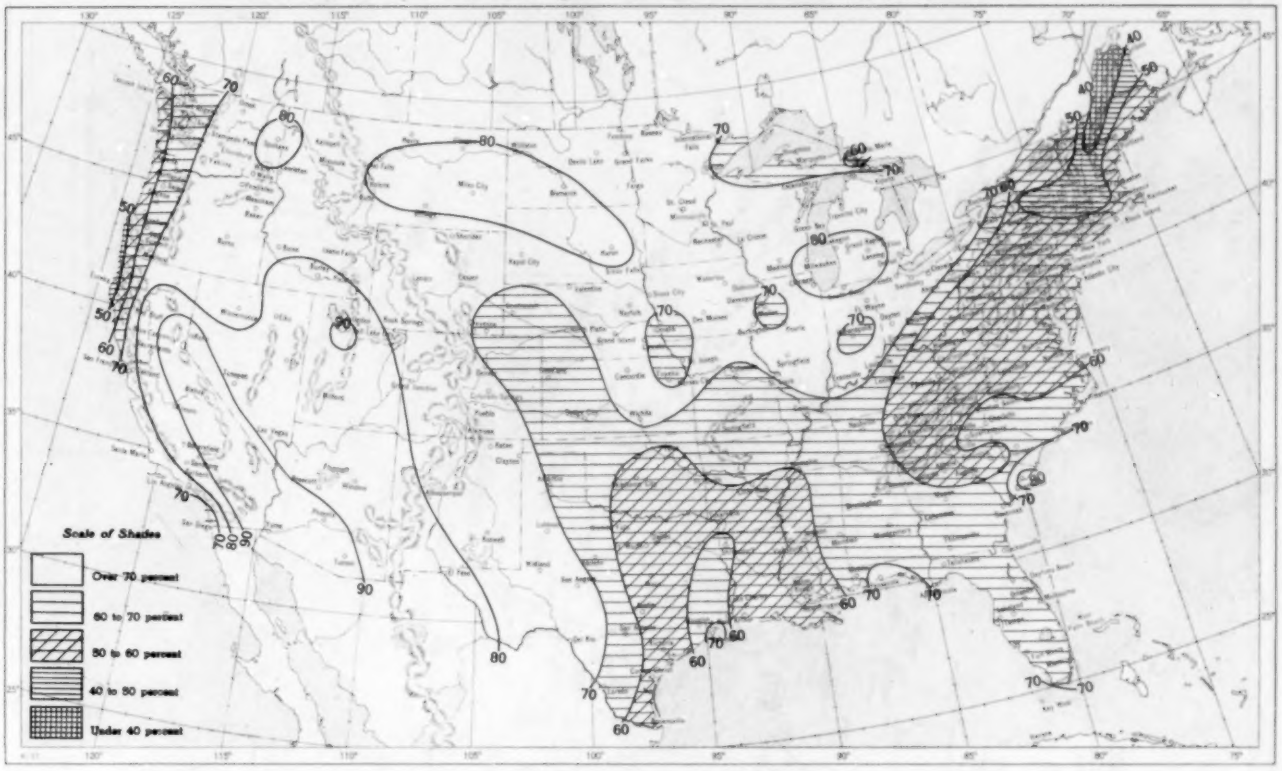

B. Percentage of Normal Sunshine, May 1958.

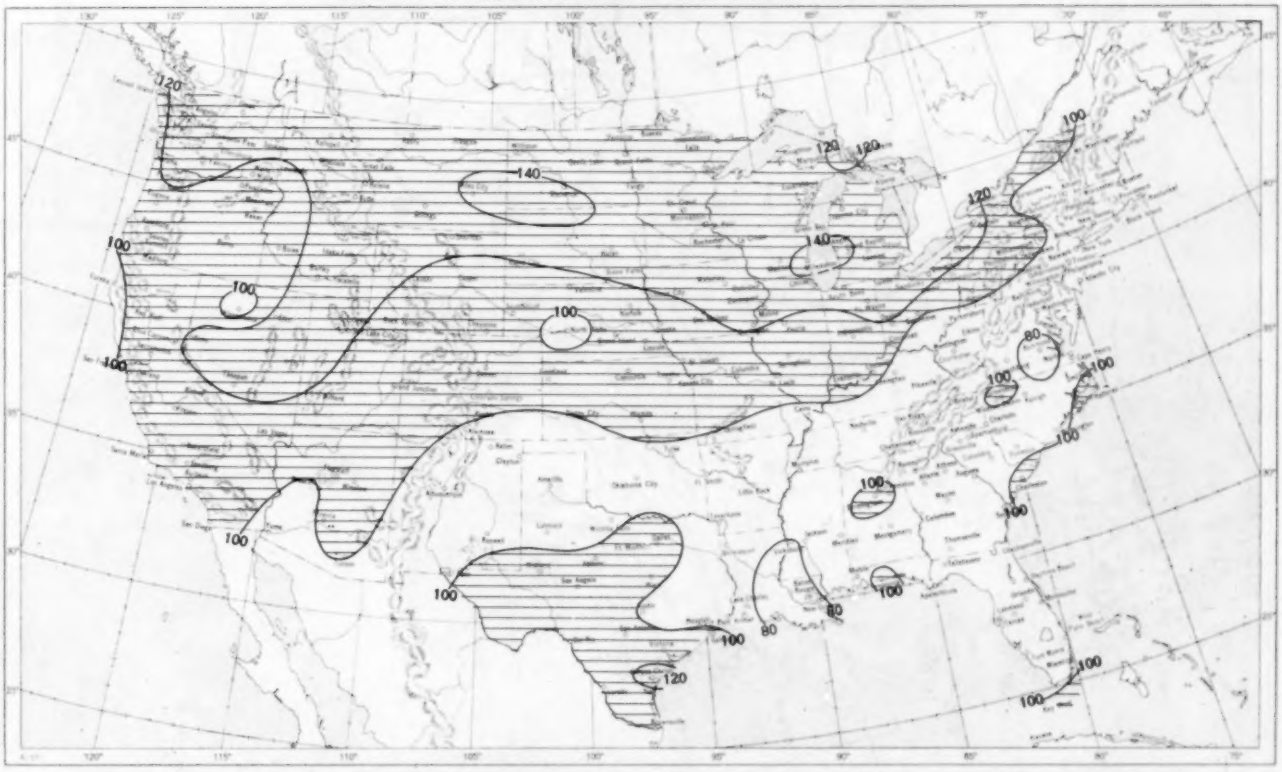

A. Computed from total number of hours of observed sunshine in relation to total number of possible hours of sunshine during month. B. Normals are computed for stations having at least 10 years of record.

Chart VIII. Average Daily Values of Solar Radiation, Direct + Diffuse, May 1958. Inset: Percentage of Mean Daily Solar Radiation, May 1958. (Mean based on period 1951-55.)

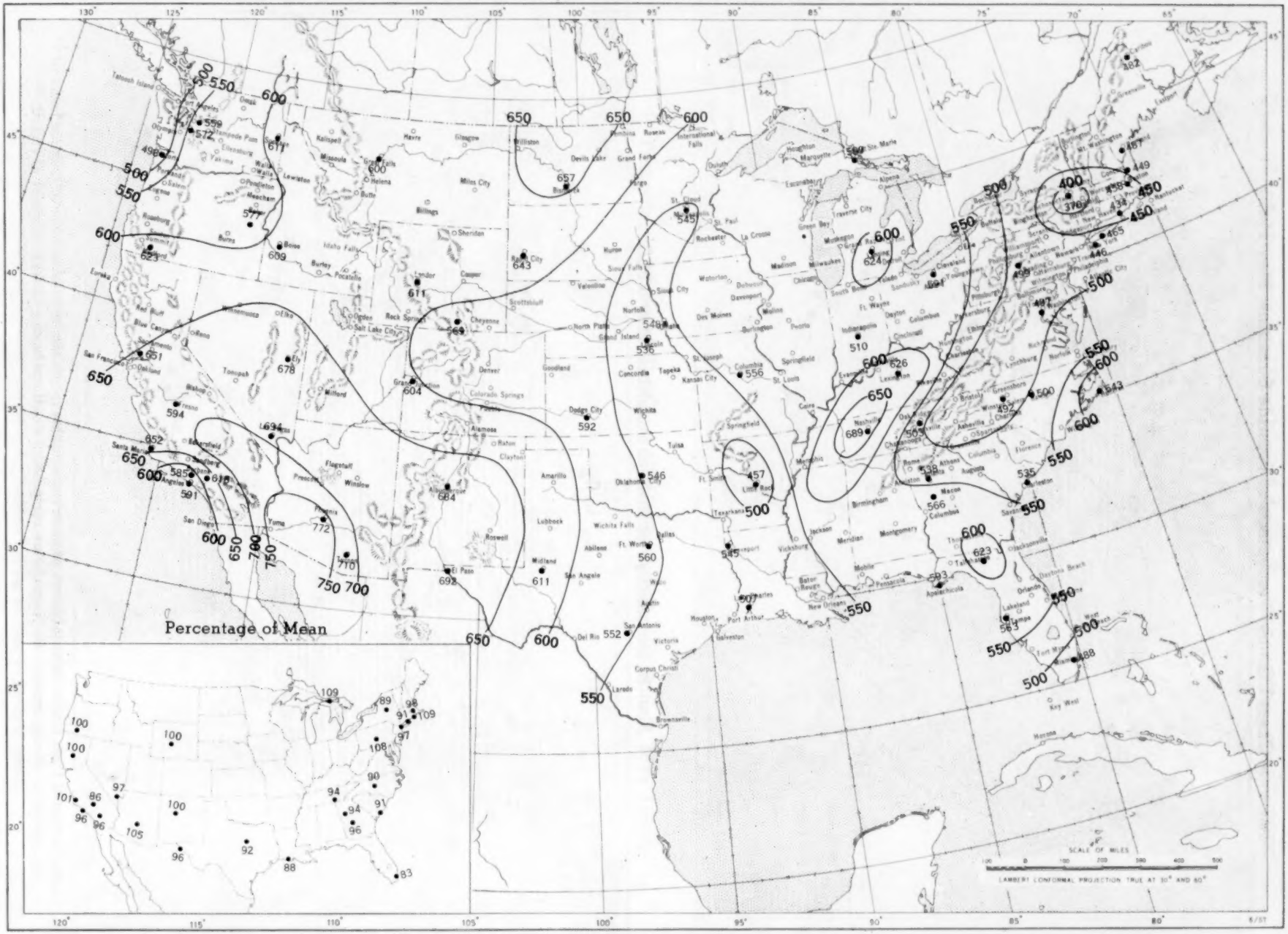

Chart shows mean daily solar radiation, direct + diffuse, received on a horizontal surface in langleys (1 langley = 1 gm. cal. cm. $^{-2}$). Basic data for isolines are shown on chart. Further estimates are obtained from supplementary data for which limits of accuracy are wider than for those data shown. The inset shows the percentage of the mean based on the period 1951-55.

Chart IX. Tracks of Centers of Anticyclones at Sea Level, May 1958.

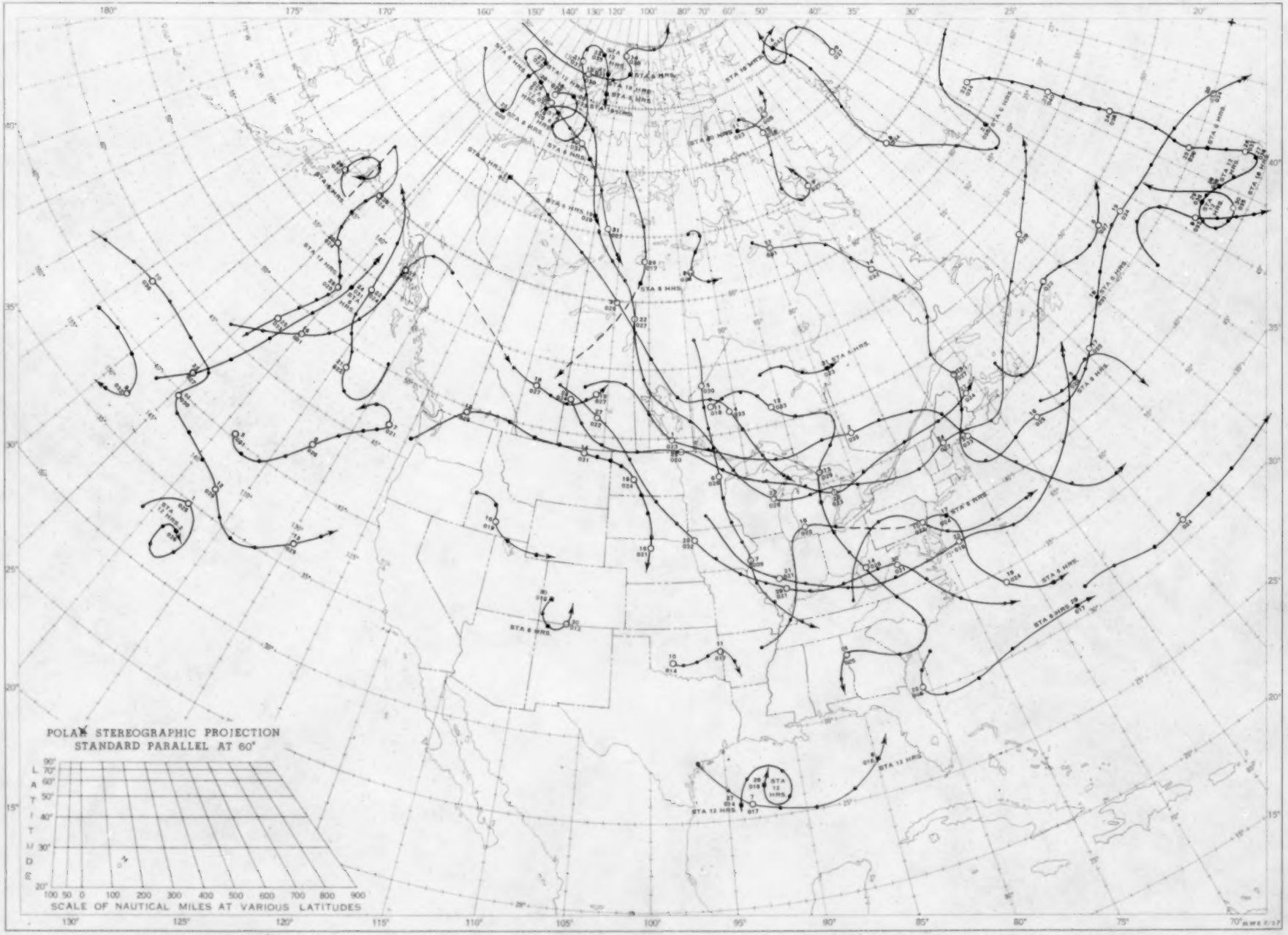

MAY 1958

Circle indicates position of center at 7:00 a. m. E. S. T. Figure above circle indicates date, figure below, pressure to nearest millibar. Dots indicate intervening 6-hourly positions. Squares indicate position of stationary center for period shown. Dashed line in track indicates reformation at new position. Only those centers which could be identified for 24 hours or more are included.

Chart X. Tracks of Centers of Cyclones at Sea Level, May 1958.

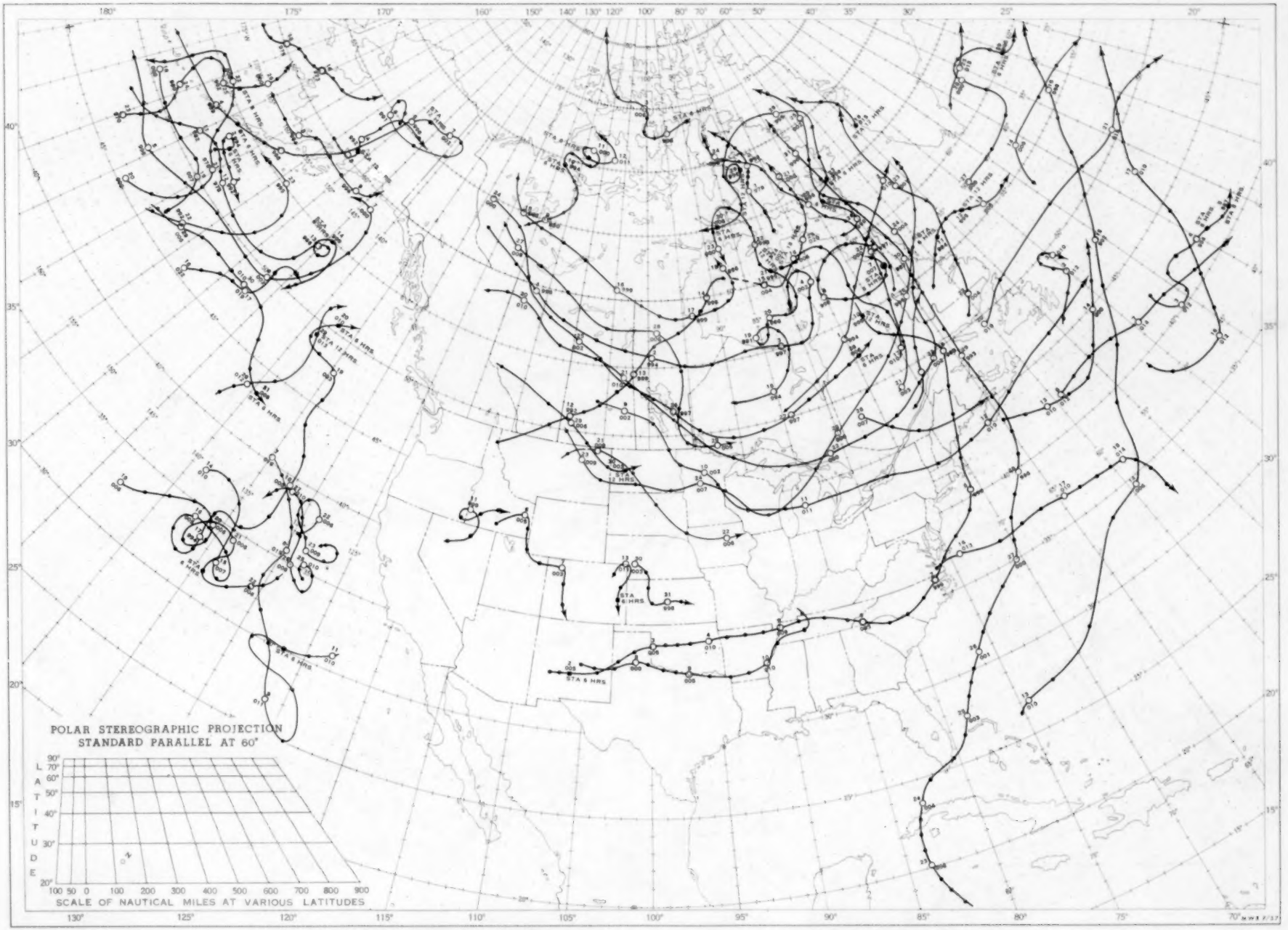
POLAR STEREOGRAPHIC PROJECTION
STANDARD PARALLEL AT 60°
LATITUDE
90° 70° 60° 50° 40° 30° 20°
100 50 0 100 200 300 400 500 600 700 800 900
SCALE OF NAUTICAL MILES AT VARIOUS LATITUDES

Circle indicates position of center at 7:00 a. m. E. S. T. See Chart IX for explanation of symbols.

Chart XI. Average Sea Level Pressure (mb.) and Surface Windroses, May 1958. Inset: Departure of Average Pressure (mb.) from Normal, May 1958.

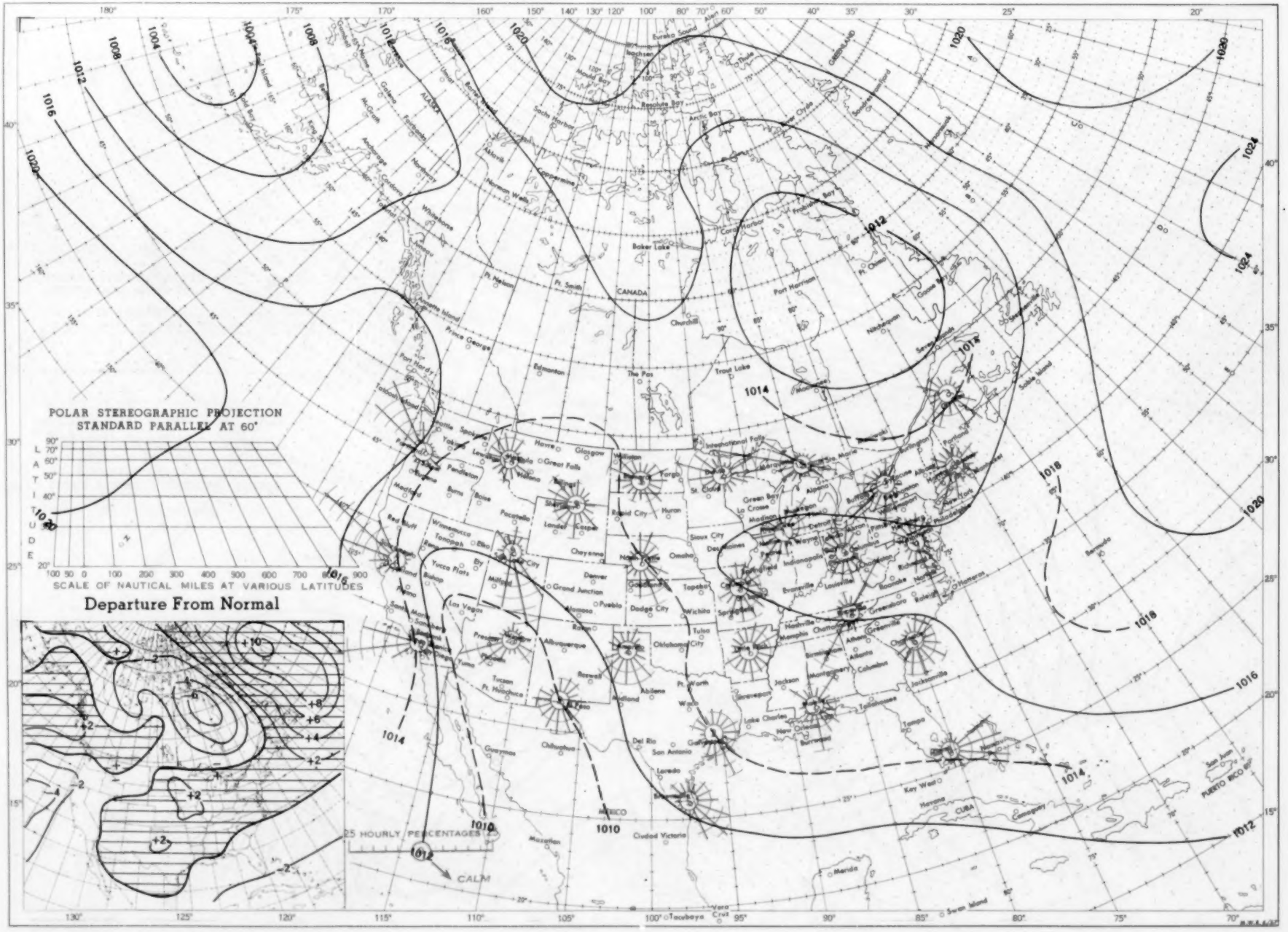

MAY 1958

Average sea level pressures are obtained from the averages of the 7:00 a. m. and 7:00 p. m. E. S. T. readings. Windroses show percentage of time wind blew from 16 compass points or was calm during the month. Pressure normals are computed for stations having at least 10 years of record and for 10° intersections in a diamond grid based on readings from the Historical Weather Maps (1899-1939) for the 20 years of most complete data coverage prior to 1940.

Chart XII. 850-mb. Surface, 1200 GMT, May 1958. Average Height and Temperature, and Resultant Winds.

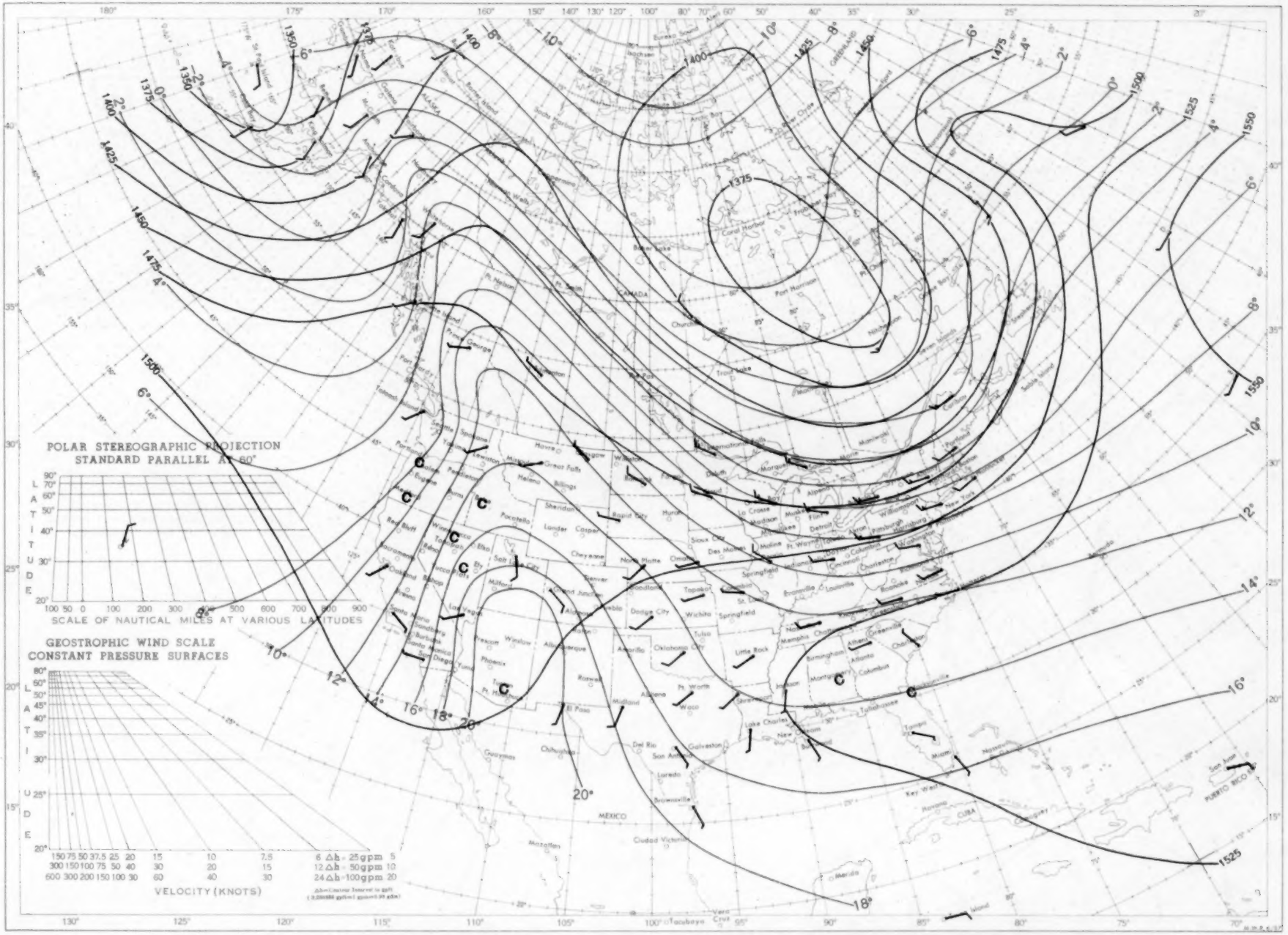

Height in geopotential meters (1 g.p.m. = 0.98 dynamic meters). Temperature in °C. Wind speed in knots; flag represents 50 knots, full feather 10 knots, and half feather 5 knots. All wind data are based on rawin observations.

Chart XIII. 700-mb. Surface, 1200 GMT, May 1958. Average Height and Temperature, and Resultant Winds.

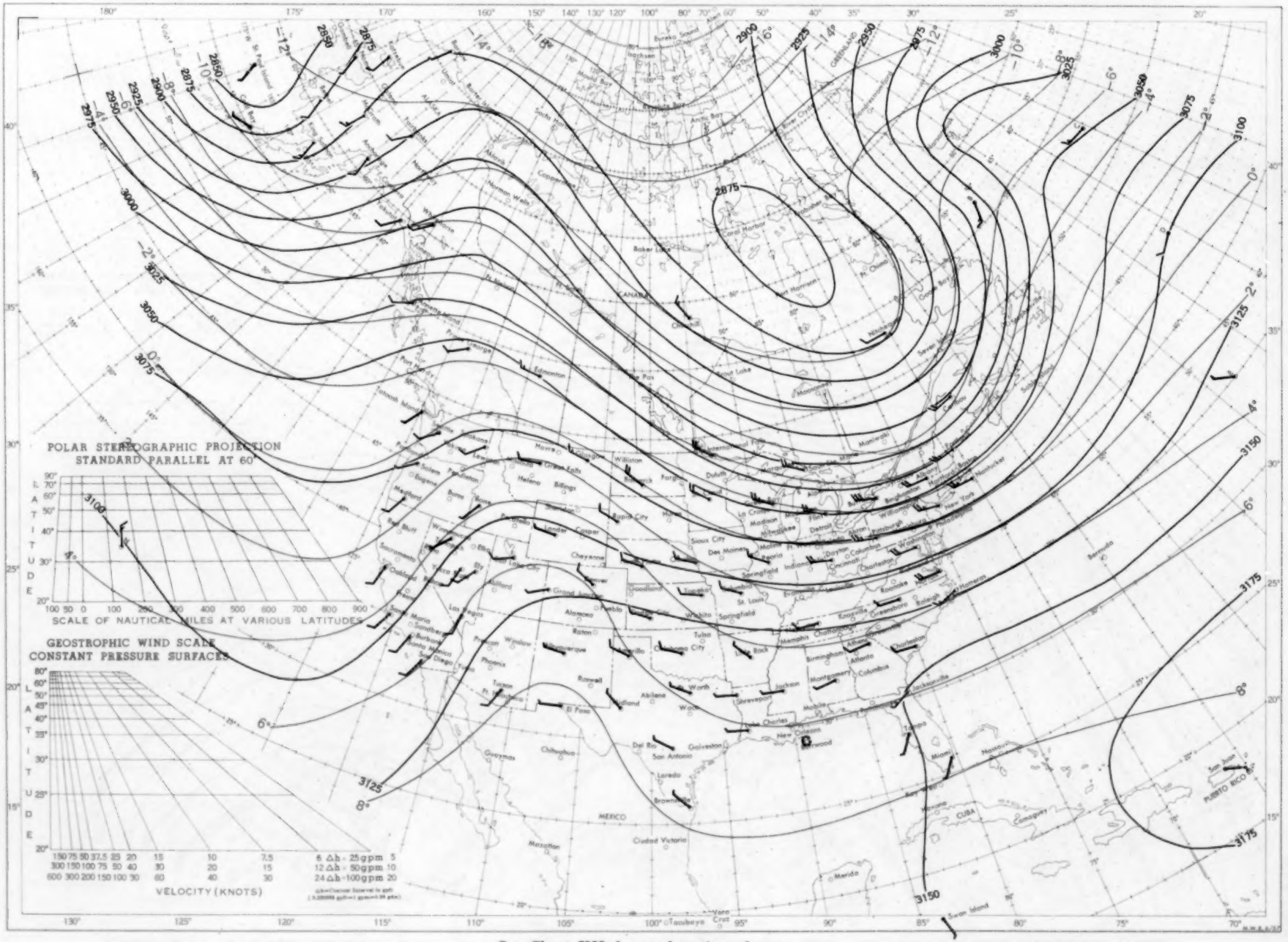

MAY 1958

See Chart XII for explanation of map.

Chart XIV. 500-mb. Surface, 1200 GMT, May 1958. Average Height and Temperature, and Resultant Winds.

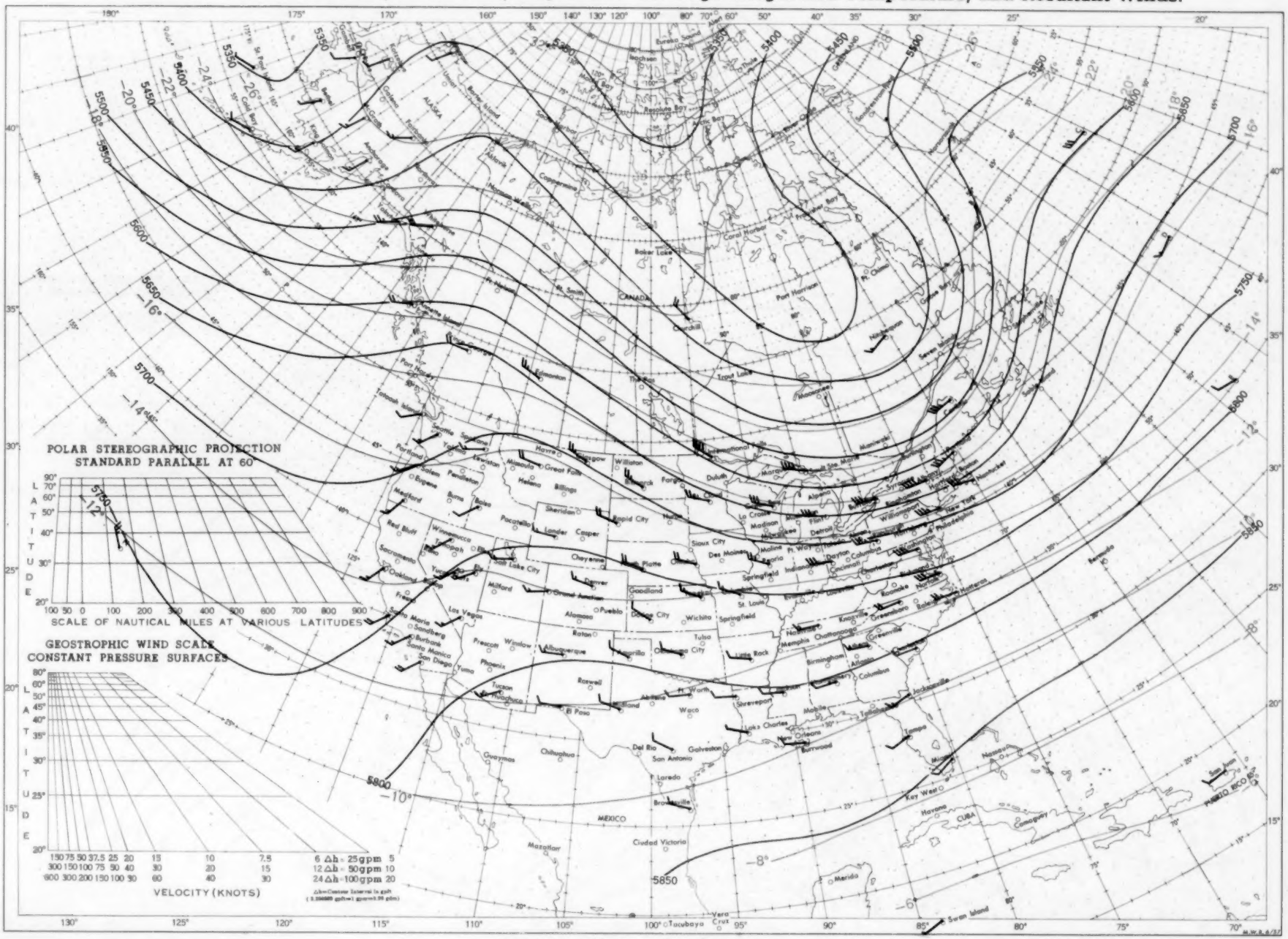
POLAR STEREOGRAPHIC PROJECTION
STANDARD PARALLEL AT 60°
SCALE OF NAUTICAL MILES AT VARIOUS LATITUDES
GEOSTROPHIC WIND SCALE
CONSTANT PRESSURE SURFACES
VELOCITY (KNOTS)
6 Δh = 25gpm 5
12 Δh = 50gpm 10
24 Δh = 100gpm 20

See Chart XII for explanation of map.

Chart XV. 300-mb. Surface, 1200 GMT, May 1958. Average Height and Temperature, and Resultant Winds.

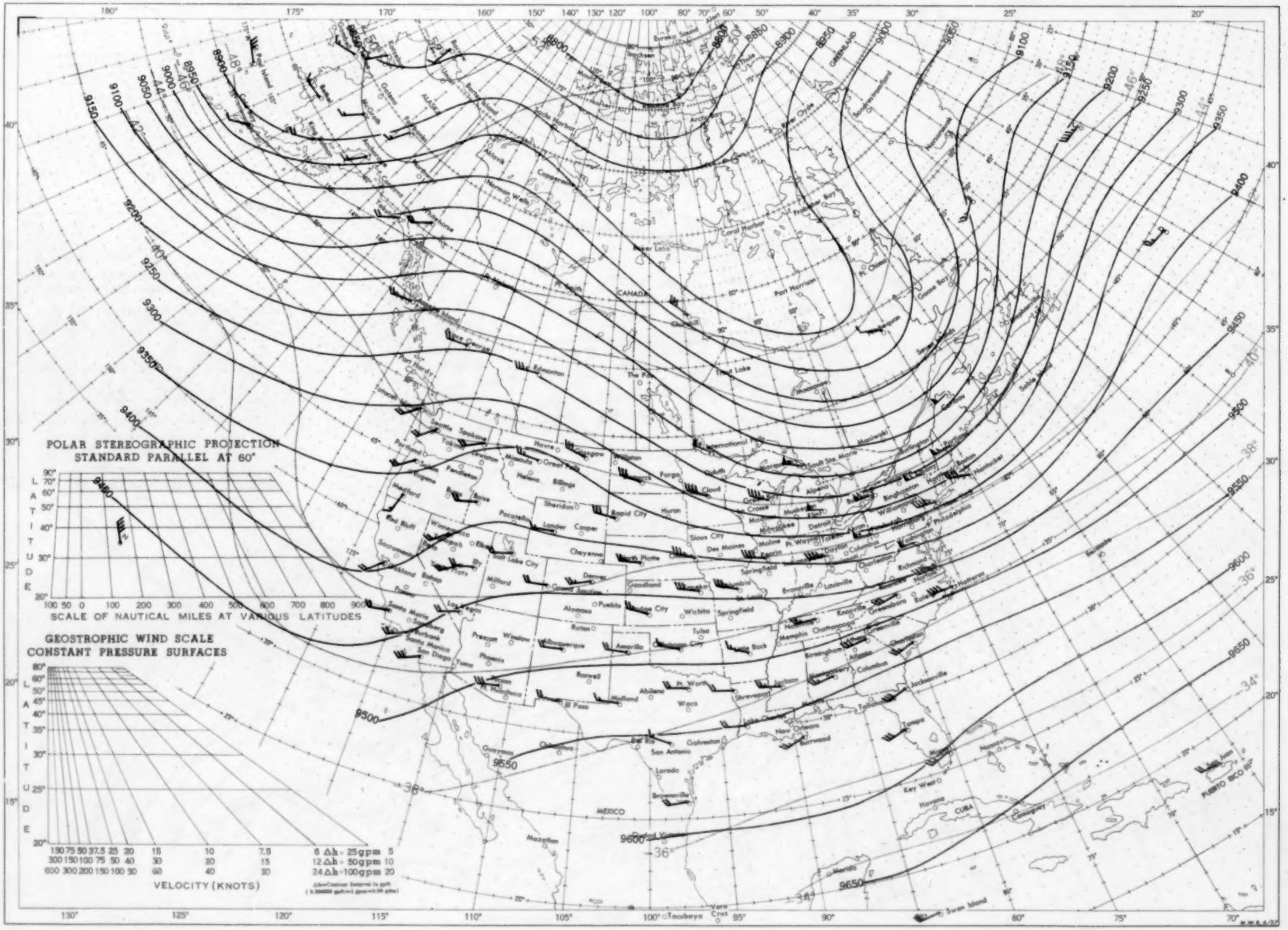

See Chart XII for explanation of map.

Chart XVI. 200-mb. Surface, 1200 GMT, May 1958. Average Height and Temperature, and Resultant Winds.

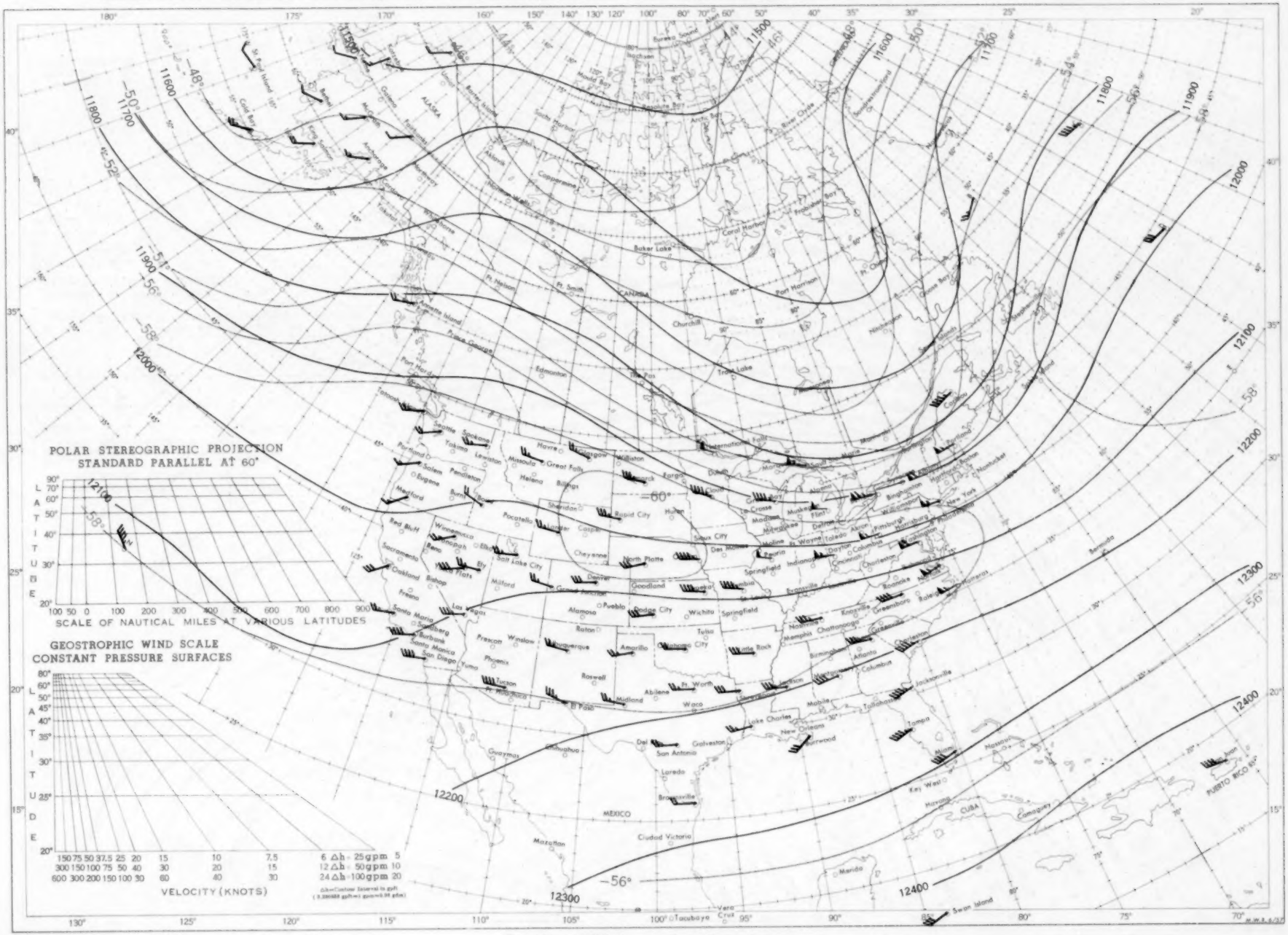

See Chart XII for explanation of map.

Chart XVII. 100-mb. Surface, 1200 GMT, May 1958. Average Height and Temperature, and Resultant Winds.

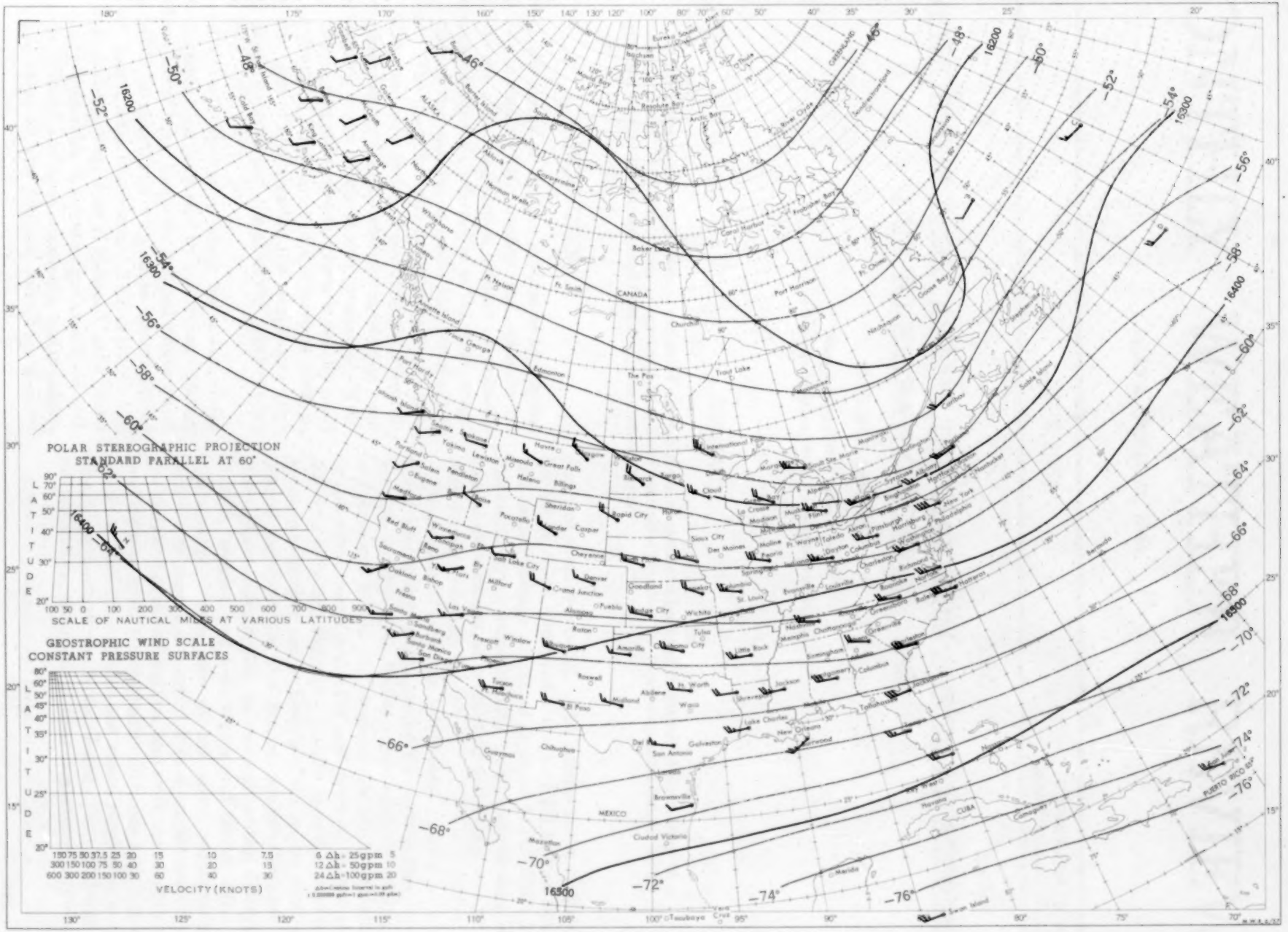

See Chart XII for explanation of map.

MAY 1958